IDENTIFICATION AND EVALUATION OF CIRCULATING BIOMARKERS FOR PANCREATIC CANCER AND THEIR CORRELATION WITH PANCREATIC STROMAL EXPRESSION

Anthony S H Evans

Department of Molecular and Clinical Cancer Medicine

Institute of Translational Medicine

University of Liverpool

Thesis submitted in accordance with the requirements of the University of Liverpool for the degree of Doctor in Philosophy

January 2016

DECLARATION

This dissertation is the result of my own work and includes nothing that is the outcome of work done in collaboration, except where specifically indicated in the text. It has not been previously submitted, in part or whole, to any university for any degree or other qualification.

ABSTRACT

Pancreatic ductal adenocarcinoma (PDAC) is the deadliest of the common cancers, with a dismal prognosis attributed in part to late diagnosis in the majority of patients. Diagnosing early stage increases the likelihood of eligibility for surgical resection, currently the only available method of cure. In this thesis I have aimed to identify serum biomarkers for the diagnosis of PDAC, as a potential means of screening for the disease in a minimally-invasive manner.

The glycoprotein tenascin C (TNC) was identified as a potential diagnostic biomarker in PDAC patient sera compared to patients with chronic pancreatitis (CP), a finding that was subsequently validated in an independent cohort of samples. As a benign inflammatory disease of the pancreas, pancreatitis commonly presents concurrently with PDAC making biomarkers that can distinguish the two a rarity. In attempting to identify the cause of increased circulating TNC in PDAC, i*n situ* hybridisation performed on PDAC and CP tissue specimens identified tumour cells as a source of TNC, producing and secreting the protein into the surrounding stroma. Tissue microarray (TMA) analysis revealed stromal TNC was more common in PDAC patients than in CP, consistent with the pattern in sera. However, when available serum samples were matched to the tissue no direct relationship was found.

Biomarker discovery work performed by other members of our group identified serum thrombospondin-1 (TSP-1) as a promising candidate biomarker for early diagnosis, decreased in sera collected up to 24 months prior to PDAC diagnosis. This observation was validated using multiple reaction monitoring, a relatively novel mass spectrometry-based method. Presented here are immunoassay results confirming the MRM data, along with serum analysis collected from a genetically engineered mouse model for PDAC suggesting that decreased TSP-1 levels may occur when PDAC is fully developed rather than at a preneoplastic stage.

Finally, in light of the lack of correlation between circulating and stromal TNC, the possibility was considered that TMAs may not be sufficient for quantifying stromal expression in PDAC. A TMA was tested as a means of quantifying components of the PDAC stroma, and revealed that prognostic analyses yielded variable results depending on what depth of the TMA was analysed. This suggests that caution should be taken when applying this technique to such a heterogeneous disease.

ACKNOWLEDGEMENTS

First and foremost I would like to sincerely thank my supervisors, Dr Eithne Costello, Dr Bill Greenhalf and Professor John Neoptolemos. Their guidance and patience has been inspirational and I can never thank them enough. My thanks go also to Professor Fiona Campbell, whose willingness to assist in any way she could helped me immeasurably.

I am also grateful to everyone here in the pancreas research group, in particular Dr Claire Jenkinson, Mrs Frances Oldfield and Dr Lawrence Barrera-Briceno for all the work we've done together. I had never imagined how enjoyable my time here would be, and that is entirely down to the people working here, past and present.

Special thanks go to Pancreatic Cancer UK, the University of Liverpool and EPC-TMNET for funding my research.

I would also like to thank Kayla Friedman and Malcolm Morgan for producing the Microsoft Word thesis template used to produce this document.

Finally, I would like to thank Rachel, my family and all my friends for their support and kindness while I've been studying.

CONTENTS

LIST OF TABLES

List of Figures

1 INTRODUCTION

The term ‘cancer’ is used to describe a number of complex diseases, all characterised by abnormal and uncontrolled cell proliferation in different organs of the body[1,2]. Hanahan and Weinberg have proposed ten hallmarks and enabling characteristics common to all cancers, namely: sustaining proliferative signalling, evading growth suppressors, activating invasion and metastasis, enabling replicative immortality, inducing angiogenesis, resisting cell death, evading immune destruction and regulating cellular epigenetics, all enabled by genome instability and mutation, and tumour-promoting inflammation[2]. These factors are the result of a complex environment within the tumour, where normal cells comprising the stroma are recruited amid a network of crosstalk signalling. Such interactions are thought to facilitate the invasive and proliferative properties characteristic of tumour cells.

In 2011, cancer was ranked second on a list of leading causes of death in the United States[3]. Pancreatic cancer, the most prevalent form of which is pancreatic ductal adenocarcinoma (PDAC), is the most lethal common cancer, with a five-year survival of approximately 5%[3–6]. Currently it is the fourth leading cause of cancer-

related death, but little improvement in survival rates has been made over the past few decades, and PDAC is projected to become the second leading cause by 2030[3,7]. This dismal prognosis is attributed to the aggressive nature of the disease, its resistance to systemic therapy and late stage at diagnosis[5]. Early stage PDAC is typically asymptomatic, with advanced disease presenting symptoms such as weight loss, obstructed jaundice, abdominal pain, fatigue and anorexia[4–6]. Consequently, only approximately 20% of diagnosed patients are eligible for surgical resection, presently the only available method of cure[5,8,9].

Patients who undergo resection followed by adjuvant chemotherapy have an improved five-year survival of approximately 25%[10–14]. Surgery alone has poorer outcome, with 6 months of treatment with gemcitabine or fluorouracil (5FU) demonstrating a significant survival benefit[11,12,14]. Chemotherapy also confers a small survival benefit in patients with locally advanced or metastatic disease, with FOLFIRINOX (fluorouracil, irinotecan, oxaliplatin, leucovorin) or gemcitabine plus nab-paclitaxel comprising the current standard treatment in patients with good performance status[5,15–18].

1.1 The biology of pancreatic cancer

One of the characteristic features of PDAC transformation is a point mutation in the *KRAS2* oncogene, occurring in ~90% of cases[19–21]. The production of constitutively active Ras protein drives cell cycle progression and survival, with these mutations reported in the most common PDAC precursor lesions, defined as pancreatic intraepithelial neoplasm (PanIN)[21–24]. *KRAS* mutations have also been identified in intraductal papillary mucinous neoplasms (IPMNs), another precursor lesion for PDAC[5,25,26]. The conventional model of disease progression begins with the formation of dysplastic PanIN lesions, with low to high dysplasia graded on a scale from 1-3, progressing to invasive carcinoma[5,23,26].

PanIN-1 lesions have been detected in non-diseased pancreata, increasing in prevalence with age, while higher grade lesions have been reported either adjacent to tumour or in individuals at a higher risk of developing PDAC[5,27]. Progression is driven by the accumulation of mutations, in particular inactivating mutations of tumour suppression genes, and disruptive epigenetic silencing through methylation of CpG islands[5,21,24]. The most commonly affected genes include *p53*, *CDKN2A* and *SMAD4*, the inactivation of which occur with increasing frequency in higher grade PanIN lesions[5,21,28].

Mutational analyses of established tumours indicate genomic instability is a key characteristic of PDAC, with heterogeneous clonal populations identified within tumours and metastases[28–32]. A recent whole-genome analysis of 100 PDAC tumours identified 5424 genes with non-silent mutations, while a seminal study that analysed 24 tumours reported an average of 63 genetic alterations per tumour, which could be broadly classified into 12 functionally-relevant signalling pathways[29,32]. This

heterogeneity of PDAC tumour cells provides one explanation for the disease's resistance to therapy, with the complex PDAC microenvironment also considered to be a crucial factor, making it the subject of intense study for the past decade.

1.2 The pancreatic cancer microenvironment

A notable feature of PDAC among other solid tumours is a particularly pronounced stromal compartment (Figure 1-1), with relatively poor vascularity[33,34]. The tissue microenvironment consists of a complex assembly of extracellular matrix, matricellular and soluble proteins, immune cells, fibroblasts and blood vessels (Figure 1-2)[33–35].

1.2.1 Inflammatory cells and PDAC

Research over the past two decades has provided a wealth of evidence suggesting inflammatory cells assist tumour development rather than hinder it[35,36]. An obvious example of this phenomenon is found in PDAC with the higher incidence of cancer among patients with the inflammatory condition chronic pancreatitis (CP)[37,38]. In genetically engineered mouse models (GEMMs) with conditional activating mutations of the *Kras* oncogene, cerulean-induced pancreatitis has been reported to accelerate the formation of PDAC[39–41].

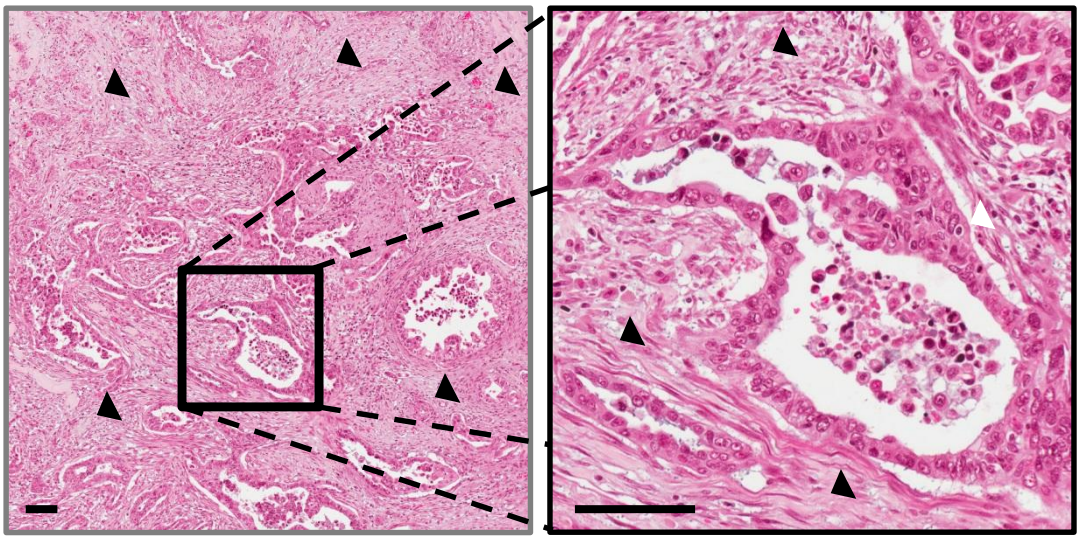

Figure 1-1. Haematoxylin and eosin stain displaying the PDAC microenvironment. PDAC is characterised by a prominent desmoplastic stroma, indicated by black arrowheads. Inset is an example of PDAC tumour cells with a ductal phenotype (white arrowheads). Scale bar=100µm.

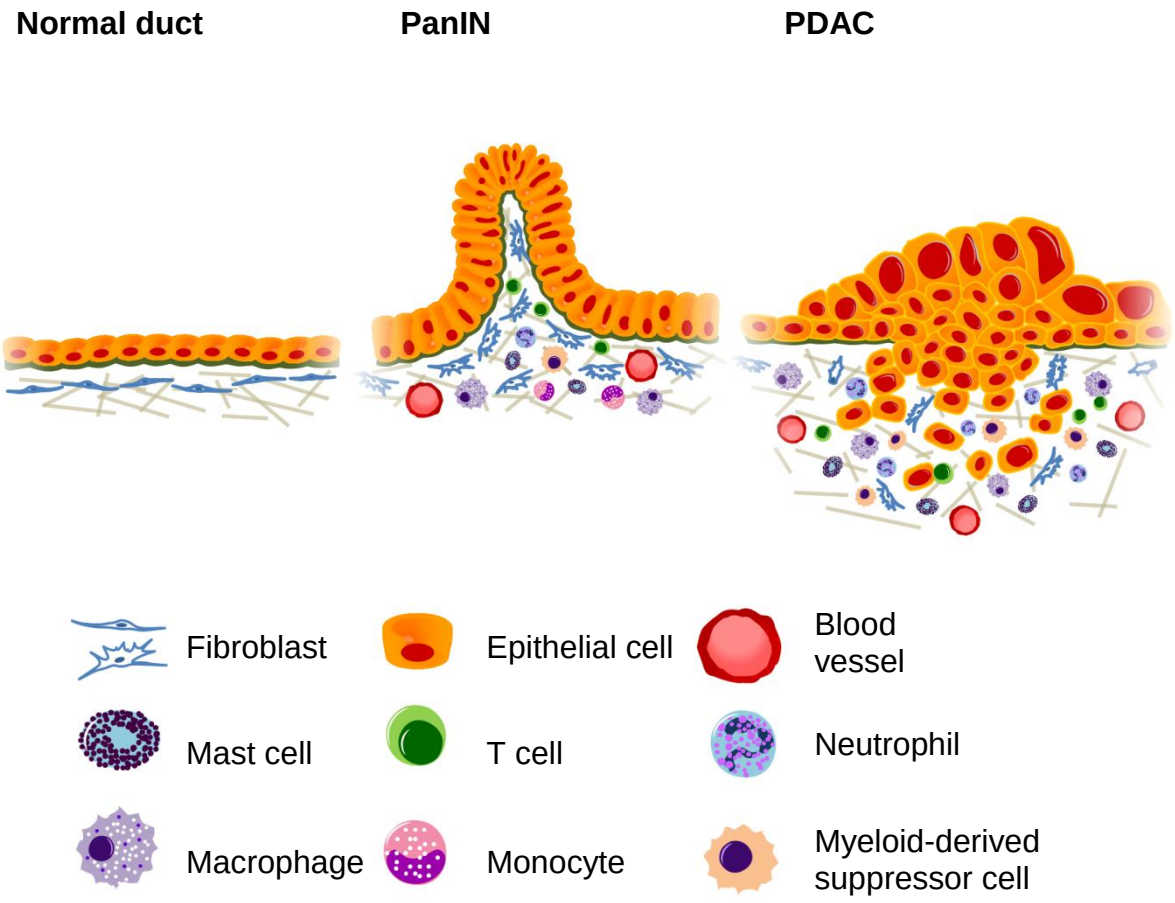

Figure 1-2. Diagram illustrating the components of the pancreas tissue microenvironment. Abbreviations: PanIN – pancreatic intraepithelial neoplasm, PDAC – pancreatic ductal adenocarcinoma. Figure adapted from Evans and Costello, 2012[35].

Cell infiltrates from the innate and adaptive immune systems have been observed in many tumour types and have been linked to prognostic outcome and response to treatment[35,36,42,42,43]. Consequently, the need for tumours to escape the immune response and hijack inflammatory components to foster growth and progression have been recognised as key characteristics of cancer[2]. The complexity of the role of immune cells in cancer has led to their intense study over the past two decades, including in relation to PDAC[34–36].

1.2.1.1 Mast cells

Several components of the immune system have been identified as promoters of PDAC cell growth and invasion. Mast cells play a key role in immune responses to microbial infection, and are thought to play a role in tissue remodelling and repair, tumour repression and tumour growth[44]. They express the receptor for stem cell factor (KIT) and are thought to be recruited and activated by tumour-derived stem cell factor, secreting inflammatory factors such as interleukin-6 (IL-6), tumour necrosis factor-α (TNF-α)and vascular endothelial growth factor (VEGF)[45]. They can also downregulate the immune response to tumours through secretion of immunosuppressive cytokines, such as IL-10, and by favouring expansion and activation of regulatory T (Treg) cells to promote immune tolerance[45].

A high influx of mast cells has been reported in the tumours of a mutant K-Ras (*KRas*^{G12V}) mouse model for PDAC, noting an even distribution of mast cells in CP and PanIN lesions but a focal accumulation in tumours along the invasive front[46]. The infiltration in CP and PanIN lesions suggests that mast cell recruitment occurs early in the development of PDAC, and is consistent with the concept of inflammation potentiating neoplasia. Chang *et al.* grew orthotopic pancreatic tumours in mast cell-deficient (*Kit*$^{-/-}$) mice and observed significantly reduced

tumour growth and improved survival times compared to control mice. They corroborated this finding in human tissues, noting that higher mast cell infiltration corresponded with poor outcome and consequently confirmed a trend observed in a previous study[46,47]. Similar work examining mast cell abundance in 103 patients with PDAC also noted a significant survival benefit to low cell counts in the cancerous border with normal tissue[48].

In a recent study by Schönhuber and colleagues, a dual-recombinase system for use in GEMMs was developed as a means of enabling secondary genetic manipulation in PDAC[49]. As a proof of concept, they crossed a mutant-*KRas* line with mast cell-deficient *Cpa3*$^{Cre/+}$ mice, thought to avoid a problem in *Kit*-deficient mice where non-immune components are altered, and observed PDAC development in mice at 12 months of age despite the complete absence of mast cells, suggesting that mast cells are dispensable for formation of the disease[49,50]. Given the results of the studies linking mast cell abundance with prognosis, it is possible that mast cells may not be essential for PDAC formation but can still assist in its development, thus providing further evidence of the complexity of the role of the immune system in PDAC.

1.2.1.2 Myeloid-derived suppressor cells

Myeloid-derived suppressor cells (MDSCs) are immature myeloid cells, thought to enhance tumour growth by suppressing components of the innate and adaptive immune system[51,52]. They are comprised of two main subsets: $CD14^+$ monocytic and $CD15^+$ granulocytic subpopulations[53]. MDSCs can actively suppress host immunity by inhibiting T cell activation and migration, expanding Treg abundance and inhibiting natural killer (NK) cells[53,54].

An analysis of a *KRas*^{G12D} GEMM revealed a slight elevation of MDSCs in PanIN lesions, with a more pronounced increase in PDAC[55]. Clark *et al*. observed that

MDSCs accumulated around periductal areas and stroma, accompanied by a corresponding lack of $CD8^+$ cytotoxic T cells[55]. Two separate GEMM studies identified tumour cells as a source of granulocyte macrophage colony-stimulating factor (GM-CSF), required for the recruitment of MDSCs, and noted that inhibiting GM-CSF inhibited tumour growth in a $CD8^+$ T cell-dependent manner[56,57]. These findings were supported by Stromnes *et al.*, who demonstrated that depleting granulocytic MDSCs in a GEMM increased intratumoral accumulation of activated $CD8^+$ T cells and apoptosis of tumour epithelial cells[58]. Interestingly, they also observed stromal remodelling in their model, noting decreased extracellular matrix and an increased number of patent blood vessels.

1.2.1.3 Tumour associated macrophages

Under normal circumstances, macrophages fight infection and facilitate wound healing, localising to sites of inflammation where they mediate the inflammatory response through the release of cytokines and growth factors[59]. They are commonly classified into two extreme phenotypes, pro-inflammatory M1 or anti-inflammatory M2, though in reality this distinction is unlikely to be discrete as most fall along a continuum[53,60,61]. It is thought that M1 macrophages facilitate tumour cell death, while M2 macrophages enhance tumour progression[53,60].

A study by Kurahara *et al*. supports this concept, reporting that higher numbers of M2 macrophages on the tumour invasive front was associated with poorer overall survival in PDAC patients[62]. They also noted that M2 abundance correlated with a high incidence of lymph node metastasis, suggesting that histological analyses of the microenvironment may be clinically informative for other features of the disease.

An analysis of mutant *KRas*^{G12D} mice has identified a potential mechanism by which macrophages enhance PDAC development. Lesina *et al.* identified Stat3 activation as an essential step for PanIN to progress to PDAC, mediated by IL-6 secreted primarily by macrophages[63]. A recent study also suggests macrophages may contribute to resistance to conventional chemotherapy, demonstrating a mechanism whereby tumour associated macrophages induce the upregulation of cytidine deaminse (CDA) in tumour cells, a metabolising enzyme that subsequently reduced the sensitivity of the cells to the drug gemcitabine[64].

1.2.1.4 T cells

T lymphocyte infiltrations have been reported in human and murine PDAC tissue specimens, with several studies focusing on the function of $CD4^+$ $FoxP3^+$ Tregs[55,65–67]. Tregs, like MDSCs, demonstrate an immunosuppressive phenotype[68]. In PDAC patients, elevated circulating Tregs have been found in the peripheral blood compared to healthy controls, and correlated with MDSC abundance[66]. Greater numbers of Tregs have also been observed in PDAC stroma than in non-neoplastic inflammatory pancreatic tissue, and were associated with a poorer prognosis[67]. The prevalence of Tregs was found to increase with grade of PanIN lesions up to invasive ductal carcinoma, with a corresponding decrease in $CD8^+$ cytotoxic T cell infiltration[67].

T helper (Th) cells have also been studied in the context of PDAC[35]. Th cells activate cells of the innate immune system, assist B cells and $CD8^+$ cytotoxic T cells, and facilitate wound repair[69]. They can be classified into several subsets, including Th1 cells that can induce microbial elimination and Th2 cells that are thought to mediate helminth immunity[69].

Both Th1 and Th2 cells have been identified in human PDAC, though skewed in both number and activity towards the Th2 subset[70]. A subsequent study supported this observation, and demonstrated that an increased ratio of tissue Th2:Th1 cells was independently associated with poor prognosis in PDAC patients[71]. Recently, a study in *KRas*^{G12D} mice has implicated Th cells in a mechanism of early neoplastic development. McAllister *et al.* observed IL-17-secreting Th17 cells were recruited to the pancreas in response to inflammation, and established that IL-17 overexpression could accelerate PanIN initiation and progression while IL-17 inhibition resulted in abrogated PanIN formation[72]. These results suggest different subsets of Th cells may have functional prominence at different stages of the development of PDAC.

1.2.2 Desmoplastic stroma

The dense desmoplastic milieu characteristic of PDAC has been studied extensively over the past decade, as there has been particular interest in developing anti-stromal therapies as an approach to enhancing chemotherapeutic delivery[33,34]. The extracellular matrix, consisting of collagen, hyaluronic acid (HA), proteoglycans, fibronectin and other matricellular proteins and enzymes, is thought to originate from activated myofibroblasts, commonly termed pancreatic stellate cells (PSCs)[33,73,74]. When isolated from tissue specimens, these cells inhabit a quiescent phenotype characterised by the accumulation of lipid droplets and are negative for α-smooth muscle actin (αSMA), but after ~48 hours adopt an activated phenotype, begin producing collagen type I and fibronectin and can be positively stained for αSMA[73,74].

Studies utilising conditioned media (CM) and co-culture methods with activated myofibroblasts and PDAC cells have demonstrated cross-talk between the two populations. Conditioned media from PDAC cell lines has been shown to stimulate myofibroblast proliferation and the production of collagen I and fibronectin, while CM from activated myofibroblasts enhanced PDAC proliferation, migration and invasion[75,76]. Co-injection of mice with PDAC cells and myofibroblasts has been demonstrated to enhance tumour size, increase metastasis and resistance to chemotherapy, and suggests that tumour cells co-migrate with myofibroblasts to form metastases[75–78]. The latter observation is supported by a recent study examining desmoplasia in primary tumours and various sites of metastasis, concluding that both contain comparable levels of desmoplasia whilst also observing a greater mean αSMA^+ area in metastases than in primary tumours[79].

It has been hypothesised that depleting the desmoplastic stroma may increase the vascular content of the tumour, facilitating the delivery of systemic therapies, which has guided investigators towards testing stromal inhibitors in GEMMs[80]. Mice expressing mutant *KRas* and *p53* oncogenes (KPC) treated with IPI-926, a Smoothened (Smo) inhibitor to inhibit the hedgehog (Hh) pathway, had a marked increase in vascular perfusion and mean vessel density, and exhibited prolonged survival when combined with gemcitabine[80]. Subsequent studies targeting hyaluronic acid in KPC mice supported this finding, demonstrating improved blood vessel density and patency leading to increased intratumoral drug delivery and extended survival[81,82]. A phase I/II clinical trial assessing the effectiveness of HA inhibitors is still ongoing (NCT01453153), but unfortunately clinical trials testing Smo inhibitors have had to be halted due to increased mortality in the treatment arm[34,83].

Recent studies depleting the stroma in GEMMs by pharmacological and genetic inhibition have also suggested this may be detrimental to survival[84–86]. Sonic hedgehog (Shh)- deleted mice with mutant *KRas* and floxed *p53* had increased tumour vascularity but reduced survival compared to mice with wild type Shh, a finding corroborated by prolonged treatment with the Smo inhibitor IPI-926[85]. A separate study using three distinct GEMMs for PDAC also confirmed that Shh deletion and Smo inhibition accelerated tumour progression and reduced desmoplasia[84]. Similarly, a study using drug-inducible αSMA deletion to deplete myofibroblasts concluded that myofibroblast loss at early and late stages of PDAC development led to reduced survival, characterised by a greater prevalence of poorly-differentiated tumours and significantly greater numbers of infiltrating Tregs[86]. These findings suggest that while the stroma may act as a barrier for drug treatment, caution should be taken when considering stromal depletion as a therapeutic approach.

More optimistically, alternative approaches to targeting the stroma have been attempted with some success[87,88]. Sherman *et al.* demonstrated that targeting the vitamin D receptor (VDR) in cancer-associated fibroblasts led to a reprogramming of the stroma, reverting the fibroblasts to a quiescent phenotype and sensitising the tumour to gemcitabine to improve survival[88]. A study by Feig *et al.* observed that depleting fibroblast activation protein (FAP)-positive fibroblasts in KPC mice slowed tumour development but not when $CD4^+$ and $CD8^+$ T cells were pharmacologically depleted[87]. FAP^+ cells were found to produce CXCL12 in the tumour, a chemokine that binds tumour cells and excludes T cells. Inhibition of its receptor, CXCR4, led to an accumulation of $CD3^+$ T cells, and increased tumour cell

death after treatment with the immune checkpoint antagonist α-programmed cell death-ligand 1 (α-PD-L1)[87].

Though many of the studies examining the role of stroma in PDAC have utilised mouse models, several have also examined the prognostic impact of desmoplastic stroma in humans. An investigation measuring αSMA expression in tissue from 162 patients enrolled in a randomised phase III clinical trial concluded that high αSMA expression was associated with reduced overall survival, though there was no association when only untreated patients were considered[89]. However, when patients were classified by stromal density determined by haematoxylin and eosin staining, a substantial survival benefit was seen in those with dense stroma in the untreated arm[89]. These findings supported a previous analysis of αSMA expression as a proportion of collagen in serial sections, termed the activated stroma index (ASI)[90]. Here, Erkan *et al.* found no significant association of αSMA expression with overall survival in 233 patients, and a modest survival benefit in patients with a high abundance of collagen. When patients were classified by ASI, those in the upper quartile had a significantly poorer prognosis than those in the lower quartile[90]. A more recent study by Özdemir *et al*. compared αSMA expression in 53 patients and found a significant positive association with overall survival in patients with high expression[86]. Different conclusions over whether an association exists between αSMA^+ fibroblast abundance and survival may be due to differences in the scoring methods used, but data appear to be consistent in identifying dense desmoplastic stroma as prognostically favourable. This is consistent with the concept of desmoplastic stroma playing a protective role in PDAC, despite potentially presenting a barrier to therapeutic delivery.

Given the lack of success in clinical trials for drugs aimed at depleting the stroma, it is apparent that more work is needed to understand its role in PDAC. Promising results from stromal reprogramming and interference of immune cell-fibroblast crosstalk suggest that it can be exploited for therapeutic gain, but more understanding of the complex relationships between components of the tumour microenvironment is required.

1.3 Diagnostic biomarkers for pancreatic cancer

Presently the only hope for cure of PDAC is surgical resection accompanied by adjuvant (post-operative) chemotherapy, with clinical trials investigating the effectiveness of neoadjuvant (preoperative) therapy currently underway[5]. The resectability of the tumour is determined by its location and degree of progression, with clinical staging determined by TNM status (Table 1.1)[6]. Tumours at stage 0 (Tis, N0, M0), stage IA (T1, N0, M0), stage IB (T2, N0, M0), stage IIA (T3, N0, M0) and stage IIB (T1-3, N1, M0) are considered resectable, with stage III (T4, any N, M0) considered borderline resectable if tumour encasement of the superior mesenteric artery (SMA) or coeliac axis is less than 180º, or if involvement is confined to the superior mesenteric vein or pulmonary vein[6]. Locally advanced stage III tumours are considered unresectable, where encasement of the SMA or coeliac arteries exceeds 180º or if venous involvement is unreconstructable, as are stage IV metastatic tumours (any T, any N, M1)[6].

Table 1.1. TNM classification definitions for PDAC.

		Definition
T: Primary tumour	TX	Primary tumour cannot be assessed
	T0	No evidence of primary tumour
	Tis	Carcinoma *in situ*
	T1	Tumour confined to pancreas, ≤ 2 cm largest dimension
	T2	Tumour confined to pancreas, > 2 cm largest dimension
	T3	Tumour extends beyond panceas, but no involvement of coeliac axis or superior mesenteric artery
	T4	Tumour involves the coeliac axis or superior mesenteric artery
N: Regional lymph node	NX	Regional lymph nodes cannot be assessed
	N0	No regional lymph nodes
	N1	Regional lymph node metastasis
M: Distant metastases	M0	No distant metastasis
	M1	Distant metastasis

With only ~20% of PDAC cases considered resectable or borderline resectable, there is an urgent need for methods of diagnosing patients at an earlier stage[5,8,9]. A study that used lineage labelling in a GEMM for PDAC discovered that epithelial-to-mesenchymal transition (EMT) and dissemination of neoplastic cells occurred from as early a stage as PanIN formation[91]. The possibility of metastasis occurring early in the development of PDAC suggests that early intervention is required, and that there may be opportunities to diagnose the disease at an earlier stage than is currently achievable[92]. Given the urgency of this requirement for improving survival, numerous approaches have been undertaken to identify biomarkers for the diagnosis of PDAC.

1.3.1 Protein biomarkers in the circulation

The use of blood-borne biomarkers to screen for PDAC is an attractive proposition, as samples can be obtained in a minimally invasive manner and are already routinely handled by clinical laboratories. Challenges are posed when attempting to identify new biomarkers in blood-based samples however, as the concentration of analytes cover a large dynamic range, and low abundance proteins can easily be masked by highly abundant proteins such as albumin[93]. These difficulties, along with the challenge of huge environmental and genetic variation across subjects, have prevented researchers from identifying robust diagnostic biomarkers for PDAC.

Currently the only serum biomarker routinely used for PDAC is the sialylated Lewis blood group antigen carbohydrate antigen 19-9 (CA19-9), informing assessments of disease recurrence and monitoring response to chemo- and radiotherapy[94,95]. It is currently considered to be unsuitable for screening, with a sensitivity and specificity for PDAC diagnosis of approximately 80%[96]. Moreover, CA19-9 is not produced in

the 5% of the population who are Lewis^{a-b-} and is consequently uninformative for this group[97]. Given the lack of progress in identifying novel single biomarkers specific for PDAC, it is likely that a panel of biomarkers may need to be identified, to use in combination with CA19-9 or otherwise. Consequently, many studies have combined several markers to improve diagnostic sensitivity and specificity[92].

Brand *et al*. performed a multiplex analysis for 83 proteins on a large cohort of serum samples, comprised of 333 PDAC patients, 144 with benign pancreatic disorders (pancreatic cysts, chronic pancreatitis and acute pancreatitis) and 227 healthy controls[98]. With their samples split into discovery and validation sets, they initially identified two panels of three markers that discriminated PDAC cases from healthy individuals and benign pancreatic disorders. Using receiver operator curves they identified a combination of CA19-9, intercellular adhesion molecule 1 (ICAM-1) and osteoprotegerin (OPG) that distinguished PDAC cases with a maximum sensitivity and specificity of 88% and 90% respectively, yielding an area under the curve (AUC) of 0.93 in the discovery set, compared to 0.83 with CA19-9 alone. This panel was similarly accurate in the validation set, resulting in an AUC of 0.91. They also found that a panel combining CA19-9, carcinoembryonic antigen (CEA) and tissue inhibitor of metalloproteinases 1 (TIMP-1) could distinguish PDAC cases from benign disorders, though the improvement over CA19-9 alone was more modest (AUC=0.86 vs 0.82). Again, this panel performed with a similar degree of accuracy in the validation set (AUC=0.83)[98]. These findings are an example of how combining biomarkers can improve diagnostic performance, particularly over CA19-9 alone, as well as demonstrating the increased difficulty of discriminating PDAC patients from benign pancreatic disorders compared to healthy subjects.

A similar study applying multiplex methods on a large serum cohort also demonstrated the effectiveness of biomarker combination, splitting a cohort of 248 PDAC patients,114 healthy subjects and 102 CP patients into training and validation sets[99]. Park *et al.* identified a panel comprised of CA19-9, matrix metalloprotease 7 (MMP-7) and cathepsin D could diagnose PDAC from all controls with an AUC of 0.90 and 0.91 in the discovery and validation cohorts respectively[99]. Similar accuracy was obtained by Gold *et al*. using an assay for PAM4, a monoclonal antibody, in combination with CA19-9 in a cohort of 298 PDAC patients, 79 healthy subjects, 120 patients with benign pancreatic disorders and 99 non-pancreatic cancer patients[100]. ROC analysis yielded an AUC of 0.91 in distinguishing PDAC cases from benign disorders, and the same again for PDAC compared to CP patients.

The results of these studies are encouraging, and suggest a diagnostic panel of proteins with close to 100% accuracy may one day be achievable. However, work conducted by our group and others has recently established that the presence of obstructive jaundice is a confounding factor in identifying circulating diagnostic biomarkers for PDAC in serum and plasma[92,101–104]. Tumours developing in the head of the pancreas, the most common site in PDAC, can obstruct the bile duct, making jaundice a common symptom among PDAC patients[5,105].

Tonack *et al*. used isobaric labelling in combination with tandem mass spectrometry to identify diagnostic proteins in sera from healthy subjects (n=29) and patients with PDAC (n=64), CP (n=48) and benign biliary obstruction caused by gallstones or liver disease (n=31)[102]. The observation was made that splitting PDAC cases according to jaundice status (total serum bilirubin> 20μmol/L) revealed reduced sensitivity in distinguishing PDAC patients without jaundice from benign disorders and healthy subjects. Correspondingly, specificity was also reduced in jaundiced

PDAC patients compared to patients with benign biliary obstruction[102]. A study by Nie *et al*. supported this conclusion, identifying a panel of serum glycoproteins that, in combination with CA19-9, had a diagnostic AUC of 0.96 for PDAC compared to CP patients, but only 0.74 when compared to patients with benign obstructive jaundice[103]. A separate study attempting to validate ICAM-1 and TIMP-1 in a cohort of serum samples from patients with CP, benign biliary obstruction, obstructed and non-obstructed PDAC and healthy controls (all n=20) observed that neither marker was significantly deregulated in PDAC patients with jaundice compared to those with benign jaundice[106]. Moreover, concentrations of both markers in PDAC patients without jaundice were not significantly different from those in CP patients, in contrast to previous studies[106]. Taken together, these studies suggest that a background of jaundice should always be considered when selecting PDAC patients to test for circulating biomarkers, and comparisons made with jaundiced patients of benign origin if possible. The lack of concordance of TIMP-1 and ICAM-1 measurements with previous studies also demonstrates the importance of validation in independent cohorts, with confounding variables taken into account.

Though cases are rarer, focusing biomarker analyses on early stage PDAC samples where the tumour is confined to the pancreas may avoid the confounding effects of jaundice. Pan *et al*. analysed a cohort of plasma from stage I-II PDAC and CP patients, as well as healthy subjects (all n=20), and discovered that combining gelsolin and lumican could discriminate PDAC cases from all control groups (AUC=0.94)[107]. They also demonstrated that the use of multiple reaction monitoring (MRM), a mass spectrometry-based method of quantification, gave comparable measurements to the more standard enzyme-linked immunosorbent assays (ELISAs) for TIMP-1 in plasma[107]. Makawita *et al*. also restricted their analysis of PDAC

patients to stage I-II cases (n=82), validating biomarkers they had previously identified in serum and comparing with healthy subjects (n=47), benign pancreatic disorders (CP and neoplasms, n=42) and non-pancreatic cancer patients (n=70)[108]. They identified a panel that could discriminate PDAC cases from all benign and healthy control groups (AUC=0.92), compared to CA19-9 alone (AUC=0.8).

The studies discussed so far have used samples collected from diagnosed patients, and may have identified informative biomarkers for diagnosis in the clinic. They are also candidates for testing in pre-diagnostic cohorts of samples, to assess their suitability as a screening tool for vital early diagnoses. Unfortunately, such cohorts of samples from individuals collected prior to PDAC diagnosis are rare. To overcome this, studies have utilised blood from GEMMs collected at different stages of disease to identify potential candidates for early diagnosis[109,110].

Faca *et al*. used tandem mass spectrometry with isotopically labelled pooled plasma samples, collected from transgenic mice with mutant *Kras* and floxed *Ink4a/Arf* with developed PanIN lesions or PDAC alongside matched controls[109]. They identified a panel of proteins that was tested in human sera from PDAC (n=30) and CP (n=10) patients, alongside healthy controls (n=20), giving a diagnostic AUC of 0.96. Interestingly, they also tested a panel of five proteins found to be upregulated in mice with PanIN lesions in a set of pre-diagnostic human sera from the CARET study. Thirteen samples obtained between 7 and 13 months prior to PDAC diagnosis were analysed for this panel alongside matched controls, yielding an AUC of 0.82[109]. Though the sample size is low for a panel of five markers, these results suggest analysing samples GEMMs for comparison with human samples is a valid approach.

A similar study conducted by Mirus and colleagues utilised an antibody microarray containing ~130 antibodies to analyse plasma from KPC mice at different stages of

disease progression, diagnosed with PanIN lesions alone or developed PDAC[110]. A simultaneous analysis of 87 PDAC samples collected up to 4 years prior to diagnosis, with matched controls, was also performed. Two proteins were identified as upregulated in both cohorts, and when combined with a third an AUC of 0.68 was achieved in the pre-diagnostic human samples. As expected, when the analysis was extended to a separate set of samples from diagnosed PDAC patients (n=24) and controls (n=24) the diagnostic accuracy was improved (AUC=0.86),[110]. The promising findings from these two studies raise the possibility that the use of GEMMs with pre-diagnostic human samples may be an effective method of identifying novel biomarkers for early diagnosis.

Many of the studies mentioned so far have focused on proteins and glycoproteins present in the circulation, quantified with the use of mass spectrometry, multiplex assays, antibody arrays, immunoblotting and ELISAs. Alternative approaches have also been undertaken, investigating cytokines and autoantibodies as potential PDAC biomarkers[104,111–114].

Zeh *et al.* demonstrated that cytokines are feasible biomarker candidates, using a panel of five cytokines to differentiate PDAC serum samples from CP patients and healthy controls, and improving upon CA19-9 alone[111]. A study by Shaw *et al.* measured 27 cytokines in sera from PDAC (n=127) and CP (n=49) patients, alongside benign obstructed jaundice patients (n=20) and healthy controls (n=45),[104]. After splitting the samples into training and validations set, panels of cytokines were identified that could be combined with serum CA19-9, yielding a diagnostic AUC of 0.84 and 0.88 in the training and validation sets respectively when discriminating PDAC cases from benign controls[104].

Recent studies have indicated that PDAC patients produce autoantibodies whose detection can distinguish cases from benign controls[112–114]. One study compared serum samples from 300 PDAC samples and 300 controls to identify several upregulated antibodies, though individually the AUC for each marker was relatively low[113]. Another group identified autoantibodies for serum phosphorylated enolase (ENOA1,2) as highly accurate biomarkers for PDAC (n=120) compared to healthy controls (n=40) and CP patients (n=46), with AUCs of 0.94 and 0.95 for advanced and resectable cancers versus all controls respectively[112]. This study was recently expanded to include autoantibodies for ezrin, identified in sera from KPC mice with PanIN lesions and PDAC as a potential early diagnostic marker[114]. Ezrin antibodies were confirmed to be significantly upregulated in human pre-diagnostic sera from the EPIC cohort (PDAC n=16, controls n=32) with a minimum time of 5 months prior to diagnosis. Combining ezrin autoantibodies with CA19-9 and antibodies for ENOA1,2 improved accuracy in a cohort of diagnosed samples, yielding an AUC of 0.96 for PDAC patients (n=45) compared to benign subjects (n=48)[114]. These findings suggest the detection of autoantibodies for tumour-associated antigens may be an effective strategy for diagnosing PDAC.

1.3.2 Protein biomarkers in urine

While much of the focus on PDAC biomarkers has been towards those in the circulation, the identification of markers in other easily-accessible samples is equally important. A recent investigation by Radon *et al*. utilised a proteomic analysis of pooled urine samples obtained from patients with PDAC, CP and healthy controls (all n=6), separated by SDS-PAGE and analysed by tandem mass spectrometry[115]. Three proteins were identified, LYVE1, REG1A and TFF1, and selected for further analysis in a large multicentre cohort of urine samples (PDAC n=192, CP n=92,

healthy control n=87). After splitting samples into a training and validation set, ROC analysis of the three proteins combined revealed diagnostic AUC for PDAC from healthy controls of 0.89 and 0.92 in the training and validation sets, respectively. Similar diagnostic accuracy was achieved when only stage I-II cancers were considered, but was improved further by combination with plasma CA19-9 measurements. Restricting the PDAC cases to stage I-IIA, for localised disease with no nodal involvement, resulted in an AUC for the panel of 0.97, compared to CA19-9 alone with 0.84, where adding CA19-9 to the panel conferred no diagnostic improvement[115]. These promising results warrant further investigation as potential early diagnostic markers, and suggest that screening urine is a valid strategy in identifying diagnostic biomarkers for PDAC.

1.3.3 MicroRNA markers in the circulation

MicroRNAs (miRNAs) are small non-coding RNA molecules that make for attractive candidates as biomarkers due to remarkably high stability in the circulation[116]. Though the breadth of studies investigating miRNA biomarkers for PDAC is much smaller than for protein, several studies have identified potential candidates. An analysis of plasma samples from 36 PDAC patients and 30 healthy controls revealed miR-18a levels were significantly higher in cancer cases, with a diagnostic AUC of 0.94[117]. A larger study analysed serum and plasma from 80 PDAC patients and 129 healthy subjects for U2 small nuclear RNA fragments (RNU2-1f), identified after detecting miR-1246 in mouse PDAC xenografts and determining RNU2-1f as the source of this miRNA sequence[118]. Though direct diagnostic AUC values for PDAC were not reported, a high degree of separation from healthy controls was observed[118]. A study conducted by Li *et al*. analysed sera from 45 PDAC patients, 32 healthy subjects and 11 patients with CP, and observed

greater levels of miR-200a and miR-200b in PDAC than healthy controls (AUC=0.86 and 0.85 respectively), but no differences between PDAC and CP[119]. The use of miRNAs for the diagnosis of PDAC may yet prove to be effective, and further analysis of larger cohorts that include benign pancreatic disorders is warranted.

1.3.4 Circulatory exosomes as biomarkers for pancreatic cancer

Exosomes are extracellular vesicles secreted by cells, containing proteins and nucleic acids. A recent study observed an abundance of exosomes expressing the cell surface proteoglycan glypican-1 (GPC1) in sera from patients with PDAC[120]. Samples from 190 PDAC patients were compared with 100 healthy controls and 26 patients with benign pancreatic disorders, revealing all PDAC cases had greater numbers of $GPC1^+$ exosomes than all of the control samples (AUC=1.0). This finding was replicated in an independent cohort of 56 PDAC, 6 benign pancreatic disorder patients and 20 healthy control samples (AUC=1.0). $GPC1^+$ exosomes quantified in sera from a GEMM for PDAC revealed exosome numbers correlated with disease progression, with notable increases preceding visible formation of tumour masses as determined by magnetic resonance imaging (MRI)[120]. These findings are extremely promising, particularly if the exceptional diagnostic accuracy can be maintained when comparing with a larger cohort of benign pancreatic disorders. The correlation of $GPC1^+$ exosome levels with disease burden in the mouse models suggest that this is a promising marker for testing in a pre-diagnostic sample cohort[120]. Even if these findings fail to be validated in independent cohorts, the measurement of exosomes with different surface markers to GPC1 may be warranted as an alternative approach to discovering diagnostic biomarkers for PDAC.

Much of the current research into pancreatic cancer, both in terms of therapy and for understanding the tumour biology, is focused on understanding the role of the stroma. Despite great progress in our understanding of the disease, survival rates have been slow to improve[4–6]. There is still an urgent need for methods of diagnosing PDAC at an early enough stage for resection, currently the only available option for cure. The use of genetically engineered mouse models has been invaluable in elucidating the role of components in the tumour microenvironment, and has enabled investigations into circulatory biomarkers at early stages of disease progression. Nevertheless, recent paradigm shifts in how to approach therapy targeting the stroma reveal more work is needed in understanding its complexity[34]. Similarly, studies investigating biomarkers using samples from pre-diagnostic cohorts are still relatively scarce, and we have yet to identify independently-validated early diagnostic markers that can discriminate PDAC cases from benign controls[92].

1.4 Hypotheses

The hypotheses to test were: proteins in the circulation can be quantified for specific early diagnosis of pancreatic cancer. Secondly, that aberrant concentration of proteins in the sera relate to their expression in the pancreatic tissue microenvironment.

1.5 Aims and objectives

1. Identify serum biomarkers for the detection of pancreatic cancer.
    a. Quantify cancer-associated proteins in two cohorts of serum samples, one comprised of pre-diagnostic sera from PDAC patients and another of diagnosed patient samples with PDAC or benign pancreatic disorders.
    b. Test candidate proteins from this analysis, and others identified by members of the group, in an independent cohort of samples to verify their suitability as diagnostic biomarkers.
2. Investigate protein biomarker expression in the pancreatic tissue microenvironment.
    a. Identify areas of protein expression in patient tissue specimens.
    b. Determine if protein levels in the circulation correspond with expression in tissue microarrays containing matched tissue specimens.
3. Determine if tissue microarrays are suitable for quantifying components of the pancreatic cancer stroma.

2 DISCOVERY AND VALIDATION OF DIAGNOSTIC SERUM BIOMARKERS FOR PANCREATIC CANCER

2.1 Introduction

2.1.1 Identification of promising diagnostic serum biomarkers for pancreatic cancer using a multiplex Luminex approach

To identify protein biomarkers for the early diagnosis of PDAC in a disease-specific manner, a multi-analyte profile panel, the Human Oncology MAP (Myriad Rules-Based Medicine; http://www.rulesbasedmedicine.com/), which enables the measurement of 101 target proteins in serum using Luminex technology was used (Table 2.1). Luminex xMAP technology relies on 5.6µm polystyrene microspheres stained with two fluorochromes to varying degrees, such that each microsphere set has a unique fluorescent signature detectable by excitation with a red diode laser[121]. This enables the mixing of multiple microsphere sets as each bead can still be uniquely identified by its fluorescent spectrum. By tagging microsphere sets with specific capture antibodies, the detection of each microsphere can be associated with a specific analyte. Once the antigens in the sera have bound to the microspheres, biotinylated detection antibodies are added followed by streptavidin-phycoerythrin as a third fluorochrome. Excitation of bound R-phycoerythrin is performed with a green yttrium aluminium garn (YAG) laser, concurrently with the red diode laser, for detection and quantification of bound protein per microsphere. Suspended microspheres are passed through the detection chamber in single file for discrete measurements of each bead, with thousands of beads read per second. These principles enable multiplex analysis of up to several analytes per reaction.

Table 2.1. Full list of Human OncologyMAP® v.1.0 proteins quantified by Myriad RBM

Human OncologyMAP® v.1.0	
6Ckine	Aldose reductase
Alpha-fetoprotein	Amphiregulin
Angiogenin	Annexin A1
B cell-activating factor	B lymphocyte chemoattractant
Bcl-2-like protein 2	Betacellulin
Cancer antigen 125	Cancer antigen 15-3
Cancer antigen 19-9	Cancer antigen 72-4
Carcinoembryonic antigen	Cathepsin D
Cellular fibronectin	Collagen IV
Endoglin	Endostatin
Eotaxin-2	Epidermal growth factor
Epidermal growth factor receptor	Epiregulin
Epithelial cell adhesion molecule	Ezrin
Fatty acid-binding protein, adipocyte	Fatty acid-binding protein, liver
Fibroblast growth factor basic	Fibulin-1C
Galectin-3	Gelsolin
Glucose-6-phosphate isomerase	Glutamate-cysteine ligase regulatory subunit
Glutathione S-transferase Mu 1	HE4
Heparin-Binding EGF-Like Growth Factor	Hepatocyte
Growth Factor	Hepatocyte growth factor receptor
Hepsin	Human chorionic gonadotropin β
Human epidermal growth factor receptor 2	Insulin-like growth factor-binding protein 1
Insulin-like growth factor-binding protein 2	Insulin-like growth factor-binding protein 3
Insulin-like growth factor binding protein 4	Insulin-like growth factor binding protein 5
Insulin-like growth factor binding protein 6	Interferon gamma induced protein 10
Interferon-inducible T-cell α chemoattractant	Interleukin-2 receptor alpha
Interleukin-6	Interleukin-6 receptor subunit β
Kallikrein 5	Kallikrein-7
Lactoylglutathione ly.ase	Latency-associated peptide of transforming growth factor β1
Leptin	Macrophage inflammatory protein 3 β
Macrophage migration inhibitory factor	Macrophage-stimulating protein
Maspin	Matrix metalloproteinase-2
Mesothelin	MHC class I chain-related protein A
Monocyte chemotactic protein 1	Monokine induced by gamma interferon
Neuron-specific enolase	Neuropilin-1
Neutrophil gelatinase-associated lipocalin	Nucleoside diphosphate kinase B
Osteopontin	Osteoprotegerin
Pepsinogen I	Peroxiredoxin-4
Phosphoserine aminotransferase	Placenta growth factor
Platelet-derived growth factor BB	Prostasin
Protein S100-A4	Protein S100-A6
Receptor tyrosine-protein kinase erbB-3	Squamous cell carcinoma antigen-1
Stromal cell-derived factor-1	Tenascin C
Tetranectin	Thyroglobulin
Tissue type plasminogen activator	Transforming growth factor α
Tumor necrosis factor receptor I	Tyrosine kinase with ig and egf homology domains 2
Urokinase-type plasminogen activator	Urokinase-type plasminogen activator receptor
Vascular endothelial growth factor	Vascular endothelial growth factor B
Vascular endothelial growth factor c	Vascular endothelial growth factor D
Vascular endothelial growth factor receptor 1	Vascular endothelial growth factor receptor 2
Vascular endothelial growth factor receptor 3	YKL-40

2.1.2 Choice of samples for analysis

Two sets of human serum samples were selected for analysis. They were designed to accommodate the challenges posed in identifying diagnostic biomarkers for PDAC. Patients with obstructed jaundice from benign causes were included in the sample set, as the presence of biliary obstruction in patients with PDAC is a confounding factor in biomarker studies[101,102,122,123]. Similarly, existing biomarkers including CA19-9 have demonstrated poor specificity for PDAC when compared to patients with chronic pancreatitis[123,124]. Thus, chronic pancreatitis patients were selected to address the specificity of potential protein biomarkers for PDAC. Finally, in the past serum biomarker discovery programs have generally used samples from diagnosed patients, with the inherent risk that changes occurring prior to diagnosis are missed. To address this concern, a pre-diagnosis cohort was employed in collaboration with a group from University College London, led by Dr John Timms. The UK Collaborative Trial of Ovarian Cancer Screening (UKCTOCS) was established by the University College London (UCL) Institute for Women's Health as a randomised controlled trial following 202,638 post-menopausal, healthy women to assess the value of screening for ovarian cancer[125]. Upon recruitment a serum sample was taken, with 50,000 women also providing annual samples such that serial samples were available dating back up to eight years. In this cohort, 226 women went on to develop PDAC; as a result the biobank contained serum samples collected up to five years prior to the diagnosis of PDAC. This offered the opportunity to detect biomarkers with aberrant expression at time points prior to conventional clinical methods of diagnosis.

2.1.3 Logistic regression analysis for the identification of potential biomarkers of PDAC

Logistic regression is a method of fitting a model with a dichotomous dependent variable, in this case PDAC diagnosis, using a set of independent variables[126]. This method can be paired with calculation of a receiver operating characteristic (ROC) curve, which plots the performance of a variable's sensitivity, the ability to detect a true signal, against false positive detection (1-specificity) over a range of thresholds for that variable[126]. Measuring the area under the curve (AUC) allows for comparison of different markers' performance in accurately classifying a dichotomous variable, with an AUC of 1 indicating perfect classification and 0.5 indicating no classification effect by the independent variable.

2.2 Samples and materials and methods

2.2.1 University of Liverpool collection

The University of Liverpool (UoL) collection consisted of serum taken from healthy subjects as well as from patients diagnosed with PDAC, chronic pancreatitis (CP) and benign diseases causing obstructive jaundice. All samples were collected at the Royal Liverpool University Hospital with ethical approval and patients and subjects participated with written informed consent. Serum was obtained from blood samples collected in Sarstedt Monovette tubes (Sarstedt Ltd., UK), left to clot at 4ºC for 15 minutes before centrifugation at 800g for 10 minutes. The serum supernatant was then aliquoted and stored at -80ºC for future use.

2.2.2 UKCTOCS collection

Each pre-clinical PDAC case from the UKCTOCS collection was matched with a healthy control sample based on the same collection centre, collection date, and equivalent age as closely as possible. Thus, 45 PDAC samples with 45 matched controls were selected for this study. Initially, the samples were divided equally into five time groups: 0-6 months, 6-12 months, 1-2 years, 2-3 years and 3-4 years prior to diagnosis. However, subsequent histological review of patient data since the experiment was conducted revealed a small number of patients had been misclassified as PDAC and had incorrect dates of diagnosis. Misclassified samples were removed from the analysis and the time to diagnosis for the remaining samples was recalculated. For this reason, there is considerable disparity in the numbers of individuals per group in this analysis.

2.2.3 Myriad RBM multiplex protein quantification

Serum samples from both sample cohorts were shipped for analysis to Myriad RBM located in Austin, Texas, where the analysis was undertaken. Using microspheres coupled with a capture-antibody sandwich approach enabled multiplex quantification of 101 proteins (Table 2.1). Briefly, each serum sample was pre-diluted and, in 96-well hard-bottomed microtitre plates, 10µL was mixed with 5µL blocker and 5µL of mixed diluted capture-antibody microspheres. Standards and controls were also mixed accordingly with the microsphere mixture before plate incubation for 1 hour at room temperature. 10µL biotinylated detection antibody was added to each well before a further 1 hour incubation. A similar addition of 10µL streptavidin-phycoerythrin per well followed, and was left to incubate again for 1 hour. A filter-membrane microtitre plate was pre-wetted with 100µL wash buffer before aspiration using a vacuum manifold device. The contents of the hard-bottomed plates were transferred to the respective wells of the filter plate then vacuum-aspirated and washed twice with 100µL wash buffer. After the final wash a further 100µL wash buffer is added to each well before thorough mixing to resuspend the microspheres. The plated protein-bead conjugates were subsequently analysed with a Luminex 100 Analyzer (Luminex, USA). For each protein analyte, a standard curve was fitted using known quantities of analyte on the same microtitre plate. Previously unknown concentrations of proteins in the serum samples were then calculated by comparing the median fluorescence intensity (MFI) for each analyte with its respective standard curve. Multiplication by the sample dilution factor then gives a final concentration of each protein for that sample. Myriad RBM defined the lower limit of quantification (LLOQ) as the concentration at which the coefficient of variation (CV) percentage equalled 30%. This was determined for each analyte by two-fold dilution of a

medium standard eight times, assaying in triplicate over three separate runs before calculating and plotting the CV against concentration. Samples whose measured concentration fell below the LLOQ were excluded from the analysis for that analyte.

2.2.4 Serum protein measurement by enzyme-linked immunosorbent assay (ELISA)

Commercially available enzyme-linked immunosorbent assay (ELISA) kits were purchased for IL-6Rβ (cat. no. DGP00, R&D Systems, UK), TNC (cat. no. 27767, IBL International, Japan) and PSAT (cat. no. CSB-EL018838HU, Cusabio, China). Each kit used sandwich immunoassay principles to quantify the protein of interest. Briefly, serum was diluted and added to antibody-coated 96-well plates then incubated so that antigen would bind to the base of the wells. This was followed by washing and addition of a horseradish peroxidase (HRP)-linked antibody, before further washing and the addition of tetramethylbenzidine (TMB) as a chromogen. TMB is converted by HRP to a coloured product such that the degree of colour change is proportional to the amount of bound antigen. Known quantities of the protein of interest were measured alongside the serum samples in order to generate a standard curve, against which the measured colour absorbance of the serum could be compared to calculate an exact protein concentration. Assays were all performed to manufacturer's instructions, with absorbance measurements performed using a Thermo Multiskan Ex (Thermo Fisher Scientific, USA) at 450nm wavelength with 595nm measurements collected for background correction. All samples were measured in duplicate, and measurements accepted if the coefficient of variation was less than 10%. Five-parameter logistic regression was used to fit the standard curves and calculate the sample concentrations using Sigmaplot, version 11.

2.2.5 Statistical Analysis

For the purposes of selecting the best fit model of protein biomarker combinations, stepwise logistic regression was performed using JMP's minimum corrected Akaike Information Criterion (AIC) procedure.

2.3 Results

2.3.1 Identification of candidate biomarkers differentially regulated prior to diagnosis (UKCTOCS cohort)

The characteristics of the pre-diagnosis patient cohort are shown in Table 2.2.

Table 2.2. Patient characteristics of UKCTOCS pre-diagnostic and matched control serum samples

	0-6 months		**6-12 months**		**12-24 months**		**24-36 months**		**36-48 months**	
	PDAC	Ctrl	PDAC	Ctrl	PDAC	Ctrl	PDAC	Ctrl	PDAC	Ctrl
n	9	11	6	9	5	9	5	8	5	8
Median age (range)	69 (53-73)	68 (58-74)	58 (51-69)	67 (50-77)	63 (52-68)	60 (52-73)	65 (57-68)	64 (52-70)	60 (56-66)	63 (51-72)

Abbreviations: PDAC – pancreatic ductal adenocarcinoma, ctrl – healthy control

Before statistical analysis of the Myriad Rules-Based Medicine data, any analytes where 20% or more of the samples were deemed to be below the LLOQ were excluded. The study was designed to include the measurement of effects from several proteins combined in a logistic regression model, so excluding a large proportion of samples due to one protein's missing data when combining with other proteins would be problematic. In the UKCTOCS sample set, 17 protein analytes out of 101 were excluded in this manner.

2.3.2 CA19-9 and CA125 serum concentration increases up to one year prior to diagnosis

Mann Whitney U tests were performed using JMP version 11 (SAS Institute Inc., USA), comparing each PDAC time group set with its respective healthy control sera. This methodology does not assume that measurements follow a Gaussian distribution, meaning it could be applied to all proteins in the analysis.

Of the proteins analysed, CA125 and CA19-9 concentration displayed the clearest relationship with time to diagnosis. Despite modest sample sizes, both proteins were significantly upregulated in PDAC sera in the 0-6 month and 6-12 month groups (Figure 2-1).

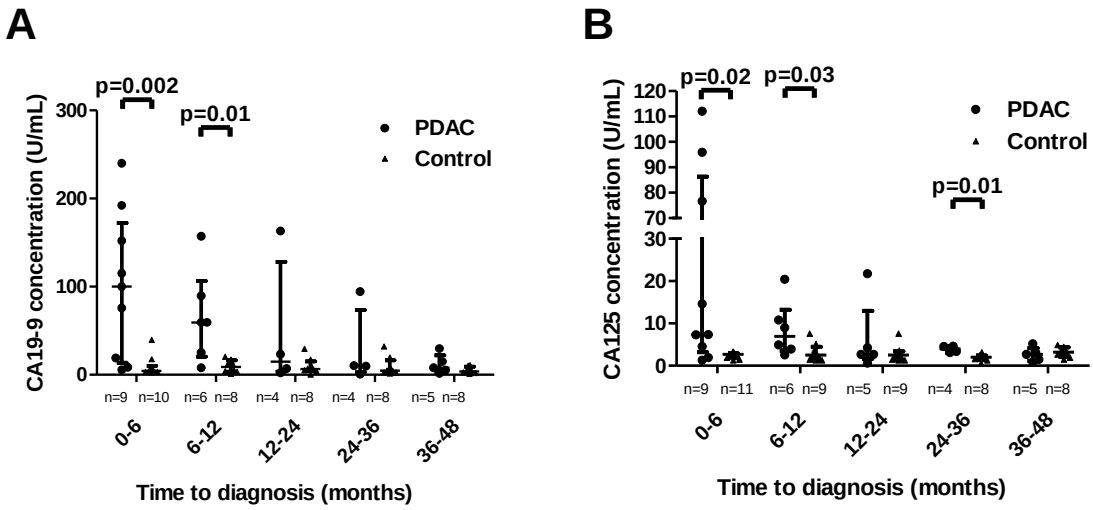

Figure 2-1. Concentration of serum CA19-9 and CA125 is significantly upregulated up to one year prior to the diagnosis of PDAC. A) CA19-9 and B) CA125 were quantified in the sera of PDAC patients prior to clinical diagnosis using a Luminex platform. Age- and centre-matched healthy control samples were also analysed for comparison. Error bars display median and interquartile range, p values calculated by Mann Whitney U.

2.3.3 Serum carcinoembryonic antigen and alpha fetoprotein increase in some PDAC patients prior to clinical diagnosis

A clear pattern of protein concentration altering as time to diagnosis decreased was not observed among the other markers, when PDAC samples were compared with controls within the same time group. However, when all healthy control samples were treated as one group a statistically significant association between carcinoembryonic antigen (CEA) and alpha fetoprotein (AFP) concentration with time to diagnosis was revealed (Figure 2-2). CEA concentration was significantly upregulated in the 0-6 month cancer case group, with a corresponding trend observed in the 6-12 month group (Figure 2-2A). Significant or trending increases of AFP concentration were also observed in all time groups prior to the diagnosis of PDAC (Figure 2-2B).

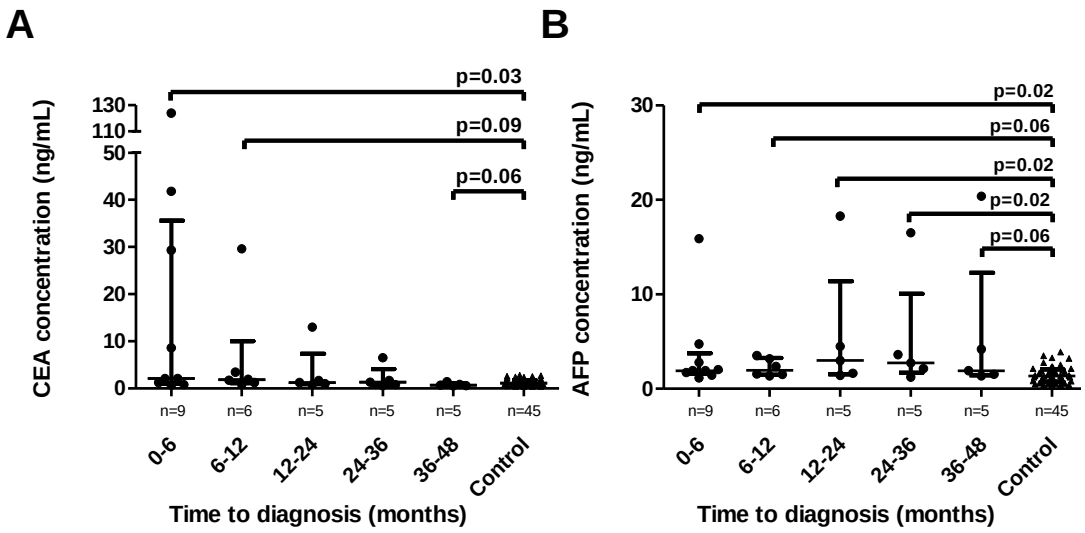

Figure 2-2. Concentration of serum CEA and AFP is significantly upregulated up prior to the diagnosis of PDAC. A) CEA and B) AFP were quantified in the sera of PDAC patients prior to clinical diagnosis samples using a Luminex platform. Age- and centre-matched healthy control samples were also analysed for comparison. Error bars display median and interquartile range, p values calculated by Mann Whitney U.

2.3.4 Discovery of disease-specific biomarkers for pancreatic cancer

The characteristics of the diagnosed patients (University of Liverpool collection) are shown in Table 2.3. As with the statistical analysis of the Myriad Rules-based Medicine data generated using UKCTOCS samples, analytes where greater than 20% of the sample measurements fell below the LLOQ were excluded from further analysis. Consequently, 20 out of 101 protein analytes were not included.

Table 2.3. Patient characteristics of diagnosed PDAC serum samples and controls with related disorders

		PDAC non-obs	PDAC-obs	BBO	CP	HC
n		20	15	10	15	15
Median age (range)		64.5 (39-78)	67 (39-78)	65.5 (24-80)	48 (36-78)	35 (23-65)
Sex	F/M	9/11	8/7	3/7	9/6	5/10
Tumour stage	T1	-	-	-	-	-
	T2	-	-	-	-	-
	T3	10	9	-	-	-
	I	10	5	-	-	-
	U	-	1	-	-	-
Resection margin	R0	1	4	-	-	-
	R1	7	5	-	-	-
	I	10	5	-	-	-
	U	2	1	-	-	-

Abbreviations: PDAC – pancreatic ductal adenocarcinoma, BBO – benign biliary obstruction, CP – chronic pancreatitis, HC – healthy control, obs – obstruction, I – inoperable, U - unknown

2.3.5 No single protein is deregulated solely in pancreatic cancer patients

Mann Whitney U tests were performed comparing sera from patients with PDAC with each benign control group. Of 81 proteins analysed, 71 had at least one significant difference between classification groups, though with so many comparisons a large number of these were likely due to chance.

No significantly differentially-expressed proteins were specific for PDAC patients compared with all of the control groups. However, several promising markers were identified that individually were significantly upregulated in PDAC sera compared with healthy controls, obstructive jaundice or chronic pancreatitis patients (Figure 2-3).

Of all the cancer-control comparisons, as expected the most commonly observed differences were between the healthy controls and the PDAC serum samples, with 43 (53%) of 81 analysed proteins showing significantly different expression in non-jaundiced PDAC patients compared with healthy controls. In comparison, proteins that could discriminate PDAC patients from those with CP or patients with benign obstructive jaundice were much less prevalent. Comparisons of non-obstructed PDAC cases against CP revealed 11 proteins (14%) with significantly different expression, while a similar comparison between jaundiced PDAC cases and benign biliary obstruction revealed 10 (12%).

CA19-9 and CA125 were again revealed as promising markers of PDAC, significantly upregulated compared with both chronic pancreatitis patients and healthy controls (Figure 2-3A, B). The hexameric glycoprotein tenascin C (TNC) was also upregulated in PDAC cases compared to CP, irrespective of obstructed jaundice status (Figure 2-3C). Of the many proteins differentially expressed in the disease groups compared with the healthy controls, the glycoprotein urokinase-type

plasminogen activator receptor (uPAR) demonstrated a particularly consistent upregulation across all disease groups (Figure 2-3D). Finally, phosphoserine aminotransferase (PSAT) and interleukin-6 receptor subunit β (IL-6Rβ, also known as gp130) were both significantly upregulated in benign obstructed jaundice cases compared with obstructed PDAC cases (Figure 2-3E, F).

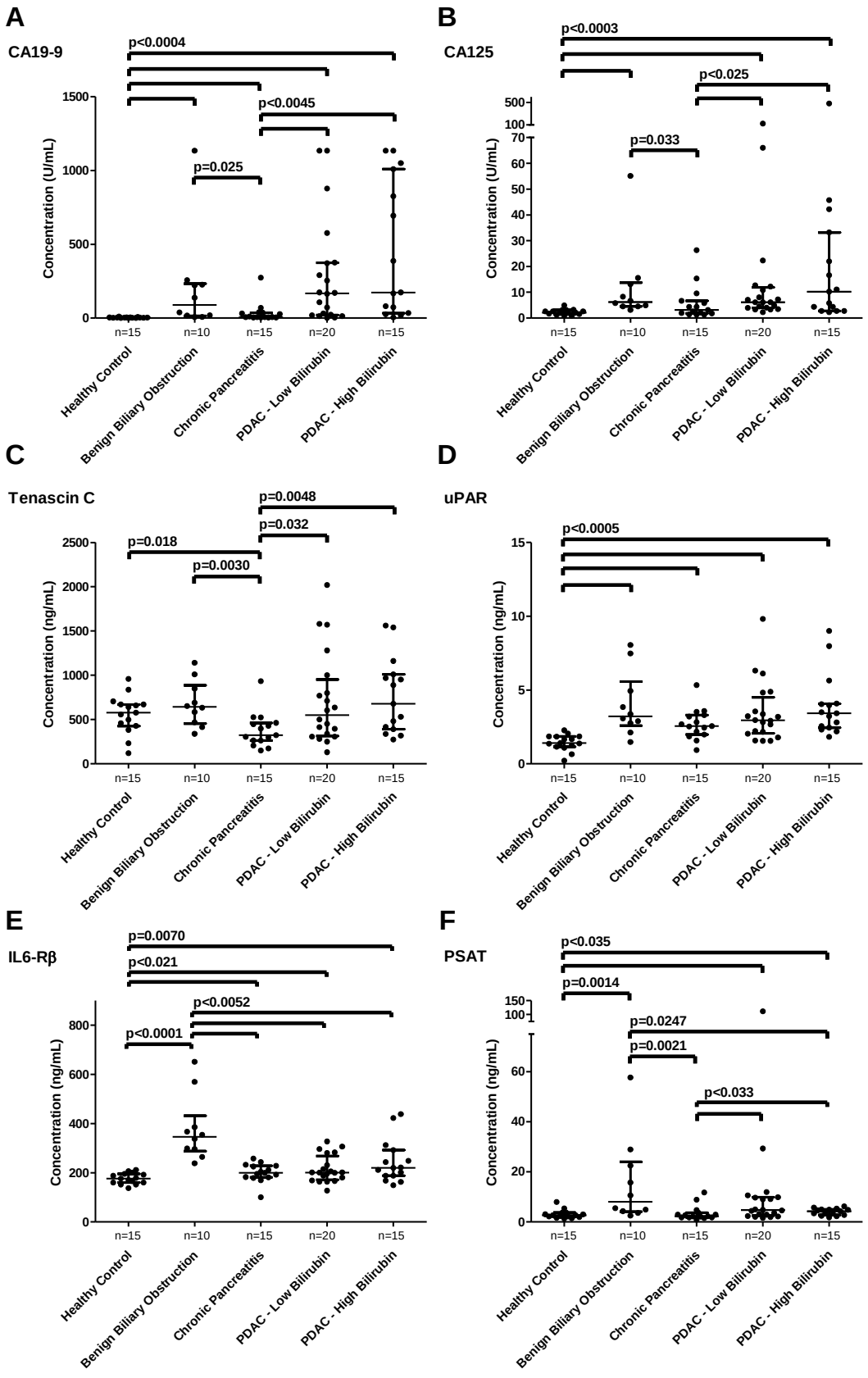

Figure 2-3. Several serum biomarkers are required for discriminating PDAC from related disorders. Univariate analysis was performed on 81 proteins quantified by Luminex assay in the sera of healthy controls and patients with PDAC, chronic pancreatitis and benign obstructive jaundice. Examples are shown of proteins showing aberrant expression in PDAC cases compared with benign control groups. Error bars display median and interquartile range, p values calculated by Mann Whitney U.

2.3.6 Logistic regression analysis identifies potential biomarkers of PDAC

All 81 proteins were entered into a stepwise logistic regression, performed using JMP's minimum corrected Akaike Information Criterion (AIC) procedure to select the best fit model of protein biomarker combinations, generating models to classify two patient sample groups: PDAC versus CP and benign obstructed jaundice versus obstructed PDAC.

For PDAC versus CP the procedure yielded five proteins to fit the model: CA19-9, TNC, receptor tyrosine-protein kinase erbB-3 (ErbB3), hepatocyte growth factor (HGF) and placenta growth factor (PlGF). The ROC curve from this combination yielded an AUC of 0.99, indicating a very high degree of accuracy.

For benign obstructed jaundice vs obstructed PDAC three proteins were selected: IL-6Rβ, uPAR and urokinase-type plasminogen activator (uPA). The ROC curve for this combination yielded a similarly high AUC of 0.97.

While the ROC analysis of these models would indicate accurate classification of the patient samples, it is highly likely that they contain too many independent variables for the sample size of this study, and as a result the models are overfit[126]. A common rule applied to logistic regression analyses when selecting sample size is to ensure there are at least 10 events per predictor variable[126,127]. Subsequent work has suggested this may be too conservative, with a range of 5-9 events per parameter suggested to be acceptable though caution should be taken when interpreting results[126,128]. Either way, with the performed analyses based on a smallest group sample size of 15 and 10 patients respectively, it would be overoptimistic to consider a model with greater than two proteins to be accurate.

The proteins selected for each model were examined to see which were contributing the greatest effect. From the PDAC versus CP model only TNC, CA19-9 and ErbB3 showed significant differential expression in PDAC sera when tested by Mann Whitney U, suggesting these were the markers classifying the bulk of the samples. In the case of ErbB3, significance was not retained when PDAC samples were classified by jaundice-status ($p=0.28$, CP vs. obstructed PDAC). ROC analysis of TNC and CA19-9 demonstrated encouraging accuracy in classifying samples, with an improved AUC when both markers were used in combination (Figure 2-4A).

From the benign obstructed jaundice vs obstructed PDAC model both IL-6Rβ and uPA were significantly upregulated in benign obstructed jaundice cases compared to PDAC. ROC analysis indicated both markers performed better than CA19-9 alone, with IL-6Rβ having the superior AUC overall and uPA proving more sensitive at the cost of specificity (Figure 2-4B).

With the aim of confirming the diagnostic utility of these biomarkers for PDAC, three proteins were selected for validation in independent sample sets: IL-6Rβ, TNC and PSAT. IL-6Rβ and TNC were selected based on performances in the relevant logistic regression analyses, while PSAT was selected based on its ability to discern some PDAC patients from both CP and benign obstructive jaundice patients in the discovery cohort. Work by other members of the group examining the most promising biomarker from the analysis, CA19-9, in serum was already ongoing before this work was undertaken.

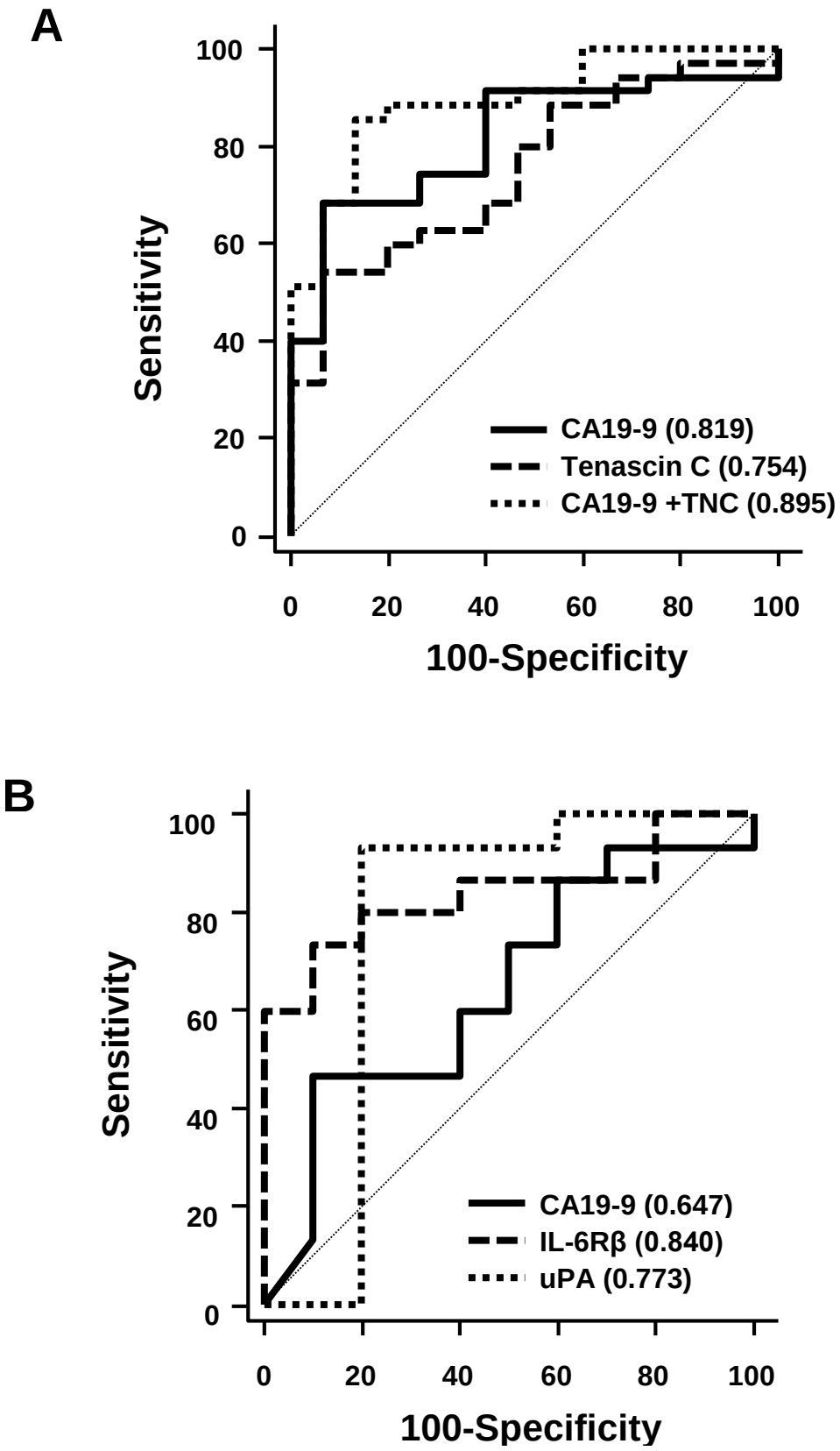

Figure 2-4 ROC curve analysis of promising markers' diagnostic performance. Serum samples from A) chronic pancreatitis (n=15) vs. PDAC (n=35) and B) benign obstructive jaundice (n=10) vs. obstructed PDAC (n=15) cases were classified by protein expression to assess diagnostic accuracy. Area under the curve (AUC) is displayed in brackets. CA19-9 and TNC combination determined using a logistic regression model.

Validation of discovery markers

2.3.7 Independent assay confirmation of IL-6Rβ, TNC and PSAT

In order to test the validity of the initial findings of the Myriad Rules-based Medicine multiplex analysis, ELISA assays were undertaken individually for IL-6Rβ, TNC and PSAT on the same UoL serum samples as were sent for assay to Myriad RBM. Mann Whitney U analysis confirmed the original observations for TNC and IL-6Rβ from the multiplex analysis, but the results were not reproducible for PSAT (Figure 2-5). TNC was significantly upregulated in PDAC cases compared with CP patients, and showed a strong positive correlation with the multiplex results (Figure 2-5A). Similarly, IL-6Rβ concentration measured by ELISA also demonstrated good correlation with the multiplex data, and the upregulation in benign obstructed jaundice cases compared with obstructed PDAC was again observed (Figure 2-5B). In contrast, PSAT measured by ELISA showed no correlation with the original data and consequently no difference was observed between PDAC patients and either CP or benign obstructive jaundice cases (Figure 2-5C).

An attempt was made at semi-quantitative analysis for PSAT using densitometric immunoblotting with a separate monoclonal antibody, probing serum samples at the high and low ends of the concentration spectrum established by the multiplex measurements, but no correlation was observed (Figure 2-6). It is possible that the antibody used for the multiplex analysis binds a particular component of the PSAT protein that is informative in this context, but as neither the ELISA nor the immunoblotting could reproduce the original results no further validation of PSAT was undertaken.

As the commercial ELISA kits suitably reproduced the results for IL6-Rβ and TNC, the analysis was subsequently extended to measure the proteins in an independent cohort of human serum samples.

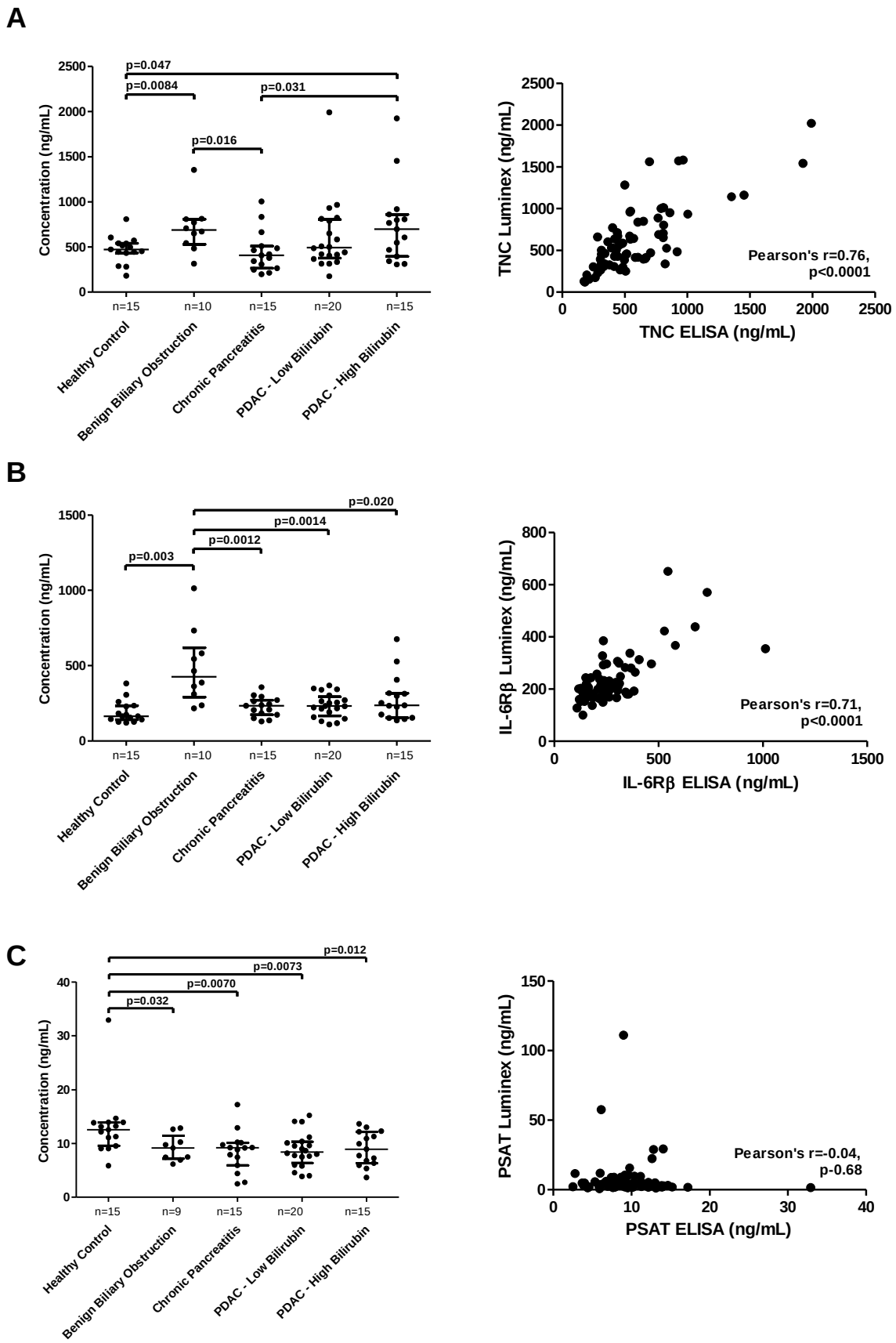

Figure 2-5. Independent assay confirmation of biomarkers of interest. Concentrations of A) tenascin C, B) IL-6Rβ and C) PSAT in the discovery UoL serum set were determined by ELISA. Measurements were compared to the original Luminex data to assess reproducibility. Error bars display median and interquartile range, p values calculated by Mann Whitney U.

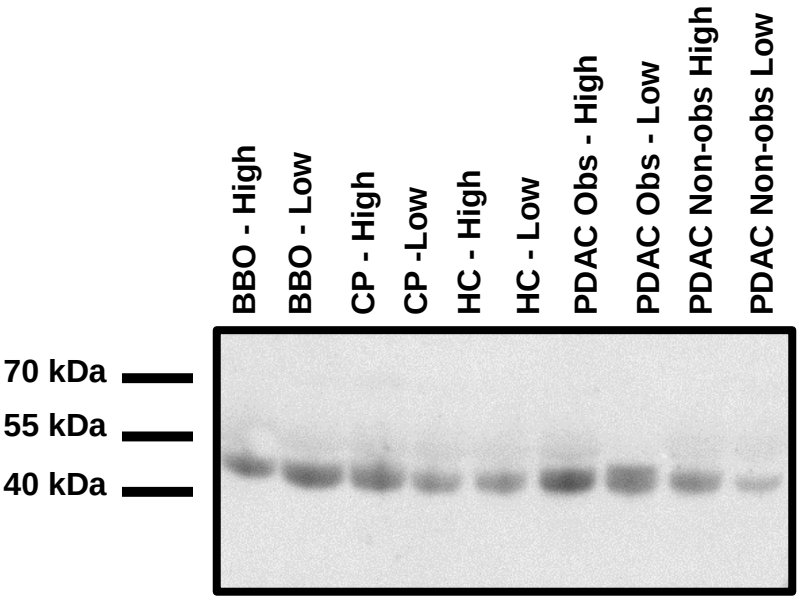

Figure 2-6. PSAT detected by immunoblotting in UoL serum samples. Pairs of serum samples were selected from each disease group. Samples with the highest and lowest PSAT concentration were chosen as measured by Myriad RBM to test for agreement.

Abbreviations: BBO – benign biliary obstruction, CP – chronic pancreatitis, HC – healthy control, PDAC – pancreatic ductal adenocarcinoma, Obs - obstructed

2.3.8 Measurement of IL-6Rβ and TNC in an independent cohort of serum samples

ELISA analysis for IL-6Rβ and TNC was repeated in a separate cohort of serum samples also collected by the University of Liverpool (Table 2.4). All conditions and protocols were consistent with those performed with the discovery sample set.

Table 2.4. Patient characteristics of diagnosed PDAC serum samples and controls with related disorders

		PDAC non-obs	PDAC-obs	BBO	CP	HC
n		35	52	29	50	36
Median age (range)		70 (51-83)	65 (45-85)	70 (23-86)	53.5 (23-78)	39 (22-77)
Sex	F/M	20/15	28/24	13/16	17/33	28/8

Abbreviations: PDAC – pancreatic ductal adenocarcinoma, BBO – benign biliary obstruction, CP – chronic pancreatitis, HC – healthy control, obs – obstruction

Unfortunately, the significant upregulation of IL-6Rβ in benign obstructed jaundice compared with obstructed PDAC cases observed in the discovery cohort was not observed in the validation set (Figure 2-7A). While IL-6Rβ concentration was still relatively high in the benign obstructive jaundice cases, a high enough proportion of patients in the obstructed PDAC group had similar concentrations, rendering IL-6Rβ an unsuitable marker for benign obstructed jaundice distinct from obstruction in PDAC.

More promisingly, Mann Whitney U analysis of TNC in the validation cohort revealed a repeat of the pattern observed in the discovery cohort, with significant upregulation in PDAC cases compared to CP (Figure 2-7B). Thanks to work from other members of the group: Drs Claire Jenkinson, Victoria Shaw, Sarah Tonack and Mehdi Jalali, CA19-9 concentrations measured by ELISA were available for 34 of

the 65 PDAC and 19 of the 35 CP samples analysed in this cohort. ROC analysis of these cases revealed TNC had greater accuracy than CA19-9 in distinguishing PDAC from CP patients, with a combination of the two markers providing the best AUC (Figure 2-8). The reproducibility of this finding in an independent cohort of serum samples suggests TNC may be a suitable biomarker in distinguishing patients with PDAC from those with CP, and is a candidate for entry into a panel of biomarkers that together would be specific and sufficiently sensitive for diagnosis of PDAC.

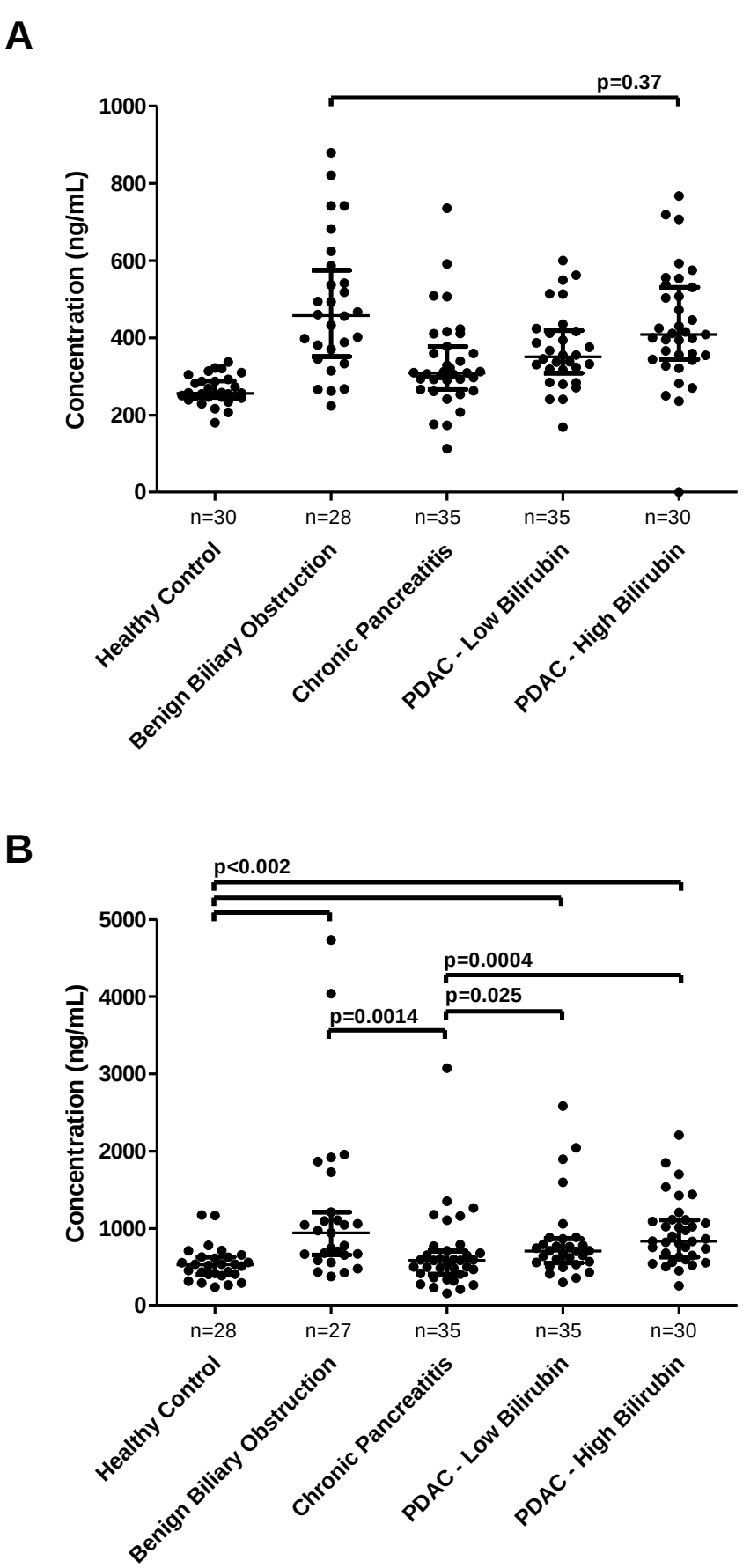

Figure 2-7. Serum IL-6Rβ and tenascin C in an independent cohort of serum samples. Concentrations of A) IL-6Rβ and B) tenascin C in an independent UoL serum set were determined by ELISA. Error bars display median and interquartile range, p values calculated by Mann Whitney U.

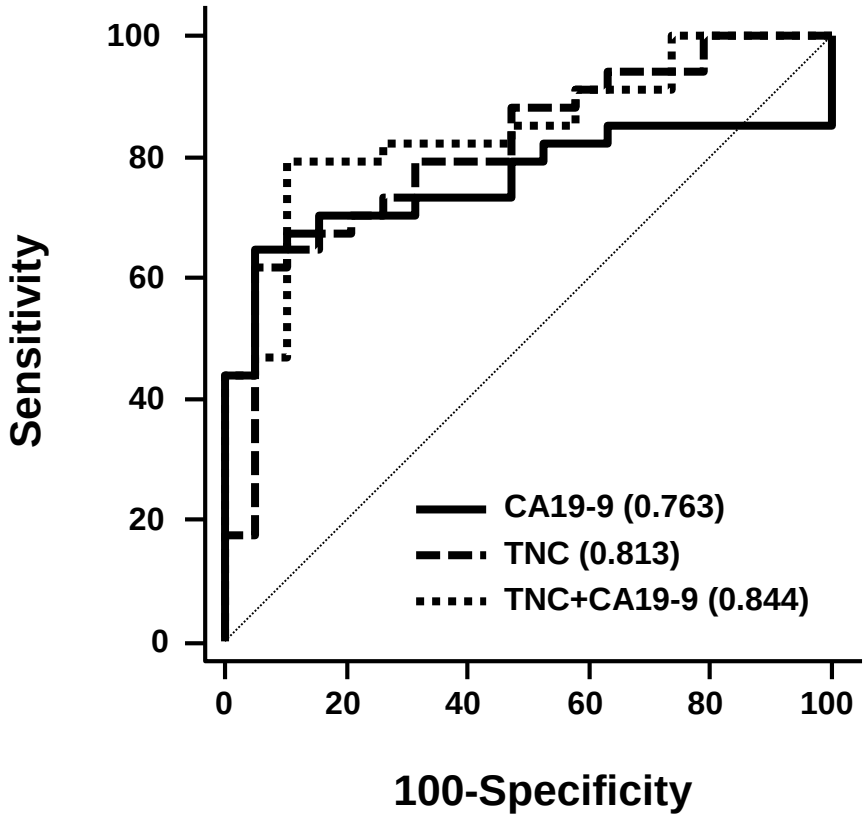

Figure 2-8. ROC curve analysis of CA19-9 against TNC in the validation cohort. Serum samples from patients with chronic pancreatitis (n=19) and PDAC (n=34) were classified by CA 19-9 and TNC concentration to assess diagnostic accuracy in the independent UoL serum cohort. Area under the curve (AUC) is displayed in brackets. CA19-9 and TNC combination determined using a logistic regression model.

2.4 Discussion

This work had a number of phases. The initial phase involved subjecting serum samples from both pre-diagnosis and already diagnosed subjects to analysis for the levels of 101 cancer-associated analytes of the Myriad Rules-Based Medicine Human Oncology MAP. In the second phase, validation of potentially useful candidates (University of Liverpool, cohort only) was undertaken in the same samples as used in the original Myriad analysis. Analytes surviving this analysis were taken to a third phase of validation in independent samples from the University of Liverpool.

In the pre-diagnostic cohort, CA125 and CA19-9, stood out as having the clearest relationship with time to diagnosis. Indeed, these promising findings confirmed results from work our collaborators were undertaking, and they have since extended the analysis to include other samples from the UKCTOCS collection, demonstrating that both markers show sensitivity up to two years prior to diagnosis[129].

Two other proteins that emerged with potential to discriminate pancreatic cancer from controls were CEA and AFP. In the case of both CEA and AFP, increases in median PDAC serum concentration were modest. CEA concentration in healthy control samples had low variation (range: 0.39-2.84 ng/mL), suggesting setting a threshold for cancer detection may be possible. CEA serum concentration as an identifier of colorectal cancer has been extensively studied and is reported to be highly specific, supporting this conclusion[94]. However, as a marker it has poor sensitivity and has been deemed unsuitable for mass screening.

AFP had larger variability in the healthy control samples and the apparent increase in median serum concentration as time to diagnosis approached zero was skewed by two patients with serial sample measurements, who had consistently high levels in

the four years prior to diagnosis. This raises the possibility that AFP may be able to identify certain patients with PDAC at earlier time points than current diagnostic methods can provide, and is a potential candidate for further investigation in independent serum samples. Unfortunately, one of the great limitations of the study, especially with respect to UKCTOCS samples was very low number of samples sent for analysis. Moreover, I did not validate the markers identified using independent samples from this set.

The University of Liverpool cohort offered the opportunity to examine for biomarker specificity. While no single marker showed up regulation or down regulation unique to the pancreatic cancer group, other interesting observations emerged, such as the identification of tenascin C as potential marker that can distinguish chronic pancreatitis from pancreatic cancer. The performance of this marker, withstood validation in an assay independent of that used by Myriad Rules-based Medicine. Having established a reliable method of testing this marker, it was important to repeat the measurements on an independent cohort of patient samples. Biomarkers measured in patients may fail to replicate initial findings in separate cohorts due to variability in ages, sex and race unaccounted for in the relatively small number of samples collected from such complex backgrounds[130]. Encouragingly, the levels of tenascin C remained significantly lower in chronic pancreatitis patients than in any other group in an independent validation set.

3 TENASCIN C IN THE PANCREATIC CANCER AND CHRONIC PANCREATITIS TISSUE MICROENVIRONMENT

3.1 Introduction

As described in Chapter 2, a commercial Luminex-based platform implemented by Myriad RBM with subsequent validation using ELISA analysis led to the identification of tenascin C as a potential biomarker for distinguishing PDAC patients from patients with chronic pancreatitis. Here I sought to determine whether this observation corresponded with TNC expression in the tissue microenvironment of pancreatic tissue from PDAC and CP patients. Staining for TNC protein and mRNA transcripts in whole tissue expression was performed to seek insight into the origin of secreted TNC, supplemented with data from primary cultured cancer-associated fibroblasts. Finally, TNC expression on tissue microarrays constructed from CP and PDAC specimens was assessed to directly compare circulatory TNC with localised pancreatic expression.

3.2 Materials and methods

3.2.1 Immunohistochemical staining for TNC on PDAC and CP tissue

IHC was performed for TNC using the same monoclonal antibody, described in section 0, that was used to coat the 96-well plate of the ELISA from the serum analysis (1:200, clone 4C8MS, cat. no. NB110-68136, Novus Biologicals, UK). Staining was performed on whole sections from PDAC and CP tissue specimens. Paraffin embedded blocks were cut into 4µm sections and mounted on histology slides (cat. no. 1014356190, Thermo Scientific, UK). After drying overnight at 40ºC, the sections were deparaffinised and antigen retrieval performed through boiling at 95ºC in pH 9 antigen retrieval buffer (cat. no. K8004, Dako, UK) using a PT Link

(cat. no. PT10126, Dako, UK). Tris buffered saline (TBS, 2.4g Tris base, 8.8g NaCl in 1L dH_2O, pH7.6) was prepared and used to make a 0.1% TBS Tween 20 solution (TBST). Sections were washed with TBST, leaving for three 1-minute incubations, before drying carefully with tissue and coating with peroxidase blocking reagent (Dako, UK) then leaving to incubate at room temperature for 10 minutes. Sections were washed again with TBST and dried, before covering with tenascin C antibody diluted 1:200 in antibody diluent (cat. no. S0809, Dako, UK) and leaving to incubate for 1 hour at room temperature. After a further wash and dry, labelled polymer anti-mouse secondary antibody was added (Dako, UK) and incubated for another hour at room temperature. Another wash followed, before the addition of DAB+ chromogen (Dako, UK) for ten minutes at room temperature to visualise bound antibody. After a final wash with TBST, the sections were left to rest in distilled water before placing the slides in Gill III haematoxylin (cat. no. 3801540BBE, Leica Microsystems, UK) to counterstain for 30 seconds. Slides were subsequently washed for 5 seconds in dH_2O, before rinsing in 0.25% hydrochloric acid for 5 seconds then placing in 2% ammonium hydroxide for a further 5 seconds. Slides were then placed in 90% ethanol for 1 minute, followed by 100% ethanol for a further 2 minutes, replacing the ethanol after the first minute. Finally, the slides were placed in xylene for two 1 minute incubations in preparation for mounting in DPX (cat. no. 06522, Sigma-Aldrich, UK).

All sections were qualitatively reviewed by specialist histopathologist, Professor Fiona Campbell.

3.2.2 Haematoxylin and eosin staining

Whole sections matched to those stained for TNC by IHC were deparaffinised in xylene and rehydrated by incubation for 2x30 seconds in serially decreasing ethanol/dH_2O solutions from 100% to 95% to 70%, before rinsing in tap water. Slides were then incubated in haematoxylin for 10 minutes, rinsed in running tap water and agitated in 0.25% HCl/dH_2O for 5 seconds. A further rinsing in tap water followed, before a 30 second agitated incubation in Scott's tap water (1g potassium hydrogen carbonate, 10g magnesium sulphate in 500mL dH_2O). After another rinse, slides were agitated in 100% ethanol for 30 seconds then placed in eosin Y (cat. no. 3801600E, Leica Microsystems, UK) to incubate for 2 minutes. The slides were then agitated in 100% ethanol for 1 minute, followed by two 30 second washes in fresh ethanol and three 30 second agitations in fresh xylene before mounting in DPX.

3.2.3 *In situ* hybridisation for TNC mRNA in PDAC and CP tissue specimens

In situ hybridisation (ISH) was performed on serial tissue sections matched to those stained for TNC by IHC, using a commercial assay platform with probes specific for TNC (RNAscope® Reagent Kit, Advanced Cell Diagnostics, USA), visualised by DAB staining (cat. no. 310033, Advanced Cell Diagnostics, USA). The assay was performed according to manufacturer's instructions. In brief, sections were deparaffinised in xylene and ethanol before permeabilisation and hybridisation of probes targeted to TNC RNA. A series of amplification steps followed through further hybridisation before a final addition of HRP-conjugated labelled probe was visualised by DAB chromogen reaction[131]. The amplification step enables visualisation of up to a single RNA molecule, with the number and size of punctate dots indicating the extent of RNA expression in each cell. Each run was

accompanied with sections probed for peptidylprolyl isomerase B (PPIB) as a positive control and dihydrodipicolinate reductase (dapB), a bacterial enzyme, as a negative control.

3.2.4 Quantitative real-time PCR for TNC

Quantitative real-time PCR (qPCR) was performed for TNC mRNA. cDNA was obtained from human fibroblasts cultured from different primary pancreas specimens with pathologies such as PDAC and CP, kindly provided by Dr Lawrence Barrera-Briceno who also assisted with the qPCR experiments. All reactions were performed in a LightCycler® 480 (Roche Diagnostics Ltd., UK). The primer sequences used for TNC (Invitrogen™, Thermo Scientific, UK) are detailed in Table 3.1. Three housekeeping genes were also tested: GAPDH, β-actin and RPLP0, (proprietary sequences, Primer Design Ltd., UK). Real-time PCR reactions were carried out in a 96-well plate in total volumes of 10µL per well, consisting of 10ng of cDNA for TNC and the housekeeping gene GAPDH plus 5µL LightCycler® 480 SYBR Green I Master mix (cat. no. 04887352001, Roche Diagnostics Ltd., UK). 500nM of forward and reverse primers for TNC and GAPDH were added. Sample reactions were run beginning with a 5 minute pre-incubation step at 95ºC, followed by 45 cycles of denaturing for 10 seconds at 95ºC, 10 seconds at 60ºC for annealing and 10 seconds at 72 ºC for extension. Reactions were carried out in triplicate for each sample. Relative quantification was performed using the comparative CT method, using a Student's t test to compare the two groups. CT values for all three housekeeping genes were consistent between CP and PDAC samples, so GAPDH was selected as the reference gene.

Table 3.1. Primers used for RT-PCR for TNC

		Sequence (5'-3')
TNC	Forward	ACCGCTACCGCCTCAATTAC
	Reverse	GTTGTCAACTTCCGGTTCGG

Abbreviations: TNC – tenascin C

3.2.5 Immunohistochemical staining for TNC on tissue microarrays of PDAC and CP patients

To compare the differences in TNC expression in PDAC and CP tissue on a larger scale, three TMAs were stained. Two of these consisted of FFPE tissue specimens from PDAC samples, with three cores sampled per patient, and were constructed by Dr Katharine Hand and Mrs Elizabeth Garner as part of a separate project. The third consisted of cores collected from fibrotic regions of CP tissue specimens as determined by a specialist histopathologist (Professor Fiona Campbell). This TMA was designed and constructed with the assistance of Mr Neal Rimmer, with four cores sampled per patient.

After staining, cores were scored independently alongside Professor Campbell, noting whether the fibrotic stroma demonstrated positive staining for TNC. Where there were disagreements, a consensus was reached. Patients with less than two suitable cores for scoring were excluded from the analysis.

3.2.6 Statistical analysis

All statistical analyses were performed with JMP (Version 11, SAS Institute Inc., USA). Differences in serum biomarker concentration were tested between groups

using Mann Whitney U tests. Clinicopathological variable associations with data obtained from the TMAs were compared using Mann Whitney U, Pearson's chi-squared and Fisher's exact tests as appropriate. Kaplan-Meier curves with log-rank tests were used to test the difference in overall survival between groups, where appropriate.

3.3 Results

3.3.1 TNC is expressed in the tumour and stromal compartment of the PDAC microenvironment

FFPE whole sections from PDAC and CP specimens were stained for TNC to assess expression within the diseased pancreas microenvironment. Heterogeneous staining was observed across and within PDAC patient sections, with strong staining occasionally observed within the tumour and stromal compartments. By contrast strong staining of the fibrotic components of CP was rarer, and was rather localised to periductal regions (Figure 3-1, left column). Strong staining of benign and malignant ductal epithelia was occasionally observed in CP and PDAC patients respectively, but there were also regions of strong staining in the desmoplastic stroma where the neighbouring epithelia remained negative.

As high levels of circulatory TNC in PDAC patients may be related to high intratumoral protein expression, *in situ* hybridisation (ISH) for TNC was performed on tissue sections matched to those for which IHC was undertaken, in order to identify the cellular origin of TNC in PDAC and CP patient tissue. Areas of protein expression confined to ductal epithelia had low mRNA expression, with no expression observed in the surrounding stroma (Figure 3-1, top row). Surprisingly, in areas of strong stromal protein expression without corresponding tumour expression, mRNA expression was often limited to isolated tumour cells, (Figure 3-1, second row from top), though this pattern varied across the tumour. In some areas only scattered cells with a fibroblastic phenotype appeared to express TNC mRNA, with no adjacent tumour expression (Figure 3-1, second row from bottom).

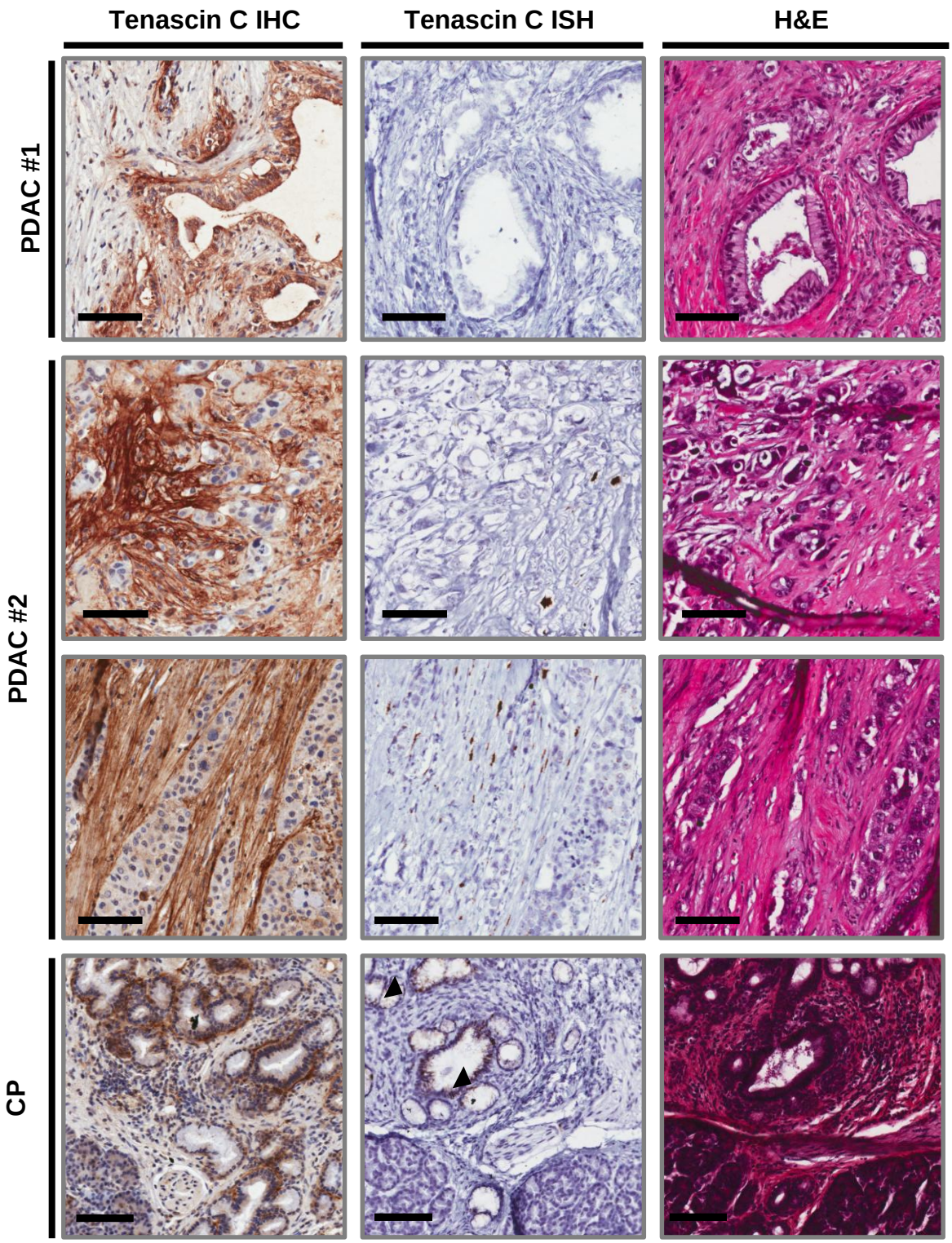

Figure 3-1. Tenascin C expression in PDAC and chronic pancreatitis. Immunohistochemistry and *in situ* hybridisation were performed for TNC in whole tissue sections from patients with PDAC and chronic pancreatitis. Arrowheads indicate the presence of strong mRNA expression in ductal cells. TNC expression varied within and between PDAC patient tissue specimens, observed in both stromal and ductal epithelial compartments of the tissue microenvironment. Stromal and ductal expression was also apparent in chronic pancreatitis. Scale bars = 100µm.

In the CP cases, areas with positive benign ductal epithelia and surrounding desmoplasia had mRNA expression confined to the ductal compartment in a similar manner to that seen in some areas of PDAC. Though other CP cases were also probed for mRNA, the tissue sections were not suitably intact after processing to enable a comparison with the IHC-stained sections. This was due to the presence of calcified stones in the specimens, a common feature of CP, preventing clean cutting with a microtome, hampering the mounting of tissue sections to the slide and rendering them vulnerable to pieces breaking away. Consequently, further histological investigations comparing PDAC with CP were limited to TMAs so that areas of calcification could be deliberately avoided.

3.3.2 Tenascin C is significantly overexpressed in PDAC stroma compared to CP

TMAs containing tissue from patients with PDAC and CP were stained for TNC and scored based on expression in the stromal compartment of each disease type (Table 3.2). Of all 35 CP patients, only 5 (14%) were positive for TNC, compared with 32 (60%) of 53PDAC cases ($p<0.0001$, Pearson's chi-square). This observation compared favourably with real-time PCR data quantifying TNC mRNA in primary human fibroblasts isolated from resected CP and PDAC tissue. Relative quantification indicated an increase in TNC expression in PDAC-associated fibroblasts compared to CP-associated (mean fold expression change=1.83), though this did not reach statistical significance ($p=0.18$, Figure 3-2).

Table 3.2 Patient characteristics of TMAs stained for TNC.

		PDAC TMA #1	PDAC TMA #2	CP TMA
n		17	36	35
Age	Median	67	68	51
	(range)	(54-81)	(52-84)	(21-77)
Sex	F/M	11/6	16/20	19/16

Abbreviations: PDAC – pancreatic ductal adenocarcinoma, CP – chronic pancreatitis

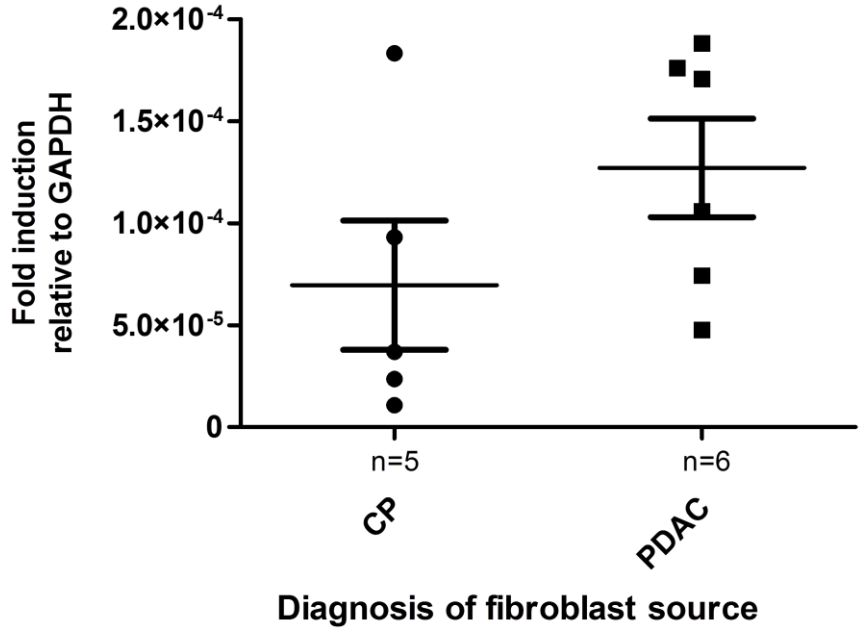

Figure 3-2. TNC mRNA expression in human fibroblasts isolated from resected pancreatic tissue from patients with CP and PDAC. Quantitative real-time PCR was performed for TNC, normalised to GAPDH. Error bars display the mean and standard error.

Twenty-nine patients across all three TMAs had matching serum samples analysed for TNC concentration. Interestingly, no direct relationship was observed between serum TNC concentration and positive stromal expression (p=0.96, Figure 3-3), which remained the case if patients were also split according to disease (p=0.83 and 0.48 for CP and PDAC, respectively).

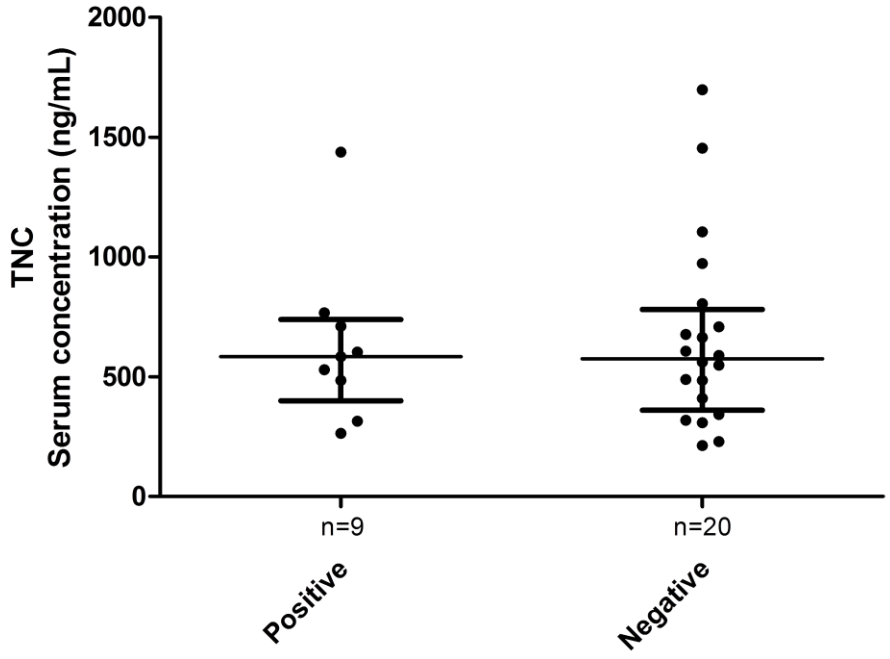

Figure 3-3. Concentration of serum TNC in PDAC and CP patients classified by protein expression in the tissue microenvironment. Error bars display median and interquartile range.

3.4 Discussion

The identification of tenascin C as a potential biomarker for PDAC compared to patients with chronic pancreatitis warranted further investigation, as circulating markers that can distinguish pancreatic cancer from chronic pancreatitis are sorely needed[92] .

This is because pancreatitis is a risk factor for PDAC, and the two conditions can present concurrently. We therefore sought to determine whether the tissue levels of TNC in pancreatic cancer and in pancreatic patients might explain the differences in the circulating levels of this protein. Of note, immunohistochemistry was performed for TNC using the same primary antibody used in the serum ELISA study, described in section 0. This was to ensure that the form of the TNC protein being measured matched that detected in the serum, as TNC has several splice variants thought to relate to certain clinical outcomes and may be associated with specific pathological contexts[132].

We observed variability in TNC expression suggesting a dynamic regulation of TNC within the PDAC microenvironment, where it can be produced and either secreted or retained by ductal epithelia and occasionally cells with a fibroblast phenotype.

Significantly, TNC expression was more frequently observed in patients with PDAC compared to patients with CP. This suggests that there may be a relationship between expression in pancreas tissue and the concentration of TNC in the circulation. Given the mRNA evidence that TNC can be produced in PDAC tumour cells and secreted into the surrounding stroma, it is possible that intratumoral TNC entering the

circulation could account for the higher serum levels observed in PDAC patients compared to CP. However, our analysis of serum TNC levels and pancreatic tissue levels failed to show any direct correlation. This suggests that while increased levels of circulatory and pancreas-localised TNC are observed in more PDAC patients than CP, the use of TMAs may not be suitable as a means of accurately quantifying tissue expression to relate to the systemic levels observed in the circulation. It is possible that the circulating TNC derives from tissues/organs other than the pancreas. TNC expression is thought to be low or absent in healthy adult tissues, with transient upregulation reported at sites of injury, with functional links to inflammation and tissue repair[132,133]. As TNC upregulation has been described at sites of skin, lung, cardiac and vascular injury there are a number of potential sites of origin for circulatory TNC. The fact that elevated serum TNC has been reported in patients with acute myocardial infarction also supports this[132,134]. With multiple splice variants of TNC thought to be functionally distinct, it is possible that the variants detected by the antibody used in this study may be more specific for PDAC compared to CP, despite both diseases involving inflammation of the pancreas.

4 EXAMINATION OF THROMBOSPONDIN-1, A PROMISING DIAGNOSTIC BIOMARKER FOR PANCREATIC CANCER, IN SERUM AND THE TUMOUR MICROENVIRONMENT

4.1 Introduction

Prior discovery work conducted by my research colleagues identified thrombospondin-1 (TSP-1) as a promising biomarker for early diagnosis in the UKCTOCS cohort. Drs Claire Jenkinson and Victoria Elliott quantified the levels of proteins in pooled serum samples by subjecting those samples to protein digestion using trypsin and tagging the resultant peptides with 8-plex isobaric tags for relative and absolute quantification (iTRAQ). Each pool contained serum from different disease categories and control groups, from 1) the UoL collection: PDAC (obstructed and non-obstructed), healthy control, benign biliary obstruction and chronic pancreatitis samples; and 2) from the UKCTOCS collection: 0-6 month and 6-12 month pre-diagnosis PDAC samples with matched controls. Unique tags labelled each group to enable relative quantification using mass spectrometry. This revealed thrombospondin-1 (TSP-1) as a promising candidate for early diagnosis, with significantly reduced fold-changes in the 0-6 month and 6-12 month PDAC cases compared to healthy controls and in the UoL sample healthy controls compared to PDAC[135].

Validation of TSP-1 levels in independent samples from the UoL and UKCTOCS cohorts was undertaken by Drs Claire Jenkinson and Victoria Elliott. Quantification was performed using multiple reaction monitoring (MRM), a mass spectrometry-based method used for absolute quantification in serum. Two target peptides were selected, unique to TSP-1, with three optimum transitions chosen and measured in trypsinised peptide digests derived from single serum samples. These measurements were compared with standard curves prepared from known concentrations of the

selected peptides, diluted in a peptide digest from human serum. MultiQuant™ software (Version 2.1) was used to analyse the peak area for each peptide transition and calculated concentrations of TSP-1 per sample using software-generated standard curves. Conventionally, studies examining circulatory proteins use ELISAs to determine concentration, including those investigating TSP-1 in the context of other cancers[136,137]. As MRM is a relatively new technique, here I used the more conventional ELISA and immunoblotting approaches to assess TSP-1 levels, and in doing so, to validate the MRM method established here. Moreover, I also assessed TSP-1 levels in sera derived from a genetically engineered mouse model for PDAC, and performed IHC for the assessment of TSP-1 levels in pancreatic cancer tissue.

4.2 Materials and methods

4.2.1 Serum ELISA for TSP-1

Pre-diagnosis PDAC serum samples from the UKCTOCS collection were selected from 27 patients up to 2 years prior to diagnosis, along with 27 matched controls for the quantification of TSP-1 by ELISA (cat. no. DTSP10, R&D Systems, UK). The assay was performed according to manufacturer's instructions, with all samples run in duplicate and accepted for further analysis if the coefficient of variation was less than 10%. Average readings for the duplicates were calculated.

4.2.2 TSP-1 knockdown

Human foreskin fibroblast cells (HFF, American Type Culture Collection, UK) were cultured at 37ºC in a 5% CO_2 atmosphere, in Dulbecco's Modified Eagle's Medium (DMEM, Life technologies, UK) supplemented with 10% foetal bovine serum (FBS, Life technologies, UK) and 1% L-glutamine (Sigma-Aldrich, UK). Cells were passaged every 2-3 days when confluence reached ~80%.

Prior to short interfering RNA (siRNA) treatment, 70,000 cells per well were seeded in a 6-well tissue culture plate (Appleton Wood, UK). After 24 hours, the cells were ready for transfection at a confluence of ~40%. SiRNA for TSP-1 (Cat no. D-0197-01-0002, Thermo Scientific, UK) was mixed in 200µL Opti-MEM I (Life technologies, UK), and incubated at room temperature for five minutes alongside a separate solution of 200µL Opti-MEM containing 4µL Lipofectamine 2000 (Life technologies, UK). The two solutions were mixed in equal volumes and left to incubate at room temperature for a further 30 minutes. 400µL of this solution was added dropwise to each well to make a final concentration of 30nM. Each siRNA treated well was run alongside three control groups: DMEM only, RISC-free siRNA (Cat. no. D-001220-01-05, Thermo Scientific, UK) and a non-targeting siRNA pool (cat. no. D-001810-10-20, Thermo Scientific, UK). Following treatment, cells were incubated for 72 hours at 37ºC before protein extraction.

4.2.3 Protein extraction

RIPA buffer (150mM sodium chloride, 1% Triton X-100, 0.5% sodium deoxycholate, 0.1%SDS, 50mM Tris pH 8.0) was prepared and mixed with a protease inhibitor cocktail (cat. no. 11 836 170 001, Roche Diagnostics GmbH, Germany) to complete the cell lysis buffer. Cells were washed with cold phosphate buffered saline (PBS, Sigma-Aldrich, UK) and 120µL lysis buffer added before cell removal from the plate using a cell scraper. The cell suspensions were mixed and incubated on ice for 5 minutes, repeating this process twice further. The lysate was then centrifuged at 17000g for 10 minutes at 4ºC. The supernatant was subsequently collected and stored at -80ºC for future use.

4.2.4 Protein quantification and western blot analysis

In preparation for western blot analysis, the total protein concentration of the cell samples were determined with a bicinchoninic acid (BCA) assay (cat. no. 23225, Thermo Scientific, UK) according to manufacturer's instructions. A 5x concentrated stock of reducing sample buffer (1g SDS, 5mL glycerol, 300mM Tris, 5mg bromophenol blue in 10mL dH_2O) was prepared and mixed with a 1M solution of dithiothreitol (DTT) in a ratio of 3:2 to produce a loading buffer. Sample volumes containing 20µg total protein were each mixed with 3µL of loading buffer and enough 1x reducing sample buffer to equalise the total volume between samples. Samples were then incubated at 90ºC for 15 minutes, cooled to room temperature and centrifuged at 17000g for 10 seconds. Samples were loaded into precast acrylamide gels (cat. no. 4569034, Bio-Rad Laboratories, UK) in running buffer (3.03g Tris base, 14.4g glycine, 1g SDS in 1L dH_2O) before running the gel at 270V for 30 minutes.

Semi-dry transfer of the proteins from the gel to a PVDF membrane (cat. no. 1704156, Bio-Rad Laboratories, UK) was performed using a Trans-Blot Turbo system (Bio-Rad Laboratories, UK) using the Mixed MW protocol (1.3A, up to 25V, 7 minutes). TBS (2.4g Tris base, 8.8g NaCl in 1L water, pH7.6) was mixed with Tween 20 (TBST, Sigma-Aldrich, UK), with 1mL Tween per 1L TBS. A blocking solution of 5% milk/TBST was prepared and used to block the PVDF membranes for 2 hours at room temperature. This was followed by overnight incubation at 4ºC with anti-TSP-1 monoclonal antibody diluted 1:400 in 5% milk/TBST.

Membranes were then washed with TBST every 10 minutes for one hour prior to a further incubation with anti-mouse HRP-bound immunoglobulins (cat. no. P0447, Dako, UK) diluted 1:3000 in 5% milk/TBST for 1 hour at room temperature. A further hour of 10 minute-interval washes followed, before a 3 minute incubation with Western Lightning Plus (cat. no. NEL105001EA, Perkin Elmer, UK) chemiluminescent substrate and visualisation of antibody-bound protein using x-ray film (cat. no. 12715325, Sigma-Aldrich, UK). To test for equal loading, membranes were washed in TBST and probed with a monoclonal anti-β-actin antibody (cat. no. A5441, Sigma-Aldrich, UK) diluted 1:10000 in 5% milk/PBST for 30 minutes, before washing and probing with secondary antibody as before.

4.2.5 Semi-quantification of TSP-1 in human and murine serum by western blotting

Serum samples from the UKCTOCS and UoL cohorts were also analysed by western blotting using the protocol described in Chapter 4 Section 4.2.4, with the exception that a fixed volume (4µL) of sample per well was used instead of a fixed quantity of protein. This was to ensure the density of the bands observed were proportional to

the amount of TSP-1 protein per unit volume, to make readings comparable with concentrations derived by quantitative methods.

With the assistance of Dr Claire Jenkinson, samples were run on 15-well gels (cat. no**.** 4569036, Bio-Rad Laboratories, UK) alongside pooled healthy control serum, loaded in 2µL, 4µL and 6µL volumes to act as standards for each gel. If the standards demonstrated a good linear fit after measurement (R>0.95) the gel was accepted and samples were normalised to the 4µL standard reading to allow comparisons across gels. All samples were run and analysed so that readings were available at least in triplicate. Densitometry was performed using ImageJ (version 1.45) to give a quantitative reading for each sample (Figure 4-1).

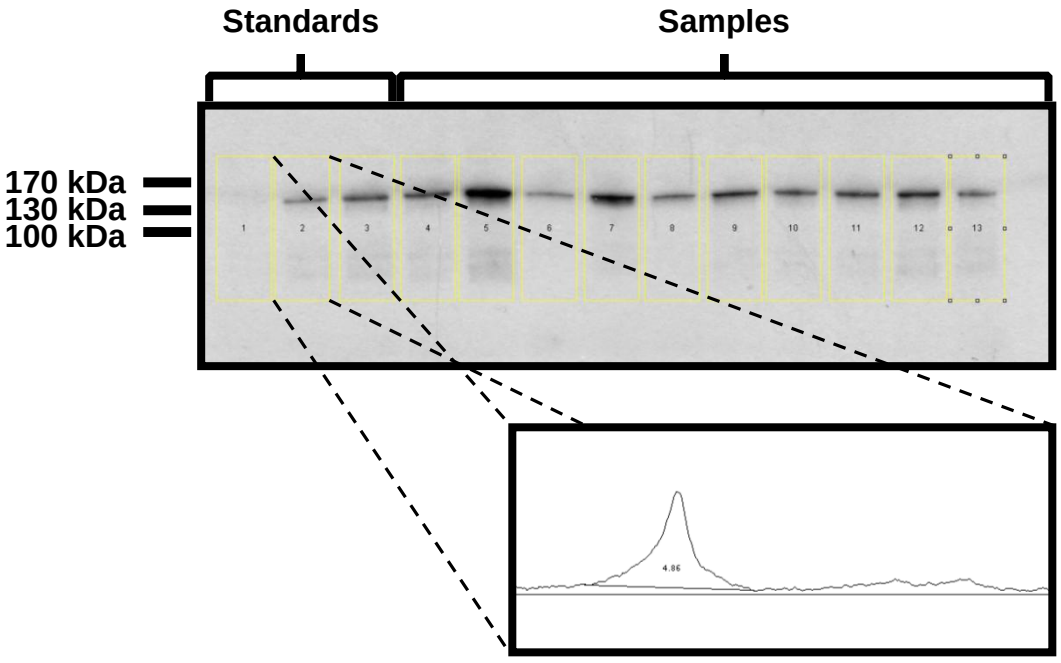

Figure 4-1. Overview of densitometric measurement of band intensity using imageJ. Shown is an example of a western blot for TSP-1, containing serum samples from the UKCTOCS collection. Each detectable band is measured as a peak, from which the background can be subtracted before the area under the peak is quantified.

4.2.6 Serum from LSL-Kras$^{G12D/+}$;LSL-Trp53$^{R172H/+}$;Pdx-1-Cre (KPC) and LSL-Trp53$^{R172H/+}$;Pdx-1-Cre (PC) mice.

Serum samples collected at the University of Cambridge from LSL-Kras$^{G12D/+}$;LSL-Trp53$^{R172H/+}$;Pdx-1-Cre (KPC) mice at different stages of PDAC, age-matched with LSL-Trp53$^{R172H/+}$;Pdx-1-Cre (PC) control mice were the kind gift of Professor David Tuveson. All mice were treated in accordance with institutional and European guidelines (Legislative Order No. 116.92). Blood was collected via cardiac bleed under isofluorane gaseous anaesthesia from 10 KPC and 9 PC controls (Table 4.1). Samples were allowed to clot for 2 hours at room temperature before centrifugation at 1000g for 20 minutes. Serum was then collected and snap frozen in liquid nitrogen prior to storage at -80ºC. Histological assessment confirmed the presence of PDAC and PanIN.

Table 4.1. Clinical characteristics of KPC mouse serum cohort.

		Normal pancreas	Low grade PanIN	PanIN III	PDAC
n		9	6	1	3
Median age/days (range)		66 (42-159)	53 (42-63)	172 (-)	157 (154-161)
Sex	F/M	9/0	6/0	1/0	3/0

Abbreviations: PanIN – pancreatic intraepithelial neoplasm, PDAC – pancreatic ductal adenocarcinoma

4.2.7 Confirmation of TSP-1 monoclonal antibody specificity by immunocytochemistry

The same monoclonal antibody used for western blotting (clone A6.1, cat. no. MA5-13398, Thermo Scientific, UK) was selected for immunohistochemical (IHC) staining to allow the direct comparison between serum and tissue TSP-1 expression. To confirm the specificity of the antibody when used for tissue staining, immunocytochemistry was performed on paraffin embedded HFF cells treated with siRNA for TSP-1 and control off-target siRNA as previously described. After 72 hours of treatment, cells were washed in PBS and harvested using a cell scraper before centrifugation at 200g for 10 minutes. The supernatant was discarded and the cell pellets stored at -80ºC ready for fixation. Formalin fixation and paraffin embedding (FFPE) of the pellets followed, kindly performed by Mrs Elizabeth Garner.

Embedded cell blocks were cut into 4µm sections and mounted on histology slides (cat. no. 1014356190, Thermo Scientific, UK). After drying overnight at 40ºC, the sections were deparaffinised and antigen retrieval performed through boiling at 95ºC in pH 9 antigen retrieval buffer (cat. no. K8004, Dako, UK) using a PT Link (cat. no. PT10126, Dako, UK). Tris buffered saline (TBS, 2.4g Tris base, 8.8g NaCl in 1L dH_2O, pH7.6) was prepared and used to make a 0.1% TBS Tween 20 solution (TBST). Sections were washed with TBST, leaving for three 1-minute incubations, before drying carefully with tissue and coating with peroxidase blocking reagent (Dako, UK) then leaving to incubate at room temperature for 10 minutes. Sections were washed again with TBST and dried, before covering with TSP-1 monoclonal antibody diluted 1:100 in antibody diluent (cat. no. S0809, Dako, UK) and leaving to incubate for 1 hour at room temperature. After a further wash and dry, labelled

polymer anti-mouse secondary antibody was added (Dako, UK) and incubated for another hour at room temperature. Another wash followed, before the addition of DAB+ chromogen (Dako, UK) for ten minutes at room temperature to visualise bound antibody. After a final wash with TBST, the sections were left to rest in distilled water before placing the slides in Gill III haematoxylin (cat. no. 3801540BBE, Leica Microsystems, UK) to counterstain for 30 seconds. Slides were subsequently washed for 5 seconds in dH_2O, before rinsing in 0.25% hydrochloric acid for 5 seconds then placing in 2% ammonium hydroxide for a further 5 seconds. Slides were then placed in 90% ethanol for 1 minute, followed by 100% ethanol for a further 2 minutes, replacing the ethanol after the first minute. Finally, the slides were placed in xylene for two 1 minute incubations in preparation for mounting in DPX (cat. no. 06522, Sigma-Aldrich, UK).

4.2.8 Immunohistochemical staining for TSP-1 on a tissue microarray of PDAC patients

A tissue microarray (TMA), constructed by Mrs Elizabeth Garner, consisting of tissue from 49 FFPE PDAC specimens was stained for TSP-1 using the same conditions as for the ICC. Two cores of tissue were mapped to the TMA per patient, with each core scored by a specialist histopathologist (Professor Fiona Campbell). Cores were scored as positive or negative based on observed staining in the tumour or stromal compartment.

4.2.9 Statistical analysis

All statistical analyses were performed with JMP (Version 11, SAS Institute Inc., USA). Differences in serum biomarker concentration were tested between groups using Mann Whitney U tests. Clinicopathological variable associations with data obtained from the TMAs were compared using Mann Whitney U, Pearson's chi-squared and Fisher's exact tests as appropriate. Log-rank tests were used to test the difference in overall survival between groups, where appropriate.

4.3 Results

4.3.1 Comparison of MRM and ELISA for analysis of TSP-1 in pre-diagnostic PDAC serum

ELISAs were performed on UKCTOCS pre-diagnosis PDAC cases and controls to compare with data obtained by MRM (Table 4.2). Comparing each time group with their respective controls, the median concentration of TSP-1 as measured by ELISA was consistently lower in each time group (Figure 4-2A), although this did not reach statistical significance. In contrast, the same samples analysed by MRM revealed significantly reduced concentration in pre-diagnosis PDAC patients in the 0-6 month category, with a trend observed in the pre-diagnosis cases up to 2 years prior to diagnosis (Figure 4-2B). This pattern was consistent with that observed in the original iTRAQ discovery work.

Table 4.2. UKCTOCS patient characteristics for samples measured by ELISA for TSP-1

	0-6 months		**6-12 months**		**12-24 months**	
	PDAC	Ctrl	PDAC	Ctrl	PDAC	Ctrl
n	8	8	8	8	11	11
Median age (range)	61.5 (53-73)	67.5 (56-73)	65 (53-74)	64 (52-76)	62 (52-71)	60 (51-73)

Abbreviations: PDAC – pancreatic ductal adenocarcinoma, Ctrl – healthy control

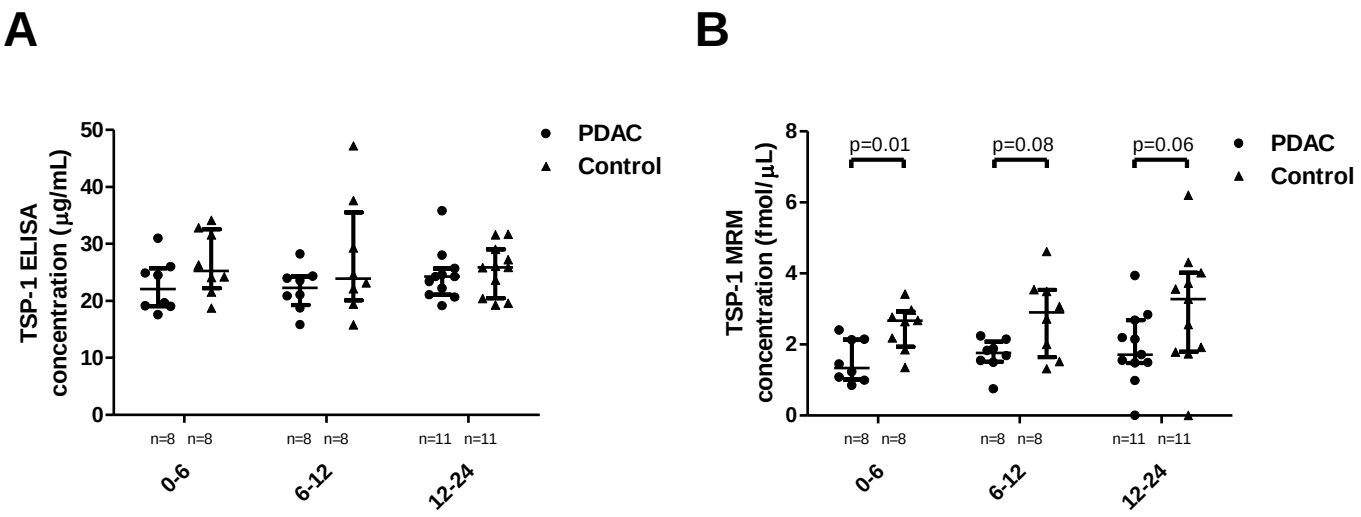

Figure 4-2. Serum TSP-1 levels in pre-diagnostic PDAC samples. TSP-1 concentrations were measured by A) ELISA and B) MRM in pre-diagnostic PDAC samples and matched healthy controls. Error bars display median and interquartile range, p values calculated by Mann Whitney U.

The pattern observed in the TSP-1 ELISA data suggested immuno-based approaches were comparable to MRM, but details on which monoclonal antibody was used to coat the plate was proprietary and thus unavailable to me. A different candidate antibody was selected for testing with the aim of confirming the MRM results with an independent assay, mainly western blotting and eventually analysing TSP-1 expression in the PDAC tumour microenvironment.

4.3.2 Monoclonal antibody for TSP-1 confirmed as specific for TSP-1 in serum and fibroblasts

Expression of TSP-1 was detectable by western blotting in untreated HFF cells, with a strong downregulation of protein observed after treatment with siRNA for TSP-1 (Figure 4-3). Probing for TSP-1 in sera alongside HFF cell lysate revealed a band at the same molecular weight, confirming antibody specificity in both clinical sample sets (Figure 4-3). Importantly, a range of band intensities were observed across samples, suggesting that densitometric analysis of the bands would be a suitable semi-quantitative method for analysis of TSP-1 levels.

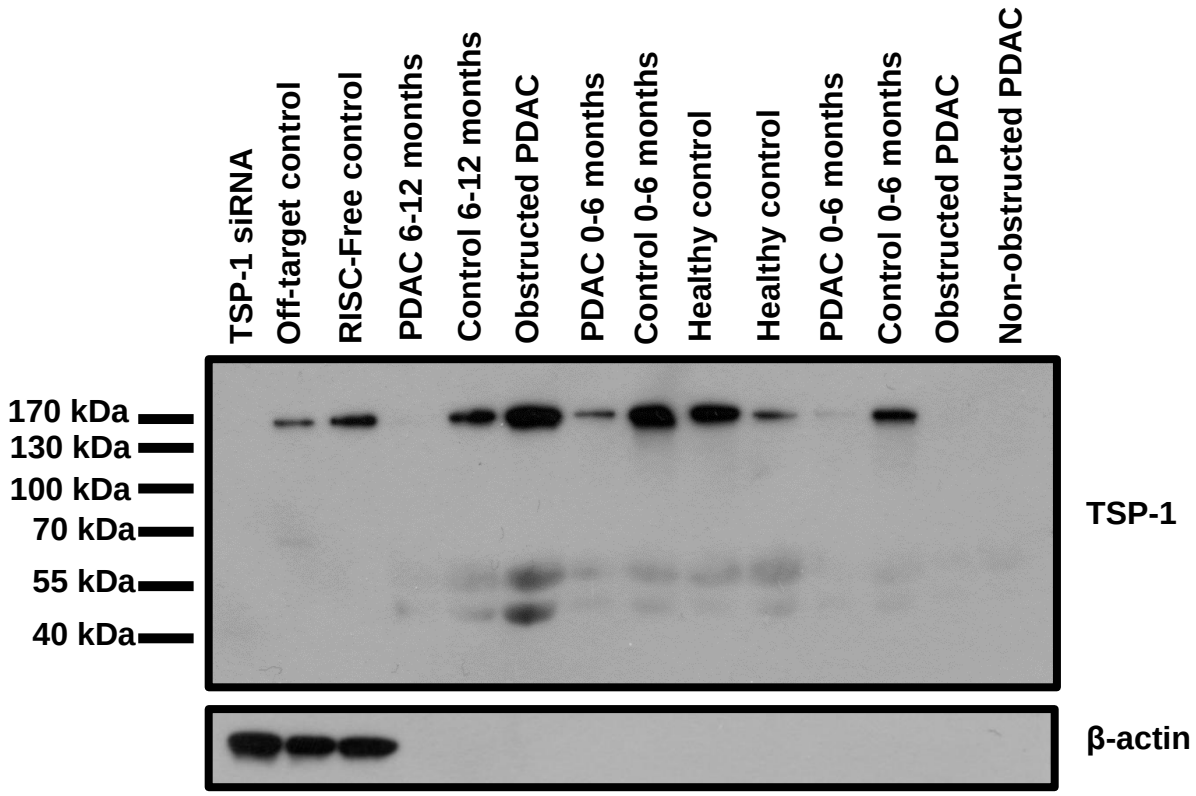

Figure 4-3. Variable concentration of TSP-1 in diagnostic and pre-diagnostic PDAC serum confirmed by western blotting. Serum from the UoL and UKCTOCS collections were blotted on a membrane and probed with a monoclonal antibody for TSP-1. The specificity of the antibody was confirmed by siRNA inhibition of TSP-1 expression in human foreskin fibroblasts. Probing for β-actin was performed as a measure of loading in the cell samples.

4.3.3 Semi-quantitative analysis of TSP-1 serum concentration in UoL and UKCTOCS samples

The analysis was expanded to include all UKCTOCS and UoL serum samples measured by MRM (Table 4.3, Table 4.4). Median TSP-1 levels were lower in cancer compared to control in all groups, and this reached statistical significance in the 6-12 months pre-diagnostic group (Figure 4-4A). In contrast, the UoL cohort measurements demonstrated significantly reduced levels of TSP-1 in the PDAC cases compared to healthy controls, irrespective of jaundice-status (Figure 4-4B). Correlative analysis also suggested the antibody performance differed between the two cohorts. A weak positive association with the MRM data was observed in the UKCTOCS cohort (r=0.27, Figure 4-4C) where a stronger one was observed in the UoL samples (r=0.48, Figure 4-4D).

Table 4.3. Patient characteristics of UKCTOCS serum samples measured for TSP- by western blotting.

	0-6 months		**6-12 months**		**12-24 months**	
	PDAC	Ctrl	PDAC	Ctrl	PDAC	Ctrl
n	30	30	17	17	17	17
Median age (range)	66 (51-74)	64 (51-76)	68 (51-74)	67 (50-76)	62 (52-71)	60 (51-73)

Table 4.4. Patient characteristics of UoL serum measured for TSP-1 by western blotting.

		PDAC non-obs	PDAC-obs	BBO	CP	HC
n		49	48	20	29	24
Median age (range)		67 (39-82)	65 (39-85)	65.5 (24-80)	52 (36-77)	34.5 (23-71)
Sex	F/M	28/21	26/22	5/15	16/13	8/16
Tumour stage	T1	1	-	-	-	-
	T2	3	2	-	-	-
	T3	31	36	-	-	-
	I	12	8	-	-	-
	U	2	2	-	-	-
Resection margin	R0	10	10	-	-	-
	R1	24	28	-	-	-
	I	12	8	-	-	-
	U	3	2	-	-	-

Abbreviations: PDAC – pancreatic ductal adenocarcinoma, BBO – benign biliary obstruction, CP – chronic pancreatitis, HC – healthy control, obs – obstruction, I – inoperable, U - unknown

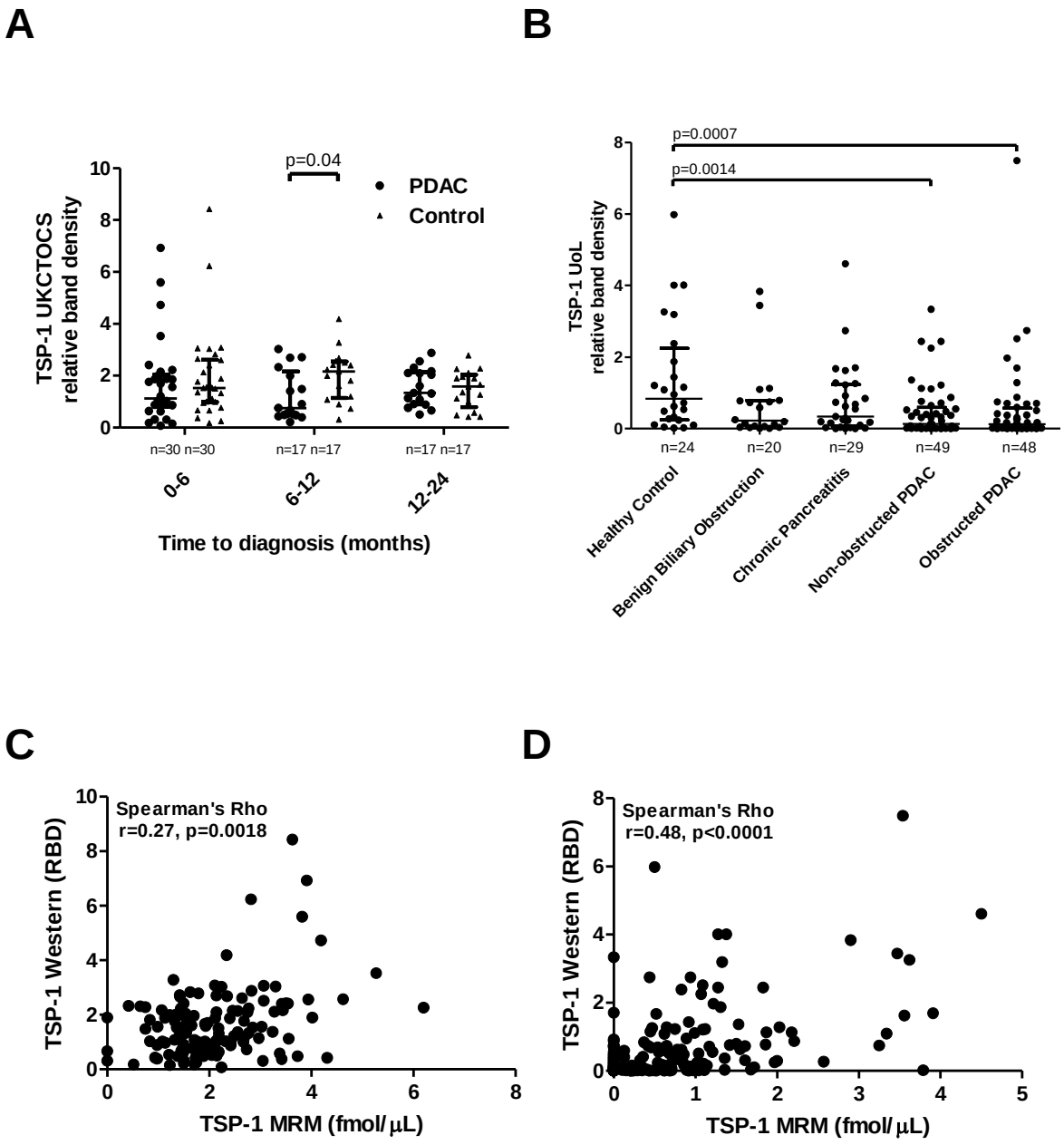

Figure 4-4. Semi-quantitative analysis of TSP-1 in sera from the UoL and UKCTOCS cohorts. A) Pre-diagnostic and B) Clinical serum samples were separated and transferred onto PVDF membranes before probing for TSP-1 with a monoclonal antibody and quantified by densitometry. Data were then compared with their respective MRM measurements in the C) UKCTOCS and D) UoL cohorts. Error bars display median and interquartile range, p values in A) and B) calculated by Mann Whitney U.

4.3.4 Confirmation of low serum TSP-1 in a genetically engineered mouse model for PDAC

KPC mouse-derived samples were immunoblotted and quantified by densitometry alongside age-matched PC control mice (Table 4.1). Low TSP-1 levels were observed in mice diagnosed with PDAC compared to high or low grade PanIN and control mice (Figure 4-5).

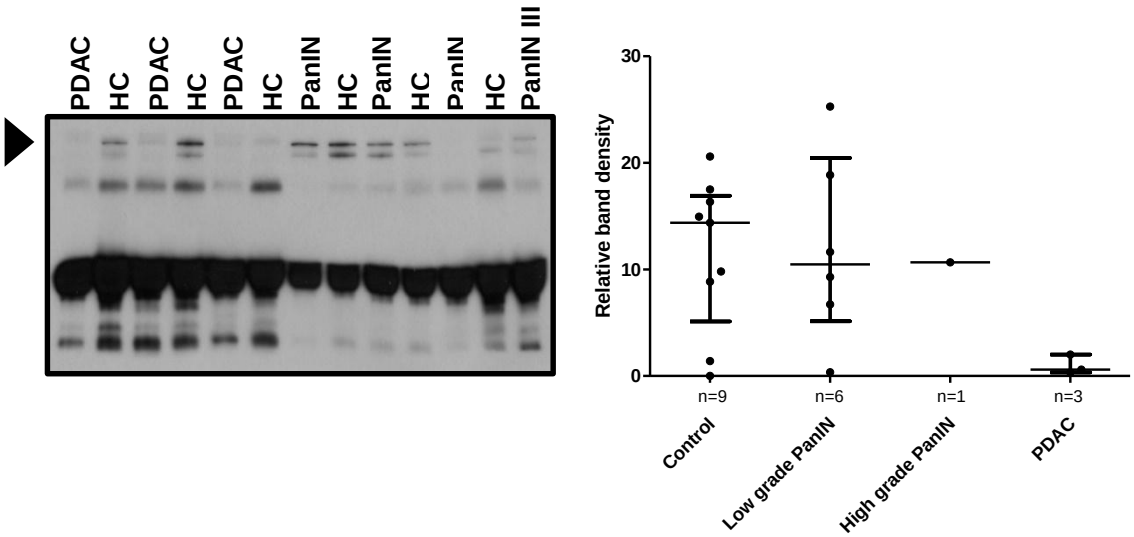

Figure 4-5. Semi-quantification of TSP-1 in KPC mouse sera with matched healthy controls. Western blotting for TSP-1 was performed on serum from KPC mice sacrificed at different stages of PDAC development, alongside age-matched healthy controls. An example blot is shown with the TSP-1 band indicated by the arrowhead. The dot plot is representative of one of three runs. The difference between PDAC and control sample measurements did not reach statistical significance across all three runs, so no p values are displayed here. Error bars display median and interquartile range. Abbreviations: HC – healthy control.

4.3.5 Clinicopathological analysis of TSP-1 expression in the PDAC tumour microenvironment

Serum TSP-1 levels as measured by MRM showed promise as an early diagnostic marker for PDAC. Kaplan-Meier analysis conducted by Dr Claire Jenkinson also suggested a prognostic role for TSP-1; patients with lower levels of TSP-1 had poorer overall survival[135]. To investigate whether varying levels of serum TSP-1 were reflected in the tumour, immunohistochemistry for TSP-1 in a tissue microarray (TMA) of PDAC specimens was performed.

4.3.6 Confirmation of immunohistochemical specificity of clone A6.1 TSP-1 antibody

Under the same RNAi conditions used for the western blot analysis, a robust confirmation of successful TSP-1 downregulation was observed when measured by ICC (Figure 4-6). Consequently, these conditions were kept constant for further immunohistochemical work on human tissue specimens.

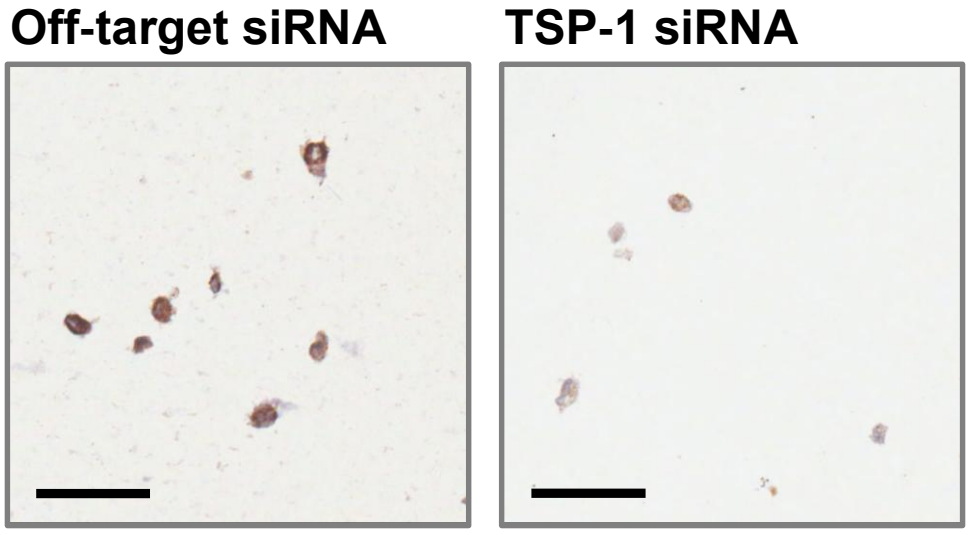

Figure 4-6. Specificity assessment of monoclonal TSP-1 antibody for immunocytochemistry. HFF cells treated with off-target siRNA and siRNA for TSP-1 were embedded in paraffin and stained for TSP-1. Scale bar=60μm

4.3.7 TSP-1 tissue expression in PDAC cases is not associated with overall survival

A TMA constructed from PDAC patient tissue specimens was stained for TSP-1. Heterogeneous staining of tumour and stromal staining was observed across patients, with TSP-1 expression observed in tumour cells and desmoplastic stroma in some patients, but no expression observed in others (Figure 4-7). In total, 32 (65%) of the 49 patients were negative for TSP-1, with 17 (35%) having positive staining in either the stroma or tumour. Univariate analysis found no association between TSP-1 expression and other clinicopathological parameters, including overall survival (Table 4.5, Figure 4-8).

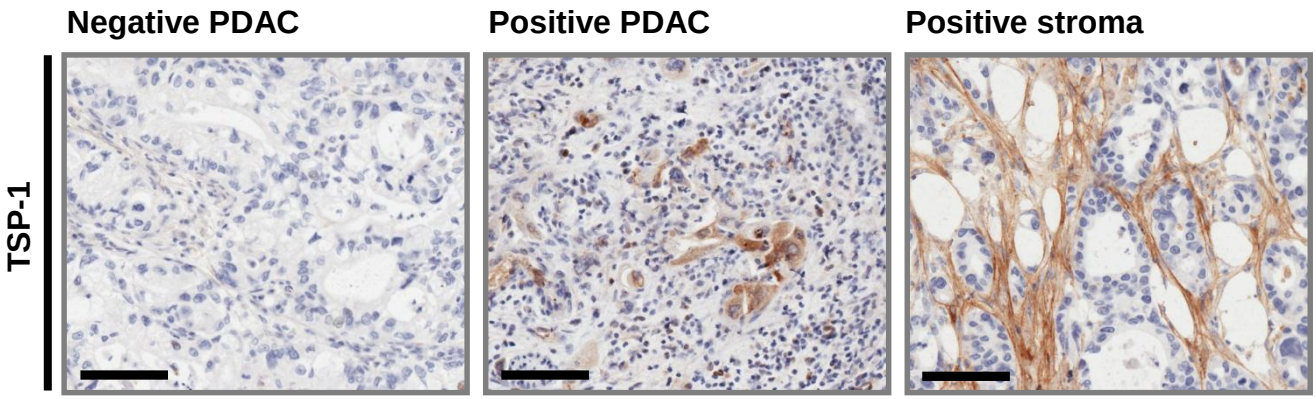

Figure 4-7. Examples of TSP-1 staining by IHC in PDAC tissue. Heterogeneous TSP-1 staining was observed in the tumour and stromal compartments of PDAC tissue. Scale bar=100µm.

Table 4.5. Univariate analysis of PDAC patient TMA stained for TSP-1.

		Cases (n=49)	TSP-1 Positive	TSP-1 Negative	P value
Age	Median (range)	67 (51-84)	67 (51-84)	66.5 (52-81)	0.77
Sex	Male	25	9	16	1.0
	Female	24	8	16	
Diabetic	Yes	11	5	6	0.46
	No	30	9	21	
	Unrecorded	8	3	5	
Resection margin	R0	10	3	7	0.66
	R1	20	4	16	
	Unrecorded	19	10	9	
Tumour stage	T1	0	0	0	0.38
	T2	3	2	1	
	T3	43	13	30	
	T4	2	1	1	
	Unrecorded	1	1	0	
Nodal involvement	R0	10	4	6	0.72
	R1	39	13	26	
Platelet count	Median (range)	303.5 (31-809)	296 (208-456)	312 (31-809)	0.70

P values determined by Mann Whitney U, Pearson's chi-squared and Fisher's Exact tests as appropriate.

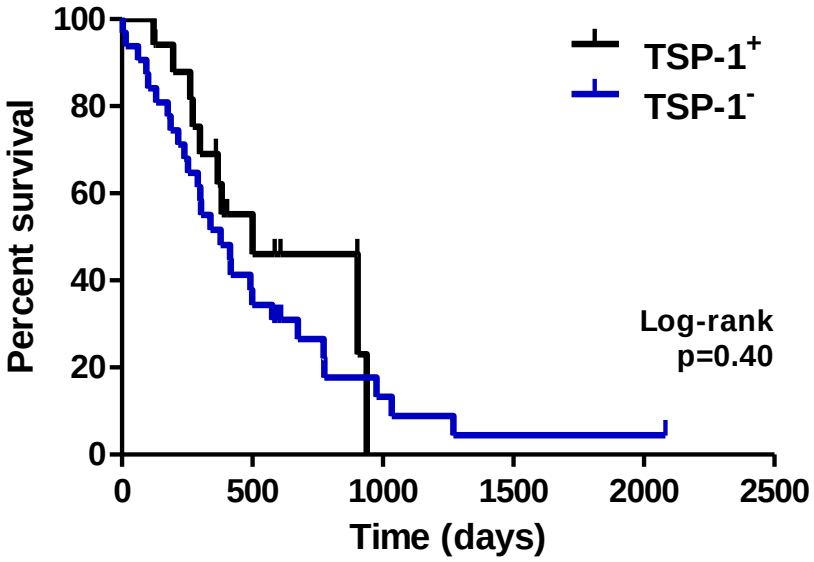

Figure 4-8. Kaplan-Meier analysis for overall survival in PDAC patients, classified by TSP-1 tissue expression. A TMA of PDAC patient tissue was scored based on positive TSP-1 expression in tumour or desmoplastic stroma. TSP-1^{+} n=17, TSP-1^{-} n=32.

4.4 Discussion

The use of a targeted mass-spectrometry based approach addresses the weaknesses of immunoassays for quantifying proteins in serum, in that they require the targeting antibody to be highly specific and are prone to interference from endogenous human anti-reagent antibodies[138,139]. However, the discovery of a potential marker, TSP-1 with lower circulating levels in PDAC patients than healthy subjects warranted independent validation in serum and investigation in primary tissue specimens using immunohistochemistry, requiring the identification of a suitable antibody.

An ELISA assay was initially employed to determine TSP-1 levels in UKCTOCS samples using a non-mass spectrometry based approach. Although I consistently measured lower levels in cancer case groups than controls, this did not reach statistical significance. It was impossible to validate the specificity of the antibody used in the ELISA, as all information pertaining to this antibody was proprietary. Therefore, a western blotting approach was adopted, with HFF cells, which have previously been reported to express TSP-1, considered a suitable positive control cell line for testing the antibody[140,141]. Western analysis on UKCTOCS samples again showed lower levels in pre-diagnostic cases compared to controls, however only reaching significance in the 6-12 month time group. The correlation between Western and MRM was better in the UoL samples, suggesting that the sample processing differences between the two cohorts may have had an effect on antibody affinity for TSP-1. This, coupled with the fact that the antibody used has shown weak cross-reactivity with thrombospondin-2 when used for western blotting[142], suggested

MRM was the most appropriate method for quantifying TSP-1 in the two human serum cohorts.

The LSL-Kras$^{G12D/+}$;LSL-Trp53$^{R172H/+}$;Pdx-1-Cre (KPC) mouse model of PDAC has been well characterised and is thought to faithfully reproduce the human disease from the pre-neoplastic stage to the development of advanced and metastatic cancer[143].

I observed that the specificity of the TSP-1 antibody was poorer when used to probe the murine samples, possibly due to the murine origin of the monoclonal antibody requiring an anti-mouse secondary antibody for visualisation, with the potential for cross-reaction with other serum proteins (Figure 4-5). Analysis of serum from KPC mice indicated that circulating TSP-1 was decreased in mice with PDAC, but not with pre-malignant PanIN lesions. This supports the findings observed in the human samples, and raises the possibility that decreases in serum TSP-1 observed in the pre-diagnostic cases are occurring in the context of fully developed PDAC. It also suggests that the use of genetically engineered mouse models for identifying early diagnostic markers may be a valid strategy.

Perhaps in contrast to the analysis of TNC expression in pancreatic cancer tissue in chapter 3, the use of IHC to identify TSP-1 expression in the tumour microenvironment did not help explain the reduced levels of TSP-1 in the serum. At present we do not have a mechanism to explain these observations.

5 EVALUATION OF STROMAL QUANTIFICATION IN PANCREATIC CANCER USING A TISSUE MICROARRAY

5.1 Introduction

In chapters 3 and 4, I attempted to relate the circulatory levels of TSP-1 and TNC to their respective pancreatic tissue levels. In the case of TNC, the higher levels observed in the circulation of pancreatic cancer patients compared to patients with chronic pancreatitis correlated with high stromal tissue expression in cancer tissue compared to chronic pancreatitis tissue ($p<0.0001$, Chapter 3 Section 3.3.2). This suggested a link between TNC protein expression in the tumour or chronic pancreatitic microenvironment and the levels of the TNC protein in the circulation. However where data were available to compare TNC levels in matched pancreatic tissue and blood a correlation between tissue and circulating TNC levels could not be established (Chapter 3 Section 3.3.2). While there are a number of possible explanations for this, one explanation relates to the possible inadequacy use of tissue microarrays as a means of quantifying elements of the PDAC tumour microenvironment. We hypothesised that TMAs may provide too small an area of tissue to accurately quantify pancreatic stromal expression.

PDAC has a complex stromal compartment consisting of extracellular matrix, immune cells, fibroblasts, endothelial cells and soluble proteins, thought to contribute to tumour cell survival, proliferation, immune evasion and resistance to therapy [33–35]. Given the heterogeneity of the disease, it is not known whether the use of TMAs is appropriate for analysing all elements of the PDAC stroma.

To address this question, myself and two other research group members, Dr Katharine Hand and Mrs Frances Oldfield, undertook a study assessing the suitability of quantifying stromal components using TMAs in relation to clinical outcome. One of the PDAC TMAs analysed for TNC expression (Chapter 3 Section 3.2.5) was produced as part of this project, enabling me to compare this with other stromal components of the PDAC tumour microenvironment.

5.2 Materials and methods

5.2.1 Tissue microarray construction

A TMA was constructed by Mrs Elizabeth Garner. Three cores per patient were sampled from FFPE tumour specimens from 47 patients with PDAC. The TMA was cut into 192 sections of 5µm thickness, dipped in paraffin wax and stored at -20ºC.

5.2.2 Immunohistochemical staining of TMA sections

Antibodies and histological stains were selected to characterise various components of the stroma. At least four sections, at different depths within the array, were stained for the detection of each marker. IHC was performed following the protocol detailed in Chapter 3 Section 3.2.1, with an extra deparaffinisation step at the beginning. Slides were equilibrated to room temperature then placed in xylene and incubated for 30 minutes, or until the paraffin coating the slide was removed. Slides were then placed in 100% ethanol for 1 minute, before insertion into a PT Link (cat. no. PT10126, Dako, UK) for antigen retrieval. Subsequent steps were performed as described in Chapter 3 Section 3.2.1, using the antibody dilutions described in Table 5.1. All TMAs were stained alongside whole PDAC sections known to express the proteins of interest, as well as with polyclonal anti-mouse immunoglobulin-HRP conjugates (cat. no. P0447, Dako, UK) to serve as negative controls. Stained TMAs were scanned with an Aperio ScanScope™ (Leica Microsystems, UK) and mapped for scoring using Definiens Tissue Studio (version 3, Definiens, Germany).

Table 5.1. Antibodies and histological stains used for stromal component visualisation

Antibody/stain	Stromal component stained	Catalogue number	Supplier	Antibody dilution	Stained by	Scored by
Anti-α-SMA	Activated fibroblasts	ab7817	Abcam, UK	1:50	AE & FO	AE & FO
Anti-CD204	M2 Macrophages	KT022	Transgenic Inc., Japan	1:200	KH	AE & FO
Anti-CD206	M2 Macrophages	ab117644	Abcam, UK	1:200	KH	AE & FO
Anti-CD68	Macrophages	M0876	Dako UK Ltd., UK	1:100	AE & FO	AE & FO
Anti-CD8	Cytotoxic T cells	M7103	Dako UK Ltd., UK	1:1000	TG	AE & FO
Anti-cytokeratin	Epithelia	4545S	Cell Signaling Technology, Inc., USA	1:300	KH	AE & FO
Anti-podoplanin	Lymphatic vessels Fibroblasts	M3619	Dako UK Ltd., UK	1:100	AE & FO	AE & FO
Haematoxylin & Eosin	All	3801540B BE 3801600E	Leica Microsystems, UK	-	KH	-
Masson's trichrome	Collagen	HT15-1KT	Sigma-Aldrich, UK	-	KH	-

Abbreviations: SMA – smooth muscle actin

Initials: AE – Anthony Evans, FO – Frances Oldfield, KH – Katharine Hand, TG – Thompson Gana

5.2.3 Scoring of tissue microarrays

All stains were optimised and scored in consultation with a specialist histopathologist, Professor Fiona Campbell. TMAs from four depths spanning the full TMA block were evaluated for the presence of tumour in all cores, to ensure that the stroma being scored in every core was associated with malignancy.

Blinded independent scoring was performed alongside Mrs Frances Oldfield. On all TMAs, cores were only scored if at least half of the core contained intact tissue. TMAs stained for α-smooth muscle actin (αSMA) and cytokeratin were scored as a percentage of non-necrotic tissue in each core. Stained podoplanin was scored as a percentage of αSMA stained tissue in the next serial section, ensuring that podoplanin-stained TMAs were always within two sections (~10μm) of matched αSMA TMAs.

Stained immune cells (CD8, CD204, CD206, CD68) were counted manually. As some cores had missing tissue as a result of the staining process, an adjustment factor was applied if necessary based on the percentage of tissue remaining, either 50%, 75% or 100%.

Where there was disagreement over cores scored by percentage, a consensus was reached. For counted markers, if count values were not within 20% of each other then both investigators performed a recount until this criterion was met. Once a consensus for all cores was reached, the average of the scores was taken as the final core value. The average of all cores per patient was then calculated as the value used for further analysis. On each TMA section, a patient was only included in the analysis if at least two cores were available for scoring, with the average of all cores used to calculate the final score per patient. To calculate the overall mean per patient across all TMA levels, at least five cores had to be present.

Activated stroma index (ASI) was determined using ImageJ (version 1.5) software, calculated as the proportion of collagen stained for αSMA for each core: ASI = αSMA area (μm^2) ÷ collagen area (μm^2)[90]. Using ImageJ's colour deconvolution plugin[144], αSMA and collagen staining were isolated from their respective cores by segregating three colours from the original images. Optimal colour settings were kept consistent across all analysed TMAs (Table 5.2). Deconvoluted images were converted to binary 8-bit greyscale images, using the 'Triangle' auto-threshold algorithm, and scaled to enable the measurement of each stained area in μm^2. ASI was calculated from two serial TMAs stained for αSMA by IHC and collagen with Masson's trichrome stain.

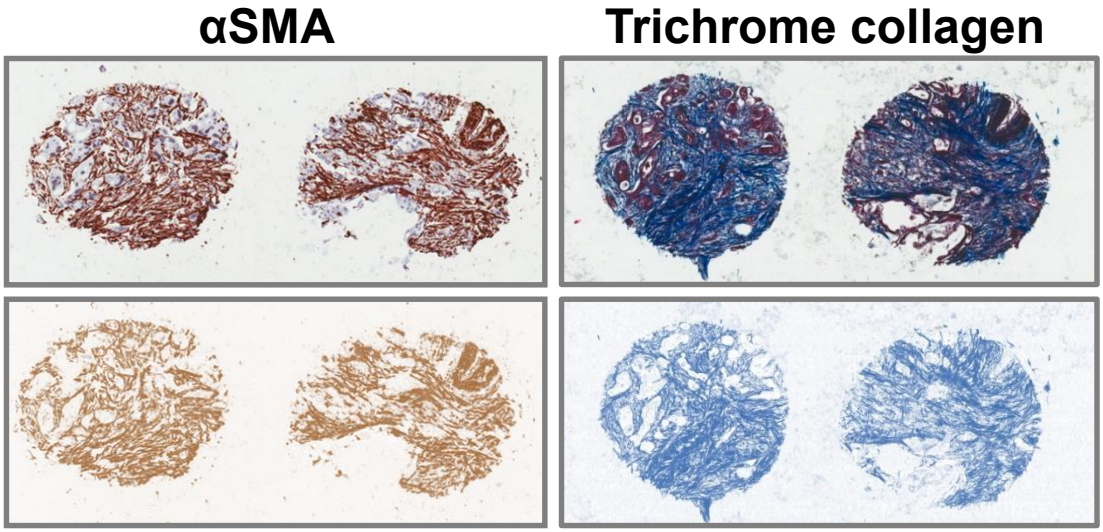

Figure 5-1. Examples of αSMA and collagen staining isolated from background counterstain using ImageJ's colour deconvolution plugin. Original core images are displayed in the top row, with isolated staining post-deconvolution shown underneath. Activated stroma index was calculated from the quantified area of αSMA staining as a proportion of collagen-stained area, both in μm^2.

Table 5.2. Settings applied for ImageJ colour deconvolution plugin.

Colour settings		αSMA	Collagen
Colour 1	R	0.6027735	0.76523894
	G	0.644836	0.5705916
	B	0.46994755	0.29805133
Colour 2	R	0.34126425	0.5437807
	G	0.56168777	0.6563658
	B	0.753688	0.52295935
Colour 3	R	0.7212509	0.34454608
	G	0.5183564	0.4935677
	B	0.45946032	0.79854804

5.2.4 Luminex quantification of serum cytokines, chemokines and growth factors

Data were available from a comprehensive analysis of sera from the University of Liverpool collection, performed by other members of the research group[104], quantifying 27 cytokines, chemokines and growth factors. These data, kindly provided by Dr Victoria Shaw, were matched with the patients on the TMA to compare stromal scores with serum cytokine concentrations.

5.2.5 Statistical analysis of TMA scored data

Clinicopathological data for each patient was matched with stroma data after scoring was completed, both at a TMA section level and at the entire TMA level, using all available scoring data across all TMA depths. Associations of stromal component scores with other clinical parameters were calculated using Pearson's chi-squared, Fisher's exact and Mann Whitney U tests as appropriate. Kaplan-Meier analysis for overall survival was performed using log-rank tests to test for differences between groups, after splitting the patients by median stromal component expression.

5.3 Results

5.3.1 Construction and staining of a TMA for the quantification of stromal components

The characteristics of the 47 PDAC patients, whose samples were used to generate the TMA in this study are shown in Table 5.3. The TMA was sectioned completely, such that TMA sections from several depths of the TMA block could be histologically stained for each marker, as illustrated in (Figure 5-2). All antibodies (Table 5.1) were optimised for IHC and deemed suitably specific for their respective targets (Figure 5-3).

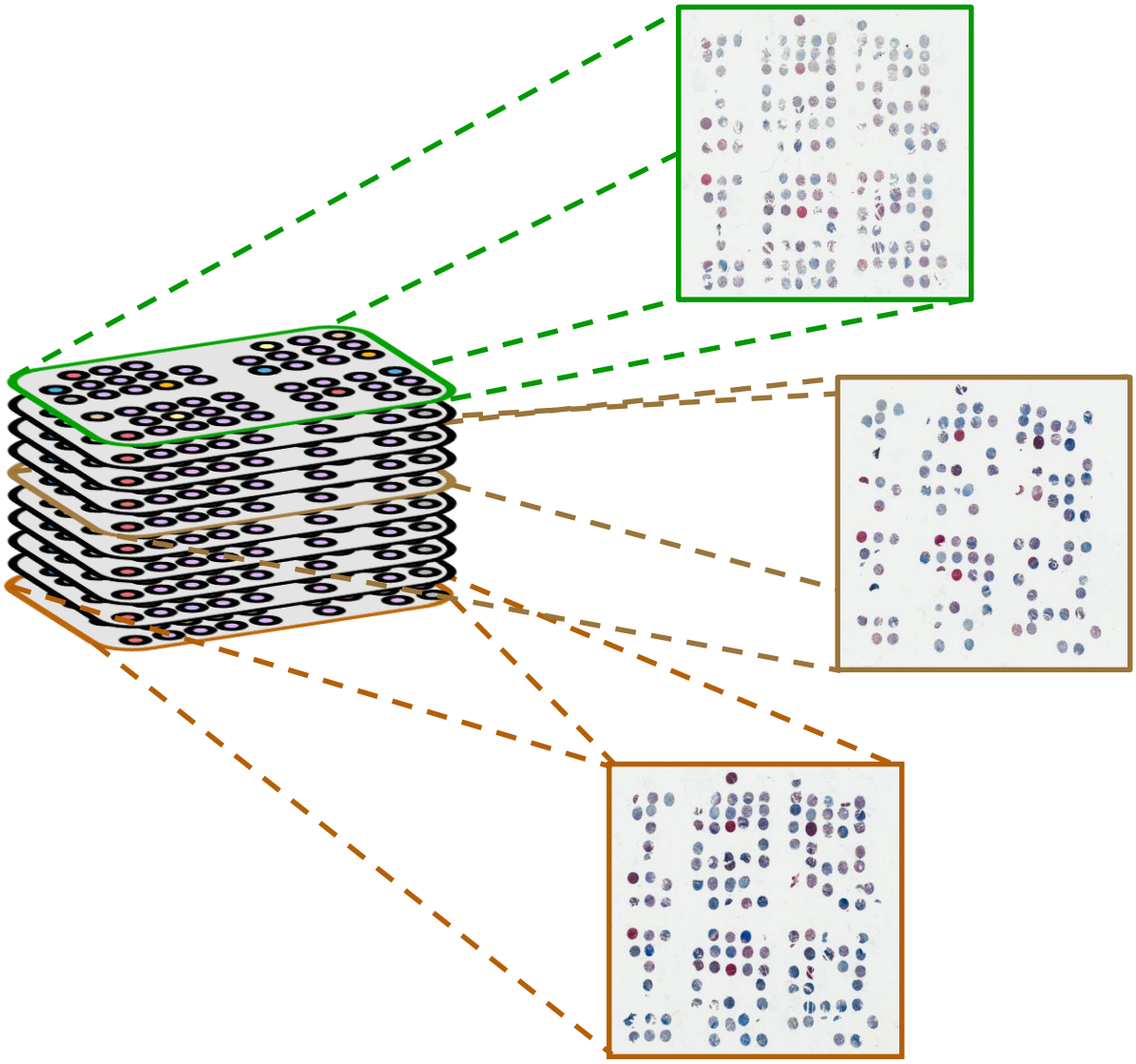

Figure 5-2. Overview of stromal quantification study design. A TMA containing cores from 47 PDAC tissue specimens were cut into 192 sections to enable staining and analysis for multiple stromal components at different depths.

Table 5.3. Patient characteristics of PDAC samples on the stroma study TMA

		Cases (n=47)
Median age (range)		68 (44-84)
Sex	F/M	22/25
Tumour stage	T1	1
	T2	2
	T3	44
Resection margin	R0	9
	R1	37
	R2	1
Lymph node involvement	N0	11
	N1	36
Median tumour size/mm (range)		30 (18-60)

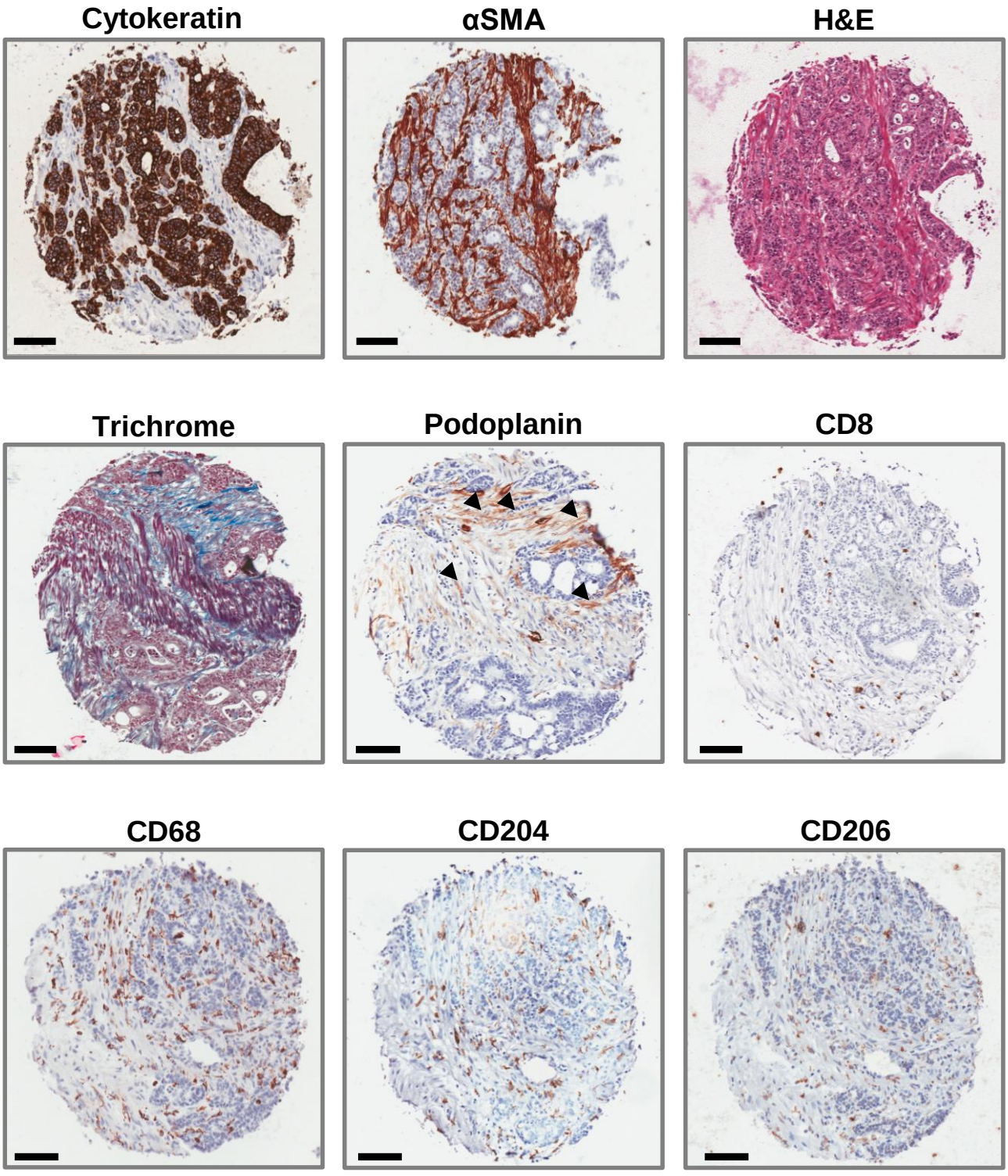

Figure 5-3. Examples of stromal components stained on a TMA of PDAC tissue specimens. Arrowheads indicate examples of fibroblasts stained for podoplanin. Scale bars=100μm.

IHC for αSMA revealed strong staining of fibrous tissue consistent with its expression in activated fibroblasts, as well as smooth muscle where present. Staining for pan-cytokeratin was also consistent with expectations, demonstrating strong cytoplasmic expression in malignant and benign epithelia. Intermittent podoplanin expression was observed in fibroblast-like cells, though its intended use as a marker was originally for lymphatic vessels. This observation was consistent with previous reports linking podoplanin expression in cancer-associated fibroblasts with prognosis in other carcinomas[145,146]. Consequently, podoplanin-stained TMAs were scored as the percentage of αSMA-positive areas from matched serial TMAs, cut within two sections (~10μm), to investigate if this prognostic effect was also observed in PDAC.

As expected, IHC for immune cells revealed scattered cytoplasmic staining of individual cells rather than areas of block staining. Cells stained for CD68, a marker of macrophages, and CD204 and CD206, both thought to be expressed in M2 macrophages, were highly abundant and phenotypically characteristic of inflammatory cells[147]. $CD8^+$ cytotoxic T cells were also stained in a specific manner, but were much lower in abundance.

5.3.2 Quantification of stromal elements reveals variable expression at different depths of the TMA

Consistent with our experience with other TMAs, for all stromal markers the number of scorable cores decreased at lower depths of the TMA block compared with upper depth levels. This resulted in reduced numbers of patients suitable for analysis at each level, as the TMA depth increased (Table 5.4).

Table 5.4. Details of TMA scored for PDAC stromal components at different depths. Slide number represents the position of the TMA section in relation to the TMA block, with Slide 1 representing the first section cut.

Scored stromal feature	Slide number	Number of patients	Scoring method	Median score
αSMA$^+$	1	40	Percentage	42.5
	30	34		51.7
	47	36		58.3
	76	29		47.9
	106	18		57.5
	Overall	41		52.6
Cytokeratin$^+$	6	41	Percentage	25.0
	36	42		18.3
	48	24		30.0
	66	36		20.0
	77	31		18.8
	96	28		22.5
	107	25		20.0
	Overall	45		19.7
Activated stroma index	1	32	Percentage	65
Podoplanin$^+$ fibroblasts	31	32	Percentage	53.3
	49	30		55
	78	29		40.8
	108	18		27.5
	Overall	37		41.6
CD68$^+$	16	44	Count	129.7
	51	34		140.6
	80	31		141.2
	110	26		120.5
	Overall	39		128.5
CD204$^+$	13	38	Count	77.8
	43	38		95.2
	73	28		109.3
	103	28		111.3
	Overall	39		91.6
CD206$^+$	15	44	Count	80.6
	45	37		87.3
	105	25		89.3
	Overall	40		92.3
CD8$^+$	10	45	Count	26.2
	40	41		21.8
	70	28		25.7
	100	29		14.9
	Overall	42		25.8

The median percentage area of αSMA-stained tissue per patient core was consistently higher than cytokeratin$^+$, suggesting the majority of tumours on the array had a pronounced desmoplastic component in comparison to areas of tumour. The median αSMA$^+$ percentage for each TMA level varied, however, ranging from 42.5-58.3% with an overall median of 52.6%, taking into account patient cores across all TMA levels. Similarly median cytokeratin$^+$ percentages also fluctuated at different TMA levels, ranging from 18.3-30%. Despite a different scoring method, podoplanin$^+$ staining scored as a percentage of αSMA$^+$ stroma was also highly variable, ranging from 27.5-55%.

All scoring and statistical analysis was performed independently by both myself and Mrs Frances Oldfield. The results of the complete analysis of αSMA, podoplanin, cytokeratin and ASI staining will be presented in her thesis, while in this thesis I will focus on the detailed analysis of the inflammatory components.

Median counts of CD204$^+$ and CD206$^+$ cells were consistently lower than CD68$^+$ cells, supporting the notion that they comprised a subset of CD68$^+$ macrophages (Table 5.4). In comparison, CD8$^+$ cytotoxic T cells were much lower in abundance than the macrophage-type cells, with an overall median of 25.8 cells per patient core.

Comparisons of the overall mean number of CD68$^+$, CD204$^+$ and CD206$^+$ cells per patient revealed a strong positive correlation between the three groups, further suggesting that the three groups are linked (Figure 5-4A-C). Interestingly, though both markers were selected to stain M2 macrophages, CD204$^+$ and CD206$^+$ cell correlation with each other was the weakest of the three, suggesting they may not be staining exactly the same macrophage subtype or that the antibodies used to strain them differed in specificity.

A weak positive relationship was also observed between $CD8^+$ cells and $CD68^+$ macrophages (Figure 5-4D) and $CD206^+$ M2 macrophages (Figure 5-4F) but not $CD204^+$ cells (Figure 5-4E).

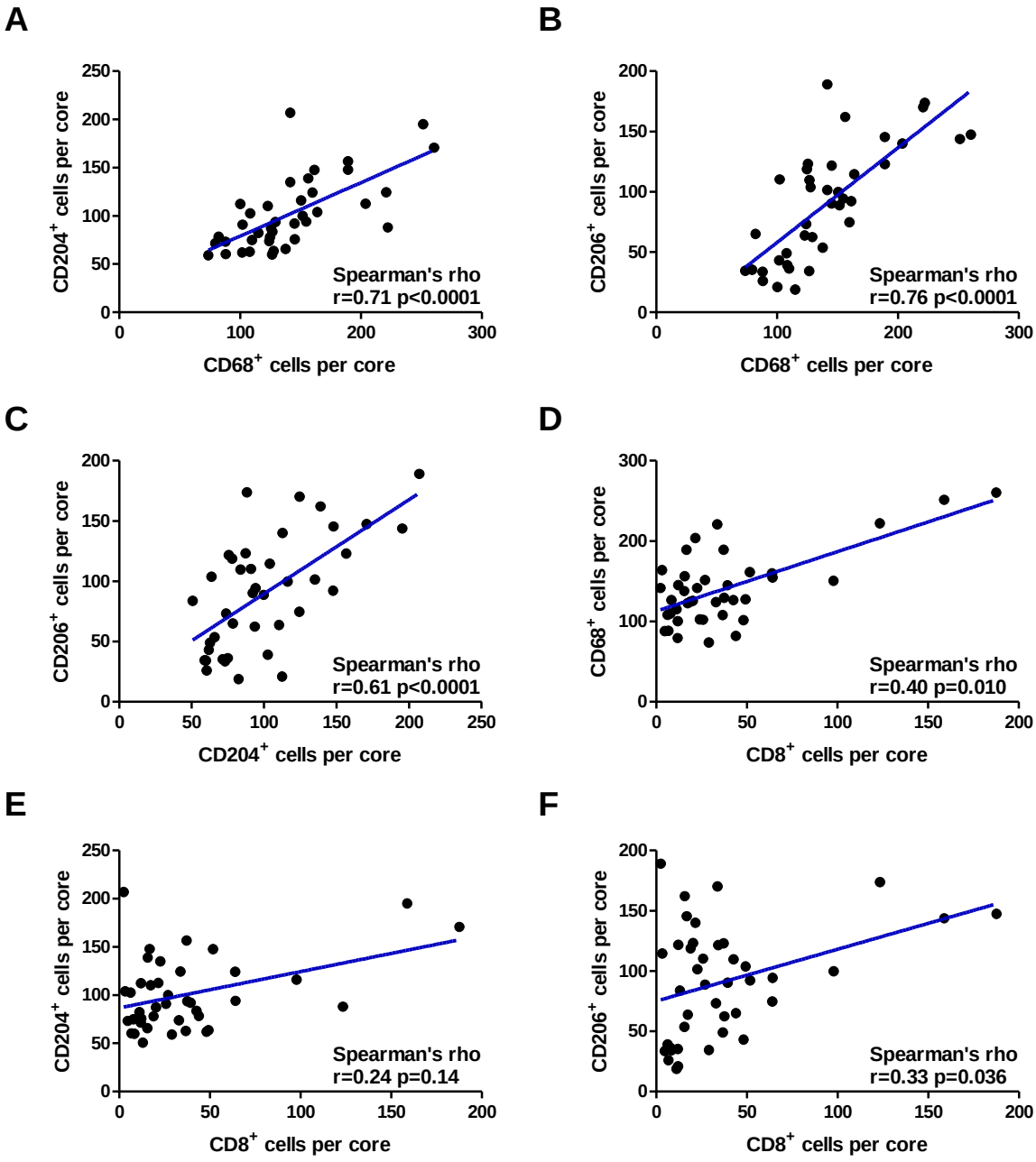

Figure 5-4 Scatter plots of immune cells quantified using a TMA of PDAC samples. A-C) Correlative comparison of $CD68^+$, $CD204^+$ and $CD206^+$ macrophages stained on a TMA of PDAC tissue, sectioned for analysis at different depths of the tissue block. D-F) Comparisons of $CD68^+$, $CD204^+$ and $CD206^+$ macrophages with $CD8^+$ cytotoxic T cells. The mean number of cells per patient, measured across all TMA levels, is plotted.

5.3.3 Inflammatory cells do not correlate with serum cytokines and chemokines

Overall mean $CD68^+$, $CD204^+$, $CD206^+$ and $CD8^+$ cell counts were correlated with matched serum concentrations of cytokines, chemokines and growth factors measured by Luminex assay. No significant relationships were identified, except for a weak positive association between $CD8^+$ cell count and serum macrophage inflammatory protein-1α (MIP-1α, Table 5.5).

Table 5.5. Correlation of mean immune cell count with matched serum cytokine, chemokine and growth factor concentration. The mean number of cells per patient, scored on a TMA sectioned for analysis at different depths, was compared with matched serum concentrations of 25 cytokines.

	Immune cell correlation (Spearman's rho)			
	$CD68^+$	**$CD204^+$**	**$CD206^+$**	**$CD8^+$**
PDGF	0.1549	0.1273	-0.0067	-0.0675
IL-1β	-0.0865	-0.0292	-0.0199	-0.0428
IL-1Ra	-0.0548	-0.1503	-0.0054	0.1886
IL-2	0.1565	0.0441	-0.0015	0.2581
IL-4	-0.0596	-0.0505	-0.0629	0.0065
IL-5	0.0005	0.0963	0.0242	-0.0675
IL-6	-0.0315	0.0327	0.0994	0.1423
IL-7	0.0224	0.0087	0.0499	-0.0613
IL-8	-0.0177	-0.0107	-0.0079	-0.0491
IL-9	0.0469	0.2541	0.0956	0.234
IL-10	0.1341	0.1639	0.211	0.033
IL-12	0.2346	0.1128	0.2299	0.2805
IL-13	0.0654	0.152	0.0537	0.0607
IL-17	0.0187	0.1508	-0.0824	0.1837
Eotaxin	-0.0718	-0.1366	0.0369	0.1109
FGF basic	-0.0961	0.0413	-0.086	0.1874
G-CSF	0.0208	0.1318	-0.0048	0.1484
IFN-γ	-0.0645	-0.0007	-0.0513	-0.0591
IP-10	0.0247	-0.0778	0.0198	0.2068
MCP-1	0.0947	0.1366	0.0921	-0.1109
MIP-1α	0.0151	0.1879	0.1219	**0.3189***
MIP-1β	-0.1343	0.0434	-0.0349	-0.0006
RANTES	0.1954	0.1811	0.1452	-0.1218
TNF-α	-0.0559	-0.0247	-0.0833	-0.052
VEGF	0.0728	0.0059	0.1163	-0.166

*Significant correlations

5.3.4 Tenascin C stromal expression is associated with increased activated stroma index and $CD68^+$ macrophage abundance

One of the PDAC TMA sections assessed for tenascin C expression, as described in Chapter 3 3.2.5, was used to investigate if TNC stromal expression related to the abundance of other stromal elements in PDAC. For the purposes of this analysis, TNC stromal expression status was categorised as present or absent and plotted against the overall mean values of inflammatory cell counts and examined for differences. Though no strong relationship was observed with either of the M2 macrophage marker scores (Figure 5-5A, B), the number of $CD68^+$ macrophages was increased in patients with positive TNC stromal expression (Figure 5-5C). Interestingly, though no difference was observed in αSMA abundance between patients positive or negative for TNC (p=1.0), activated stroma index values, a measure of αSMA-stained collagen, were higher in TNC^+ patients (Figure 5-5D), suggesting that TNC expression is associated with the activation of fibroblasts in the desmoplastic stroma.

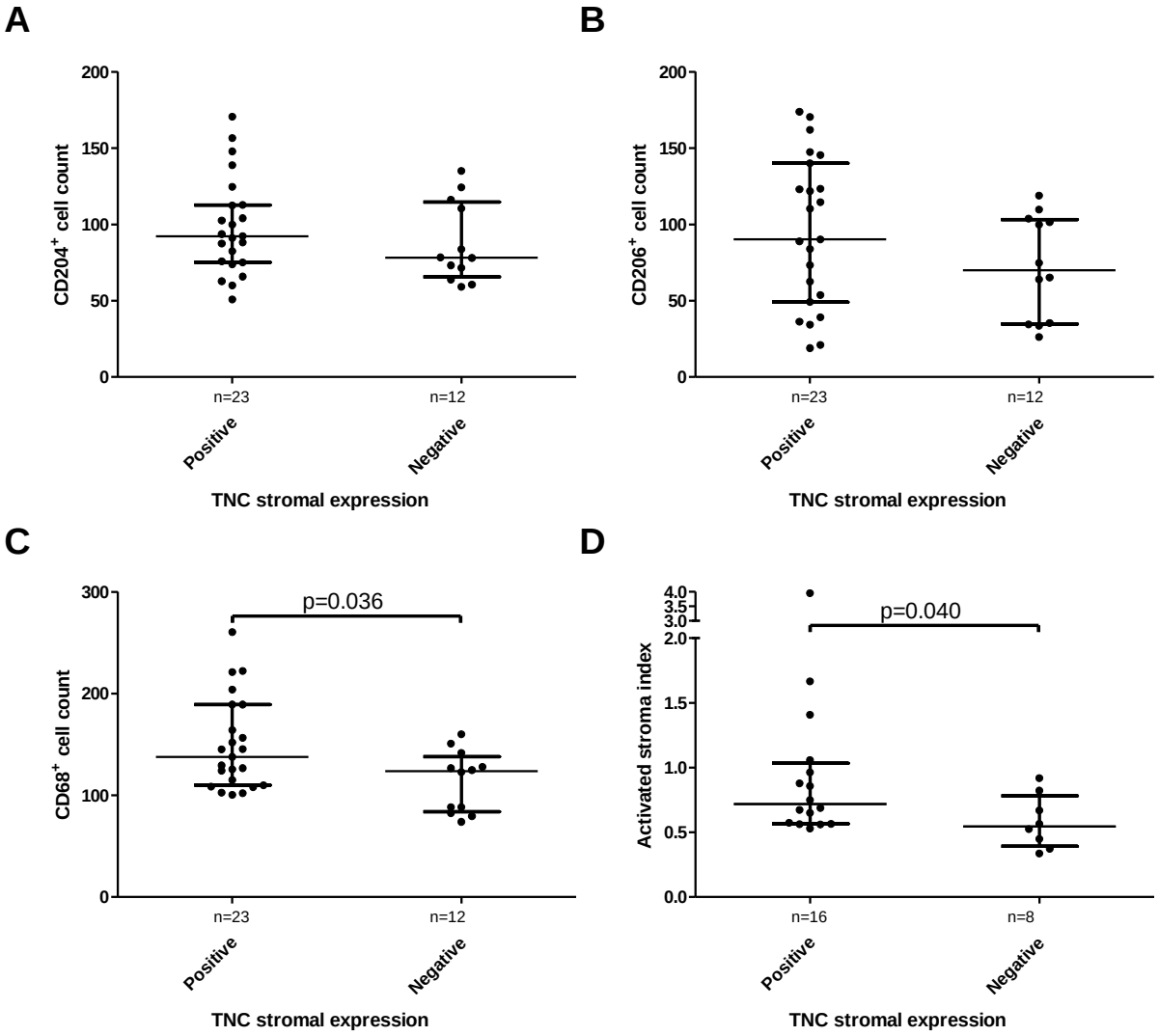

Figure 5-5. CD68$^+$ cell numbers and activated stroma index are increased in PDAC patients with positive stromal TNC expression. PDAC patients were classified by TNC stromal expression on a TMA sectioned and stained for stromal analysis at different depths. A) CD204$^+$, B) CD206$^+$, and C) CD68$^+$ mean cell counts per core and D) ASI values are plotted. P values derived by Mann Whitney U test, error bars display the median and interquartile range.

5.3.5 Survival analyses based on the inflammatory cell counts at different depths of the TMA yield variable conclusions

Kaplan-Meier analysis for overall survival was performed for all TMA levels, categorising patients as 'high' (higher than the median count) and 'low' (lower the median count) for each marker. Preliminary analyses were performed at the individual TMA levels, treating each depth as a separate entity to reflect how an analysis would be performed were only one section of TMA analysed per marker.

Four TMA sections were stained for each immune cell marker, though in the case of CD206 one section was insufficiently mounted in DPX and could not be scored. When analysed individually, high numbers of $CD68^+$ and $CD206^+$ cells were positively association with overall survival (OS) at the top level of the TMA (Figure 5-6, top row), but not at any other level. The lack of association observed between OS and $CD204^+$ cell count provided further evidence that population is not identical to that stained for CD206, or that there are differences in the specificity of the two antibodies used.

$CD8^+$ cells, though lower in abundance than the macrophages, demonstrated a similar pattern with overall survival, with a favourable prognosis associated with higher numbers at the top level of the TMA, but not at any other level (Figure 5-7).

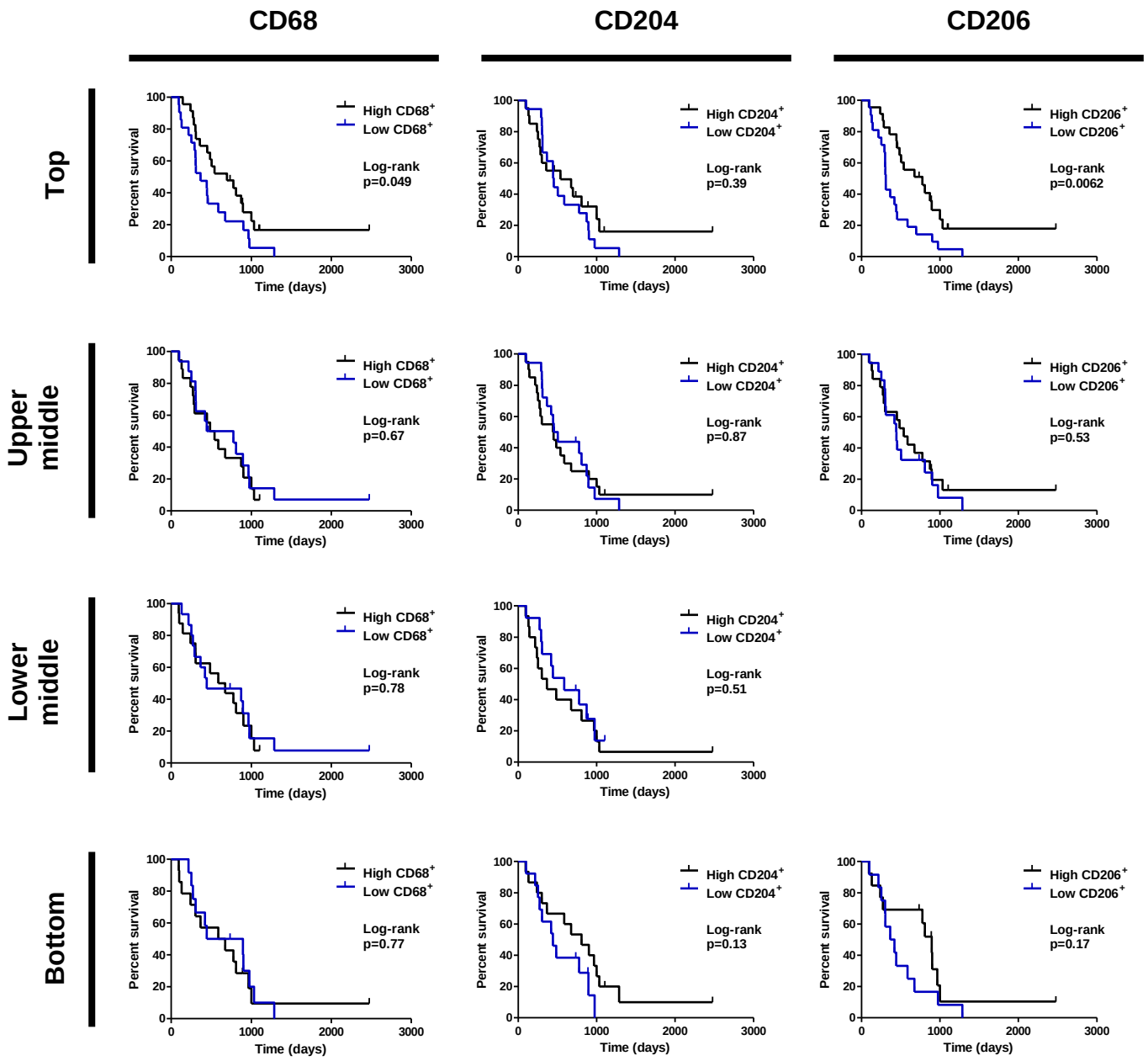

Figure 5-6. Kaplan-Meier analysis for overall survival of PDAC patients on a TMA, sectioned for analysis at different depths. TMAs stained for the macrophage markers CD68, CD204 and CD206 were scored and patients grouped above and below the median number of cells per core. At least three TMA sections were stained per marker, with each section selected to be at least 150µm apart from each other.

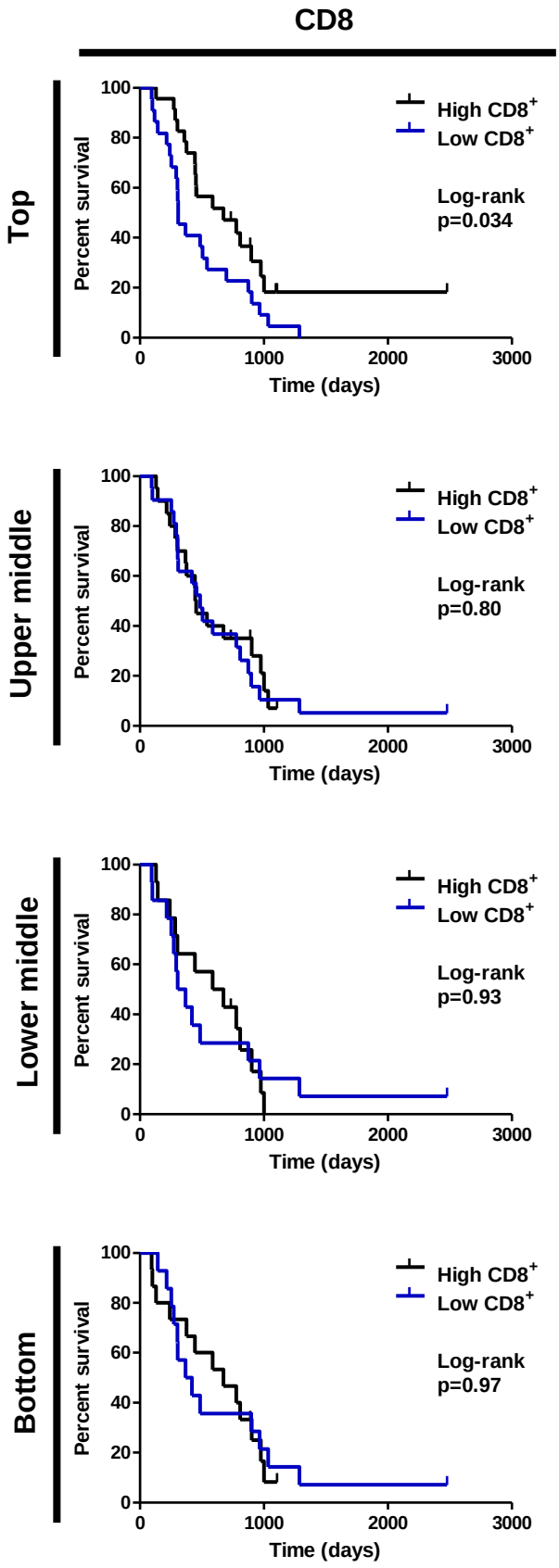

Figure 5-7. Kaplan-Meier analysis for overall survival of PDAC patients on a TMA stained for CD8⁺ cells, sectioned for analysis at different depths. TMAs stained for CD8⁺ cytotoxic T cells were scored and patients grouped above and below the median number of cells per core. Four TMA sections were stained, with each section selected to be at least 150µm apart from each other.

5.3.6 Kaplan-Meier analysis of inflammatory stromal elements across all TMA levels reveals no prognostic benefit to high abundances of $CD8^+$, $CD68^+$, $CD204^+$ and $CD206^+$ cells

Given the inconsistent conclusions drawn from analysing each TMA at distinct depths, Kaplan-Meier analyses were repeated using the combined stromal scoring data from across all TMA levels. Accordingly, all available data per patient were used to calculate a final mean count per patient. Association with overall survival were not observed when patients were categorised as having high or low $CD68^+$, $CD204^+$ or $CD8^+$ cell counts (Figure 5-8A, B, D). However, high numbers of $CD206^+$ cells were still significantly associated with longer overall survival (Figure 5-8C).

The number of evaluable patients per section decreased when depth into the TMA block increased (Table 5.4). The possibility therefore arose that the greater patient numbers in the top level TMA stained for CD206 was a source of bias with respect to the overall mean values. The analysis was therefore repeated for CD206-stained TMAs, but included only 22 patients for whom scores were available on all three TMA levels. With this stipulation, the association of $CD206^+$ cell abundance with OS was not observed on any level including when overall data per patient were applied (Figure 5-9).

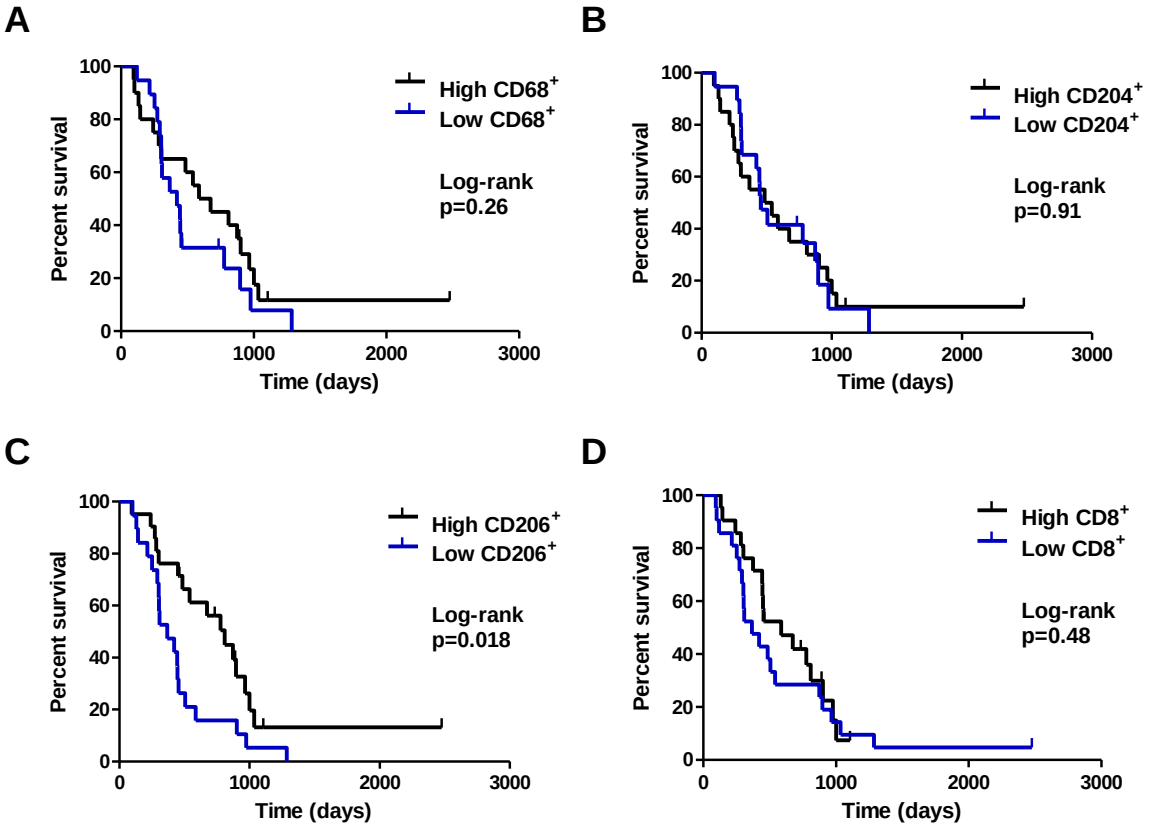

Figure 5-8. Kaplan-Meier analysis for overall survival of PDAC patients on a TMA stained for cell markers at different depths. TMA sections stained by IHC for A) $CD68^+$, B) $CD204^+$, C) $CD206^+$ and D) $CD8^+$ cells were scored and averaged across all TMA depths. Patients were grouped above and below the median number of cells per core. At least three sections were stained per marker, with each section situated at least 150µm apart from each other.

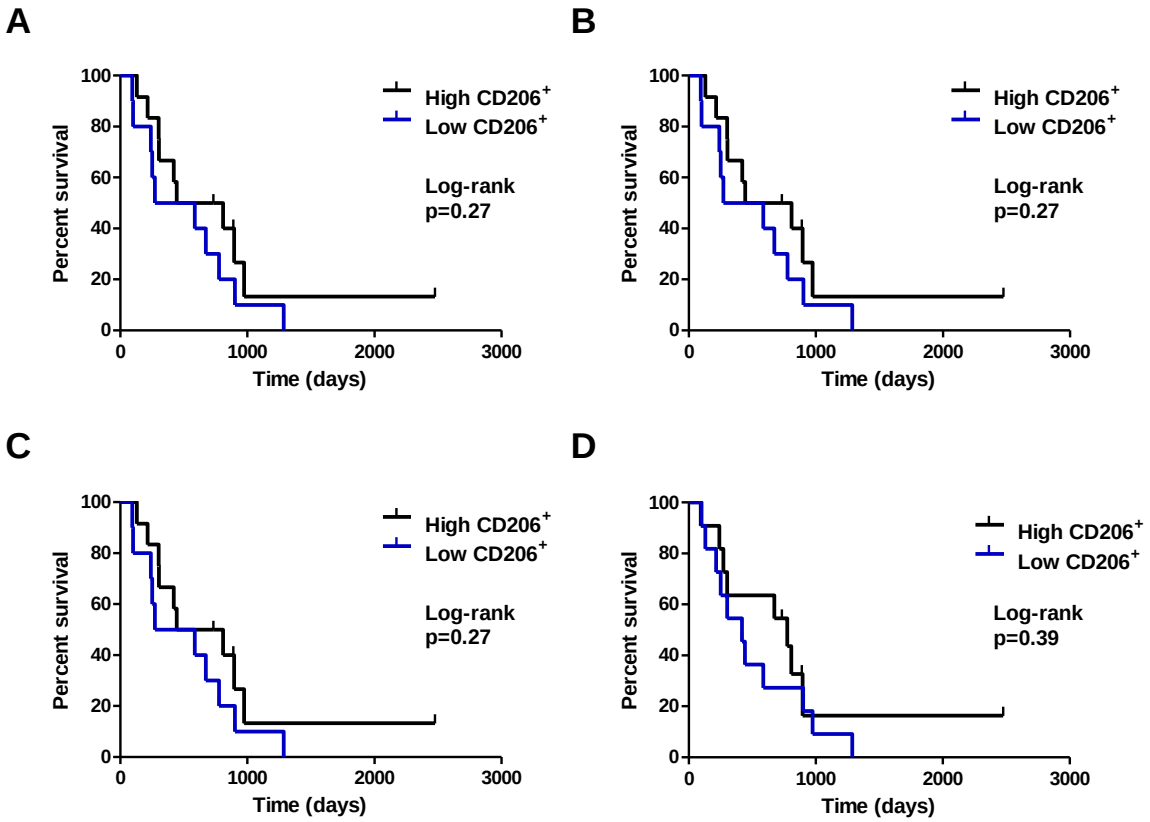

Figure 5-9 Kaplan-Meier analysis for overall survival of PDAC patients on a TMA stained for CD206 at different depths. TMA sections stained for CD206 were scored and patients grouped above and below the median number of cells per core. Only patient samples present on all TMA levels were included. Plotted are survival curves for TMAs at the A) top, B) upper middle and C) bottom levels of the TMA, along with D) overall $CD206^+$ cell counts per patient calculated from across all sections.

5.4 Discussion

The lack of concordance between blood-borne TNC and stromal expression in the tumour microenvironment raised questions about the use of TMAs to quantify stromal characteristics in PDAC. TMAs are commonly used for histological staining assessment in cancer studies, providing numerous benefits over studying whole tissue sections when the analysis of large numbers of patients is desired[148,149]. The main benefit is in the time saved, as the retrieval of blocks for the cutting of sections followed by staining and assessment can take several months, and the process has to be repeated if the analysis of other markers is required. The assembly of a TMA is far more efficient, as once constructed a TMA can be sectioned potentially hundreds of times with each section providing a cohort of patients for analysis of distinct markers. By mapping numerous patient samples to the same section, this can account for staining performance affected by any batch variation. The portability of TMAs also eases collaboration between groups, providing opportunities for multi-centre studies and potentially more robust analyses of patient cohorts.

These benefits are useful if an analysis of markers expressed in tumour cells is desired, as these can be identified on an array and scored with an appropriate method. Whether the use of TMAs is appropriate for studying stroma in PDAC, which in most cases forms the bulk of the tumour microenvironment, was one of the focuses of our group.

In this chapter I have focused on the immune cell component quantified in this study. Positive correlations in the mean abundance of macrophages and M2 macrophages per TMA core were identified, suggesting that our method of quantifying these cells was robust and reproducible. Interestingly, $CD204^+$ and $CD206^+$ cells did not

correlate as strongly with each other as each did with $CD68^+$ cells, despite both being putative markers for M2 macrophages[147]. A possible explanation could be differences in performances of the antibodies used to detect each marker, with differences in sensitivity and cross-reactivity affecting what cell types are quantified. Alternatively the M1/M2 macrophage paradigm is thought to represent extremes of macrophage classification, when it is more likely that the dynamic process of macrophage activation results in cells falling along a continuum[61]. If the expression of CD204 and CD206 varies for cells falling at different stages of the continuum, this could affect the final quantification of stained cells.

More problematically, when investigating the relationship between immune cell prevalence and patient outcome, the conclusions drawn from TMA sections at different depths of the array were not consistent. This raises concerns that if only one section were cut from the array and stained for a particular stromal marker, as is typical in prognostic studies utilising TMAs, then the conclusions from the analysis may vary depending on where in the array that section was cut. Whether this possibility could be minimised by implementing certain measures in the study design, such as ensuring the number of cores per patient exceeds three, has not been addressed in this study. Guidelines suggest that the number of cores selected per patient be chosen based on the heterogeneity of the tumour being studied [150]. Studies investigating the effect of core number in colorectal cancer, lung cancer and prostate cancer tissue conclude that 3-4 cores are optimal depending on the degree of heterogeneity of the tumour[151–153]. It is therefore possible that PDAC stroma heterogeneity requires at least four cores per patient to be sampled, especially given our observation that the number of total remaining cores decreases as the depth into the TMA increases.

Interestingly, the association of $CD68^+$, $CD206^+$ and $CD8^+$ cell number with overall survival was only observed at the top level of TMAs stained for these markers. It is possible that the cores at this level share some characteristic to reveal this observation, though we have been unable to identify what this might be. Median expression of αSMA and cytokeratin, surrogate markers for desmoplastic stroma and tumour epithelia respectively, did not deviate highly at this level compared to others, suggesting that if there is an explanatory feature it is unlikely to be linked simply to bulk composition of the cores in terms of tumour and stroma.

One of the TMA sections was stained for TNC expression, enabling comparisons with the other stromal elements to identify potential relationships. An association was found between positive TNC stromal expression and ASI, a measure of cancer-associated fibroblast activity previously linked to patient outcome[90]. This provides a possible explanation for the heterogeneity of TNC expression in the PDAC tumour microenvironment. The fact that ASI is calculated by quantifying one stromal component as a proportion of another, suggests that scoring TMA cores relative to others can be informative, and may be useful for investigating crosstalk by elements of the stroma. This may also offer a method of bypassing the depth-dependent inconsistencies we have identified in this TMA, when comparing quantified stromal features with patient outcome.

6 Discussion

6.1 Identification and validation of diagnostic biomarkers for pancreatic cancer

The initial aims of this thesis were to identify and validate serum biomarkers for the diagnosis of PDAC, and investigate the expression of these markers in the tumour microenvironment. From there, with the assistance of Mrs Frances Oldfield, I investigated the suitability of using tissue microarrays for the quantification of stromal elements of PDAC.

Myriad RBM-based quantification of 101 cancer-associated proteins in samples from UKCTOCS identified CA125 and CA19-9 as the most obvious markers associated with time to diagnosis, each significantly elevated up to a year prior to PDAC diagnosis compared to healthy controls. These findings corroborated observations in a study already underway by our collaborators, which included a larger set of samples from the UKCTOCS collection[129]. Both of these markers showed sensitivity up to two years prior to diagnosis[129].

CA19-9 was confirmed to be an informative marker in the UoL collection, with significantly increased concentrations in the PDAC cases compared to chronic pancreatitic and healthy controls. Though CA19-9 has been extensively studied, and deemed insufficiently specific as a screening tool for PDAC, I would suggest that CA19-9 should be used as part of a panel of biomarkers for this purpose[94,95,99,100,108]. CA19-9 is best recognised as a tool for disease management, used alongside imaging as an indicator of recurrence, progression or response to therapy[94]. The study by O'Brien *et al*. challenges this notion, suggesting that screening high risk populations for CA19-9 may lead to earlier diagnosis of PDAC in some patients[129].

The complete analysis of the UoL cohort found no single marker uniquely distinguished PDAC cases from benign controls. However, several individual markers appeared to discriminate PDAC cases from specific control groups, in a manner that could be used in combination to increase the sensitivity and specificity for diagnosing PDAC from benign controls. Reliable assays were established to verify the Myriad RBM measurements for tenascin C and IL-6Rβ, markers that significantly discriminated PDAC from CP and benign obstructed jaundice cases respectively. These were tested in an independent cohort of patient samples from the UoL collection. Many biomarkers fail to replicate initial results due to the nature of relatively small sample sizes used for discovery work, especially when considering the variability and complexity of a potential screening population[130]. Reassuringly, significantly higher levels of TNC in PDAC patients compared to CP were also observed in the independent samples, demonstrating superior sensitivity and specificity to CA19-9 for the discrimination of these two groups. Logistic regression modelling to combine the two markers improved the diagnostic accuracy above either marker alone, further supporting the notion that a panel of biomarkers may be required to obtain suitable sensitivity and specificity for screening.

Tenascin C is a large hexameric extracellular matrix glycoprotein that is highly expressed in the developing embryo but negligibly so in most healthy adult tissues[132,154]. Instead, transient expression is observed in sites of high cell turnover and tissue remodelling, and has been detected in areas of chronic inflammation including the stroma of several cancers such as breast, lung and ovarian tumours[154]. In PDAC, functional analyses of cell lines by Paron *et al.* suggest that TNC may play a complex role[155]. They identified a heterogeneous response to increasing doses of

exogenous TNC and growth on a TNC-rich matrix, inhibiting cell growth and migration in some cell lines but with the opposite occurring in others[155].

Identifying biomarkers that can distinguish pancreatic cancer from chronic pancreatitis has proven challenging, in part because pancreatitis is a risk factor for PDAC and the two conditions can present concurrently[92,156]. Consequently, we sought to explain the different TNC levels observed in the circulation of PDAC and CP patients by examining protein expression in the pancreatic tissue (Chapter 3). What emerged was a picture of dynamic regulation of TNC in the PDAC microenvironment, where TNC can be produced and secreted or retained in ductal epithelia of the tumour. Scattered stromal cells with a fibroblast-like phenotype were also occasionally observed to be sources of strong TNC expression in the desmoplastic stroma, a finding supported by *in vitro* analysis of cultured fibroblasts isolated from patient CP and PDAC tissue specimens. A relatively novel RNA *in situ* hybridisation technique identified tumour cells as the source of TNC protein expression in regions of positive stromal, even where no expression was observed in the epithelia[131]. This observation suggests that combining ISH and IHC to examine protein and mRNA expression in the context of a tissue microenvironment is a powerful technique, particularly in elucidating crosstalk between elements of the tumour and stroma.

Studies from other groups have also reported diffuse TNC expression in the stroma surrounding malignant cells and PanIN lesions in a murine and human PDAC setting[110,157,158]. Esposito *et al.* reported moderate to strong TNC expression in eight (80%) out of ten CP tissue sections, a considerably higher percentage than the 14% of CP patients with TNC-positive stroma characterised in our study. Our use of a tissue microarray compared to whole section profiling could be a possible

explanation for this disagreement, as the area of tissue examined in this manner is much smaller than the area of tissue available in a whole section. However the use of a TMA was considered necessary, avoiding problems associated with cutting CP tissue blocks containing calcified stones. Another possible explanation is the difference in choice of antibody between studies. Tenascin C has several splice variants, and our choice of antibody (clone 4C8MS) was specific for those containing the FNIII B domain while that used in the Esposito *et al.* study (clone BC-24) is thought to recognise all isoforms of human tenascin[132,154]. The BC-24 antibody could therefore stain for an alternative splice variant of TNC, present in the stroma of many CP cases, where 4C8MS would not recognise the same. Our choice of antibody replicated the findings from the Myriad RBM serum analysis, and consequently was appropriate for meeting the primary aim of identifying diagnostic biomarkers. By using the 4C8MS antibody for both the serum and tissue analyses, we ruled out affinity for different TNC splice variants as the reason for differences in expression between the two compartments.

We observed that TNC-positive stroma was present in significantly more PDAC patients than CP, supporting the findings of the serum analysis. As the 4C8MS antibody was selected for IHC to match the ELISA used for the serum samples, this corroboration suggests it is important to keep antibodies consistent when comparing a protein's tissue expression to circulatory levels.

Despite the comparable overall pattern of increased TNC tissue expression and circulatory levels in PDAC compared to CP cases, no direct association was found between positive stromal expression and serum concentration. This could be explained by effects on circulating TNC by other tissues and organs, such as other sites of inflammation or fibrosis[132,133]. We also considered the possibility that TMAs

may not be a suitable method for accurately quantifying tissue expression, particularly for comparison with systemic measures of a marker.

Mirus *et al*. also identified TNC as a diagnostic marker for PDAC in plasma from GEMMs and a pre-diagnostic human sample set[110]. Though they did not compare PDAC samples with plasma from CP patients, they did demonstrated that combining their panel of biomarkers with CA19-9 improved diagnostic accuracy, in agreement with our biomarker studies and others[92,110,135].

Discovery work on sera from the UKCTOCS and UoL collections by our group identified thrombospondin-1 as a promising candidate for early diagnosis of PDAC, using multiple reaction monitoring as a means of quantification. The use of a mass spectrometry-based method ensured unambiguous identification and quantification of the marker of interest, but as a relatively novel method I wanted to compare it with TSP-1 levels measured in both UKCTOCS and UoL serum collections using more conventional immunoassays. In doing so I also confirmed that the TSP-1 antibody (clone A6.1) was suitably specific for tissue analysis by IHC.

Quantification of serum TSP-1 by ELISA and western blotting demonstrated a trend consistent with that observed when measured by MRM, though not as consistently statistically significant. However, the correlation between western blotting and MRM was stronger in the UoL samples compared to UKCTOCS, suggesting that the differences in sample processing had affected the antibody's affinity for TSP-1. Moreover, a study by Annis *et al.* had reported weak cross-reactivity of our selected antibody (clone A6.1) with thrombospondin-2 when used for western blotting[142]. Together, this would suggest MRM is the most suitable method for quantifying TSP-1 in our serum cohorts. Though optimising MRM assays for each protein of interest

can be time-consuming, the results of this study suggest it is an excellent technique if a suitably specific antibody cannot be acquired[159].

The observation that circulating TSP-1 levels were reduced in cases from the UKCTOCS cohort compared to controls suggested that this marker may change prior to the development of PDAC. We sought to independently address this question using sera from KPC mice collected at different stages of disease. This particular mouse model has been extensively studied and is thought to faithfully reproduce the development of PDAC from the formation of pre-neoplastic lesions to advanced and metastatic cancer[143,160]. Serum analysis for TSP-1 revealed low circulatory levels of TSP-1 in mice with PDAC but not in healthy mice nor in those bearing PanIN lesions alone. This raises the possibility that decreased TSP-1 levels observed in pre-diagnostic sera occur in a background of already developed PDAC. It also suggests that genetically modified mouse models are an appropriate tool for identifying diagnostic biomarkers, as utilised by other studies[92,110,120].

At present we have not been able to identify a mechanism explaining the lower circulating levels of TSP-1. TSP-1 is a matricellular glycoprotein thought to be an attenuator of inflammation and inhibitor of angiogenesis, through interacting with endothelial cells in a CD36-dependent manner to induce apoptosis and inhibit cell-cycle progression, as well as antagonising VEGF function in the extracellular matrix[161,162]. Consequently, it is thought to have anti-carcinogenic properties[161]. Reports investigating circulatory TSP-1 levels in other tumour contexts are mixed, with elevated plasma levels reported in breast cancer but decreased levels in serum from lung and prostate cancer patients[163–165]. Pan *et al.* measured TSP-1 in plasma from healthy subjects and patients with PDAC and chronic pancreatitis, using the

same ELISA kit used in Chapter 4, and observed slightly increased levels of TSP-1 in cancer compared to the benign controls[166].

My colleagues extended the analysis of TSP-1 and demonstrated that combining with CA19-9 significantly improved diagnostic accuracy over either marker alone[135]. They also discovered a link between TSP-1 and PDAC-associated diabetes, noting significantly lower levels in the diabetic PDAC samples compared to non-diabetic cases and all other controls[135]. Though further work is needed to reveal the extent of this relationship, the identification of biomarkers specific for cancer-associated diabetes (type IIIC) compared to type II diabetes patients would be invaluable for use as a screening tool[167]. Future investigations into biomarkers for PDAC should consider diabetic subjects when selecting control groups to test against[92].

6.2 Evaluation of tissue microarrays as a means of quantifying stromal elements of pancreatic cancer

Both tenascin C and thrombospondin-1 circulating levels were compared with respective tissue expression to attempt to discern a relationship. Though the overall trends for TNC expression in tissue and serum between PDAC and CP patients were consistent, no direct correlation was found. We hypothesised that the use of TMAs for this analysis may be the cause, with too small an area of tissue examined to accurately quantify the pancreatic stromal expression. Given more time and sample availability, a comparison of circulatory levels with matched whole tissue sections may fully address this question.

Elucidating the features and functions of stroma in PDAC is currently a highly active area of research, both in understanding the roles the various features play in tumour biology and as a target for therapy[33,34]. PDAC has a particularly pronounced stromal compartment, both at the site of origin and at distant metastases, consisting of extracellular matrix, soluble proteins, blood vessels, lymphatic vessels, immune cells and fibroblasts[33–35,79]. Tissue microarrays are commonly used for high powered cancer studies when histological assessment is required[148,149]. PDAC is no exception, where several studies have investigated the tumour and stromal compartments in tissue samples using this method[89,168–170]. The time saved using a TMA compared to analysing an equivalent number of patients separately, coupled with the overcoming of staining variation problems from batch effects, makes it a convenient method for quantifying and studying elements of the microenvironment. Given the results of the analysis of TNC and TSP-1 in Chapter 3 and Chapter 4 I, along with my colleagues,

undertook a study investigating if the use of TMAs for quantifying stromal components was appropriate for PDAC.

To address this question, a TMA of PDAC patient samples was sectioned completely and stained for immune cells, desmoplasia and epithelia, to investigate stromal composition and consistency at different depths of the array. Counts for macrophages, stained for CD68, and M2 macrophages, stained for CD204 and CD206, strongly correlated with each other when mean patient values were matched, suggesting that our method of quantifying these cells was robust and reproducible.

Macrophages are commonly classified as M1 or M2 macrophages, though most fall along a continuum, with M2-polarised macrophages thought to be more abundant in a tumour context[61]. Kurahara *et al.* reported greater numbers of M2 macrophages at the tumour invasive front associated with poorer overall survival in patients with PDAC, with a near-significant association also observed for $CD68^+$ macrophages[62]. Our analysis of the relationship between macrophage abundance and prognosis yielded mixed results. At the top level, high $CD68^+$ and $CD206^+$ but not $CD204^+$ cell counts were associated with a favourable prognosis, in contrast to the study by Kurahara *et al*. No association was observed at any of the other TMA depths, suggesting there was some as-yet-unidentified property of the cores at the top level TMA that gave this conclusion. It is possible that the random nature of what constitutes the cores on a TMA section, particularly once a TMA has been sectioned extensively, leads to a loss of information that can abrogate the usefulness of quantifying these cell types for prognostic analyses. Kurahara *et al*. limited areas of scoring to the invasive edge of the tumour before conducting their analysis, suggesting that such an approach may be required for the association of M2 macrophages with survival to become apparent.

Ene-Obong *et al.* took a similar approach when noting an association between high numbers of $CD8^+$ cytotoxic T cells and a more favourable prognosis post-resection[168]. Here they quantified $CD8^+$ cells in separate stromal areas, classified by proximity to tumour cells; they noted a significant survival benefit to high $CD8^+$ abundance in the tumour-adjacent regions, but not when counting those from the rest of the stromal compartment. In a similar manner to the macrophage results, our analysis revealed a significant association between $CD8^+$ cell count and prolonged survival but only at the top level of the TMA. In this context, it is possible that a greater number of cores at the top level contained tumour-adjacent stroma than at other levels, though the median cytokeratin-positive area per core at the top level was not drastically different to any other TMA depth (Table 5.4). Repeating our analysis by reclassifying $CD8^+$ cell scores by proximity to tumour, may address whether such a method overcomes the problem of inconsistency we observed at different TMA depths.

Another possible explanation for the inconsistency lies in the number of cores selected per patient when constructing the array. Previous studies recommend that the number of cores be selected based on the heterogeneity of the tumour being studied, with analyses of colorectal, lung and prostate cancer TMAs concluding that 3-4 cores are optimal[150–153]. Given the heterogeneity of stromal components noted in this study, a similar analysis for PDAC may be warranted, testing core numbers in excess of the three used for our TMAs to see if more consistent conclusions can be reached at different depths.

In summary, we aimed to identify diagnostic markers in the serum of pancreatic cancer patients and relate this to expression in the pancreas microenvironment. I have identified a candidate biomarker that can distinguish patients with PDAC from chronic pancreatitis, and have discovered a potential mechanism to explain this based on expression in the tissue microenvironment. I have helped to validate a promising biomarker for the early diagnosis of PDAC, both in human and murine samples, and compared different methods of quantifying proteins in the serum. From there I investigated whether tissue microarrays are appropriate for quantifying components of the pancreatic tumour stroma, concluding that caution should be taken when comparing the abundance of stromal elements with clinical outcome. Instead, quantifying in relation to other features of the microenvironment may be required.

7 REFERENCES

1. Hanahan, D. & Weinberg, R. A. The Hallmarks of Cancer. *Cell* **100,** 57–70 (2000).
2. Hanahan, D. & Weinberg, R. A. Hallmarks of Cancer: The Next Generation. *Cell* **144,** 646–674 (2011).
3. Siegel, R. L., Miller, K. D. & Jemal, A. Cancer statistics, 2015. *CA. Cancer J. Clin.* **65,** 5–29 (2015).
4. Hidalgo, M. Pancreatic Cancer. *N. Engl. J. Med.* **362,** 1605–1617 (2010).
5. Ryan, D. P., Hong, T. S. & Bardeesy, N. Pancreatic Adenocarcinoma. *N. Engl. J. Med.* **371,** 1039–1049 (2014).
6. Vincent, A., Herman, J., Schulick, R., Hruban, R. H. & Goggins, M. Pancreatic cancer. *The Lancet* **378,** 607–620 (2011).
7. Rahib, L. *et al.* Projecting Cancer Incidence and Deaths to 2030: The Unexpected Burden of Thyroid, Liver, and Pancreas Cancers in the United States. *Cancer Res.* **74,** 2913–2921 (2014).
8. Wray, C. J., Ahmad, S. A., Matthews, J. B. & Lowy, A. M. Surgery for Pancreatic Cancer: Recent Controversies and Current Practice. *Gastroenterology* **128,** 1626–1641 (2005).
9. Bilimoria, K. Y. *et al.* National Failure to Operate on Early Stage Pancreatic Cancer. *Ann. Surg.* **246,** 173–180 (2007).
10. Neoptolemos JP, Stocken DD, Bassi C & et al. Adjuvant chemotherapy with fluorouracil plus folinic acid vs gemcitabine following pancreatic cancer resection: A randomized controlled trial. *JAMA* **304,** 1073–1081 (2010).
11. Neoptolemos, J. P. *et al.* A Randomized Trial of Chemoradiotherapy and Chemotherapy after Resection of Pancreatic Cancer. *N. Engl. J. Med.* **350,** 1200–1210 (2004).
12. Neoptolemos, J. P. *et al.* Adjuvant 5-fluorouracil and folinic acid vs observation for pancreatic cancer: composite data from the ESPAC-1 and -3(v1) trials. *Br. J. Cancer* **100,** 246–250 (2009).

13. Regine WF, Winter KA, Abrams RA & et al. Fluorouracil vs gemcitabine chemotherapy before and after fluorouracil-based chemoradiation following resection of pancreatic adenocarcinoma: A randomized controlled trial. *JAMA* **299,** 1019–1026 (2008).
14. Oettle H, Post S, Neuhaus P & et al. Adjuvant chemotherapy with gemcitabine vs observation in patients undergoing curative-intent resection of pancreatic cancer: A randomized controlled trial. *JAMA* **297,** 267–277 (2007).
15. Sultana, A. *et al.* Meta-Analyses of Chemotherapy for Locally Advanced and Metastatic Pancreatic Cancer. *J. Clin. Oncol.* **25,** 2607–2615 (2007).
16. Conroy, T. *et al.* FOLFIRINOX versus Gemcitabine for Metastatic Pancreatic Cancer. *N. Engl. J. Med.* **364,** 1817–1825 (2011).
17. Von Hoff, D. D. *et al.* Increased Survival in Pancreatic Cancer with nab-Paclitaxel plus Gemcitabine. *N. Engl. J. Med.* **369,** 1691–1703 (2013).
18. Goldstein, D. *et al.* nab-Paclitaxel Plus Gemcitabine for Metastatic Pancreatic Cancer: Long-Term Survival From a Phase III Trial. *J. Natl. Cancer Inst.* **107,** dju413 (2015).
19. Smit, V. T. *et al.* KRAS codon 12 mutations occur very frequently in pancreatic adenocarcinomas. *Nucleic Acids Res.* **16,** 7773–7782 (1988).
20. Almoguera, C. *et al.* Most human carcinomas of the exocrine pancreas contain mutant c-K-ras genes. *Cell* **53,** 549–554 (1988).
21. Feldmann, G., Beaty, R., Hruban, R. H. & Maitra, A. Molecular genetics of pancreatic intraepithelial neoplasia. *J. Hepatobiliary. Pancreat. Surg.* **14,** 224–232 (2007).
22. Maitra, A., Fukushima, N., Takaori, K. & Hruban, R. H. Precursors to invasive pancreatic cancer. *Adv. Anat. Pathol.* **12,** 81–91 (2005).
23. Hruban, R. H. *et al.* Pancreatic intraepithelial neoplasia: a new nomenclature and classification system for pancreatic duct lesions. *Am. J. Surg. Pathol.* **25,** 579–586 (2001).

24. Kanda, M. *et al.* Presence of Somatic Mutations in Most Early-Stage Pancreatic Intraepithelial Neoplasia. *Gastroenterology* **142,** 730–733.e9 (2012).

25. Amato, E. *et al.* Targeted next-generation sequencing of cancer genes dissects the molecular profiles of intraductal papillary neoplasms of the pancreas. *J. Pathol.* **233,** 217–227 (2014).

26. Hruban, R. H. *et al.* An illustrated consensus on the classification of pancreatic intraepithelial neoplasia and intraductal papillary mucinous neoplasms. *Am. J. Surg. Pathol.* **28,** 977–987 (2004).

27. Canto, M. I. *et al.* Frequent Detection of Pancreatic Lesions in Asymptomatic High-Risk Individuals. *Gastroenterology* **142,** 796–804 (2012).

28. Biankin, A. V. *et al.* Pancreatic cancer genomes reveal aberrations in axon guidance pathway genes. *Nature* **491,** 399–405 (2012).

29. Jones, S. *et al.* Core Signaling Pathways in Human Pancreatic Cancers Revealed by Global Genomic Analyses. *Science* **321,** 1801–1806 (2008).

30. Yachida, S. *et al.* Distant metastasis occurs late during the genetic evolution of pancreatic cancer. *Nature* **467,** 1114–1117 (2010).

31. Campbell, P. J. *et al.* The patterns and dynamics of genomic instability in metastatic pancreatic cancer. *Nature* **467,** 1109–1113 (2010).

32. Waddell, N. *et al.* Whole genomes redefine the mutational landscape of pancreatic cancer. *Nature* **518,** 495–501 (2015).

33. Feig, C. *et al.* The pancreas cancer microenvironment. *Clin. Cancer Res. Off. J. Am. Assoc. Cancer Res.* **18,** 4266–4276 (2012).

34. Neesse, A., Algül, H., Tuveson, D. A. & Gress, T. M. Stromal biology and therapy in pancreatic cancer: a changing paradigm. *Gut* (2015). doi:10.1136/gutjnl-2015-309304

35. Evans, A. & Costello, E. The role of inflammatory cells in fostering pancreatic cancer cell growth and invasion. *Front. Physiol.* **3,** 270 (2012).

36. Wörmann, S. M., Diakopoulos, K. N., Lesina, M. & Algül, H. The immune network in pancreatic cancer development and progression. *Oncogene* **33,** 2956–2967 (2014).

37. Lowenfels, A. B. *et al.* Pancreatitis and the risk of pancreatic cancer. International Pancreatitis Study Group. *N. Engl. J. Med.* **328,** 1433–1437 (1993).

38. McKay, C. J., Glen, P. & McMillan, D. C. Chronic inflammation and pancreatic cancer. *Best Pract. Res. Clin. Gastroenterol.* **22,** 65–73 (2008).

39. Guerra, C. *et al.* Chronic pancreatitis is essential for induction of pancreatic ductal adenocarcinoma by K-Ras oncogenes in adult mice. *Cancer Cell* **11,** 291–302 (2007).

40. Morris, J. P., Cano, D. A., Sekine, S., Wang, S. C. & Hebrok, M. Beta-catenin blocks Kras-dependent reprogramming of acini into pancreatic cancer precursor lesions in mice. *J. Clin. Invest.* **120,** 508–520 (2010).

41. Guerra, C. *et al.* Pancreatitis-induced inflammation contributes to pancreatic cancer by inhibiting oncogene-induced senescence. *Cancer Cell* **19,** 728–739 (2011).

42. Pagès, F. *et al.* Immune infiltration in human tumors: a prognostic factor that should not be ignored. *Oncogene* **29,** 1093–1102 (2010).

43. Roxburgh, C. S. D. & McMillan, D. C. The role of the in situ local inflammatory response in predicting recurrence and survival in patients with primary operable colorectal cancer. *Cancer Treat. Rev.* **38,** 451–466 (2012).

44. Gilfillan, A. M. & Beaven, M. A. Regulation of mast cell responses in health and disease. *Crit. Rev. Immunol.* **31,** 475–529 (2011).

45. Ribatti, D. & Crivellato, E. Mast cells, angiogenesis and cancer. *Adv. Exp. Med. Biol.* **716,** 270–288 (2011).

46. Chang, D. Z. *et al.* Mast Cells in Tumor Microenvironment Promotes the in vivo Growth of Pancreatic Ductal Adenocarcinoma. *Clin. Cancer Res. Off. J. Am. Assoc. Cancer Res.* **17,** 7015–7023 (2011).

47. Esposito, I. *et al.* Inflammatory cells contribute to the generation of an angiogenic phenotype in pancreatic ductal adenocarcinoma. *J. Clin. Pathol.* **57,** 630–636 (2004).

48. Cai, S.-W. *et al.* Prognostic significance of mast cell count following curative resection for pancreatic ductal adenocarcinoma. *Surgery* **149,** 576–584 (2011).

49. Schönhuber, N. *et al.* A next-generation dual-recombinase system for time- and host-specific targeting of pancreatic cancer. *Nat. Med.* **20,** 1340–1347 (2014).

50. Feyerabend, T. B. *et al.* Cre-Mediated Cell Ablation Contests Mast Cell Contribution in Models of Antibody- and T Cell-Mediated Autoimmunity. *Immunity* **35,** 832–844 (2011).

51. Ochando, J. C. & Chen, S. H. Myeloid-derived suppressor cells in transplantation and cancer. *Immunol. Res.* **54,** 275–285 (2012).

52. Ostrand-Rosenberg, S. & Sinha, P. Myeloid-derived suppressor cells: linking inflammation and cancer. *J. Immunol. Baltim. Md 1950* **182,** 4499–4506 (2009).

53. Ostrand-Rosenberg, S., Sinha, P., Beury, D. W. & Clements, V. K. Cross-talk between myeloid-derived suppressor cells (MDSC), macrophages, and dendritic cells enhances tumor-induced immune suppression. *Semin. Cancer Biol.* **22,** 275–281 (2012).

54. Kusmartsev, S., Nefedova, Y., Yoder, D. & Gabrilovich, D. I. Antigen-specific inhibition of CD8+ T cell response by immature myeloid cells in cancer is mediated by reactive oxygen species. *J. Immunol. Baltim. Md 1950* **172,** 989–999 (2004).

55. Clark, C. E. *et al.* Dynamics of the immune reaction to pancreatic cancer from inception to invasion. *Cancer Res.* **67,** 9518–9527 (2007).

56. Pylayeva-Gupta, Y., Lee, K. E., Hajdu, C. H., Miller, G. & Bar-Sagi, D. Oncogenic Kras-induced GM-CSF production promotes the development of pancreatic neoplasia. *Cancer Cell* **21,** 836–847 (2012).

57. Bayne, L. J. *et al.* Tumor-derived granulocyte-macrophage colony stimulating factor regulates myeloid inflammation and T cell immunity in pancreatic cancer. *Cancer Cell* **21,** 822–835 (2012).

58. Stromnes, I. M. *et al.* Targeted depletion of an MDSC subset unmasks pancreatic ductal adenocarcinoma to adaptive immunity. *Gut* **63,** 1769–1781 (2014).

59. Coussens, L. M. & Werb, Z. Inflammation and cancer. *Nature* **420,** 860–867 (2002).

60. Ruffell, B., Affara, N. I. & Coussens, L. M. Differential macrophage programming in the tumor microenvironment. *Trends Immunol.* **33,** 119–126 (2012).

61. Sica, A. & Mantovani, A. Macrophage plasticity and polarization: in vivo veritas. *J. Clin. Invest.* **122,** 787–795 (2012).

62. Kurahara, H. *et al.* Significance of M2-polarized tumor-associated macrophage in pancreatic cancer. *J. Surg. Res.* **167,** e211–219 (2011).

63. Lesina, M. *et al.* Stat3/Socs3 Activation by IL-6 Transsignaling Promotes Progression of Pancreatic Intraepithelial Neoplasia and Development of Pancreatic Cancer. *Cancer Cell* **19,** 456–469 (2011).

64. Weizman, N. *et al.* Macrophages mediate gemcitabine resistance of pancreatic adenocarcinoma by upregulating cytidine deaminase. *Oncogene* **33,** 3812–3819 (2014).

65. von Bernstorff, W. *et al.* Systemic and local immunosuppression in pancreatic cancer patients. *Clin. Cancer Res. Off. J. Am. Assoc. Cancer Res.* **7,** 925s–932s (2001).

66. Gabitass, R. F., Annels, N. E., Stocken, D. D., Pandha, H. A. & Middleton, G. W. Elevated myeloid-derived suppressor cells in pancreatic, esophageal and gastric cancer are an independent prognostic factor and are associated with significant

elevation of the Th2 cytokine interleukin-13. *Cancer Immunol. Immunother.* **60,** 1419–1430 (2011).

67. Hiraoka, N., Onozato, K., Kosuge, T. & Hirohashi, S. Prevalence of FOXP3+ Regulatory T Cells Increases During the Progression of Pancreatic Ductal Adenocarcinoma and Its Premalignant Lesions. *Clin. Cancer Res.* **12,** 5423–5434 (2006).
68. Josefowicz, S. Z., Lu, L.-F. & Rudensky, A. Y. Regulatory T cells: mechanisms of differentiation and function. *Annu. Rev. Immunol.* **30,** 531–564 (2012).
69. O'Shea, J. J. & Paul, W. E. Mechanisms Underlying Lineage Commitment and Plasticity of Helper CD4+ T Cells. *Science* **327,** 1098–1102 (2010).
70. Tassi, E. *et al.* Carcinoembryonic Antigen-Specific but Not Antiviral CD4+ T Cell Immunity Is Impaired in Pancreatic Carcinoma Patients. *J. Immunol.* **181,** 6595–6603 (2008).
71. De Monte, L. *et al.* Intratumor T helper type 2 cell infiltrate correlates with cancer-associated fibroblast thymic stromal lymphopoietin production and reduced survival in pancreatic cancer. *J. Exp. Med.* **208,** 469–478 (2011).
72. McAllister, F. *et al.* Oncogenic Kras Activates a Hematopoietic-to-Epithelial IL-17 Signaling Axis in Preinvasive Pancreatic Neoplasia. *Cancer Cell* **25,** 621–637 (2014).
73. Apte, M. *et al.* Periacinar stellate shaped cells in rat pancreas: identification, isolation, and culture. *Gut* **43,** 128–133 (1998).
74. Bachem, M. G. *et al.* Identification, culture, and characterization of pancreatic stellate cells in rats and humans. *Gastroenterology* **115,** 421–432 (1998).
75. Hwang, R. F. *et al.* Cancer-associated stromal fibroblasts promote pancreatic tumor progression. *Cancer Res.* **68,** 918–926 (2008).

76. Bachem, M. G. *et al.* Pancreatic carcinoma cells induce fibrosis by stimulating proliferation and matrix synthesis of stellate cells. *Gastroenterology* **128,** 907–921 (2005).

77. Vonlaufen, A. *et al.* Pancreatic stellate cells: partners in crime with pancreatic cancer cells. *Cancer Res.* **68,** 2085–2093 (2008).

78. Xu, Z. *et al.* Role of Pancreatic Stellate Cells in Pancreatic Cancer Metastasis. *Am. J. Pathol.* **177,** 2585–2596 (2010).

79. Whatcott, C. J. *et al.* Desmoplasia in primary tumors and metastatic lesions of pancreatic cancer. *Clin. Cancer Res.* clincanres.1051.2014 (2015). doi:10.1158/1078-0432.CCR-14-1051

80. Olive, K. P. *et al.* Inhibition of Hedgehog Signaling Enhances Delivery of Chemotherapy in a Mouse Model of Pancreatic Cancer. *Science* **324,** 1457–1461 (2009).

81. Provenzano, P. P. *et al.* Enzymatic Targeting of the Stroma Ablates Physical Barriers to Treatment of Pancreatic Ductal Adenocarcinoma. *Cancer Cell* **21,** 418–429 (2012).

82. Jacobetz, M. A. *et al.* Hyaluronan impairs vascular function and drug delivery in a mouse model of pancreatic cancer. *Gut* **62,** 112–120 (2013).

83. McCarroll, J. A. *et al.* Role of pancreatic stellate cells in chemoresistance in pancreatic cancer. *Front. Physiol.* **5,** 141 (2014).

84. Lee, J. J. *et al.* Stromal response to Hedgehog signaling restrains pancreatic cancer progression. *Proc. Natl. Acad. Sci. U. S. A.* **111,** E3091–3100 (2014).

85. Rhim, A. D. *et al.* Stromal elements act to restrain, rather than support, pancreatic ductal adenocarcinoma. *Cancer Cell* **25,** 735–747 (2014).

86. Özdemir, B. C. *et al.* Depletion of carcinoma-associated fibroblasts and fibrosis induces immunosuppression and accelerates pancreas cancer with reduced survival. *Cancer Cell* **25,** 719–734 (2014).

87. Feig, C. *et al.* Targeting CXCL12 from FAP-expressing carcinoma-associated fibroblasts synergizes with anti-PD-L1 immunotherapy in pancreatic cancer. *Proc. Natl. Acad. Sci. U. S. A.* **110,** 20212–20217 (2013).

88. Sherman, M. H. *et al.* Vitamin D receptor-mediated stromal reprogramming suppresses pancreatitis and enhances pancreatic cancer therapy. *Cell* **159,** 80–93 (2014).

89. Sinn, M. *et al.* α-Smooth muscle actin expression and desmoplastic stromal reaction in pancreatic cancer: results from the CONKO-001 study. *Br. J. Cancer* **111,** 1917–1923 (2014).

90. Erkan, M. *et al.* The activated stroma index is a novel and independent prognostic marker in pancreatic ductal adenocarcinoma. *Clin. Gastroenterol. Hepatol. Off. Clin. Pract. J. Am. Gastroenterol. Assoc.* **6,** 1155–1161 (2008).

91. Rhim, A. D. *et al.* EMT and dissemination precede pancreatic tumor formation. *Cell* **148,** 349–361 (2012).

92. Jenkinson, C. *et al.* Biomarkers for early diagnosis of pancreatic cancer. *Expert Rev. Gastroenterol. Hepatol.* **9,** 305–315 (2015).

93. Tonack, S., Aspinall-O'Dea, M., Neoptolemos, J. P. & Costello, E. Pancreatic cancer: proteomic approaches to a challenging disease. *Pancreatol. Off. J. Int. Assoc. Pancreatol. IAP Al* **9,** 567–576 (2009).

94. Locker, G. Y. *et al.* ASCO 2006 Update of Recommendations for the Use of Tumor Markers in Gastrointestinal Cancer. *J. Clin. Oncol.* **24,** 5313–5327 (2006).

95. Wong, D. *et al.* Serum CA19-9 decline compared to radiographic response as a surrogate for clinical outcomes in patients with metastatic pancreatic cancer receiving chemotherapy. *Pancreas* **37,** 269–274 (2008).

96. Huang, Z. & Liu, F. Diagnostic value of serum carbohydrate antigen 19-9 in pancreatic cancer: a meta-analysis. *Tumour Biol. J. Int. Soc. Oncodevelopmental Biol. Med.* **35,** 7459–7465 (2014).

97. Tempero, M. A. *et al.* Relationship of carbohydrate antigen 19-9 and Lewis antigens in pancreatic cancer. *Cancer Res.* **47,** 5501–5503 (1987).

98. Brand, R. E. *et al.* Serum Biomarker Panels for the Detection of Pancreatic Cancer. *Clin. Cancer Res. Off. J. Am. Assoc. Cancer Res.* **17,** 805–816 (2011).

99. Park, H.-D. *et al.* Serum CA19-9, cathepsin D, and matrix metalloproteinase-7 as a diagnostic panel for pancreatic ductal adenocarcinoma. *Proteomics* **12,** 3590–3597 (2012).

100. Gold, D. V. *et al.* PAM4 Immunoassay Alone and in Combination with CA19-9 for the Detection of Pancreatic Adenocarcinoma. *Cancer* **119,** 522–528 (2013).

101. Yan, L. *et al.* Confounding Effect of Obstructive Jaundice in the Interpretation of Proteomic Plasma Profiling Data for Pancreatic Cancer. *J. Proteome Res.* **8,** 142–148 (2009).

102. Tonack, S. *et al.* iTRAQ reveals candidate pancreatic cancer serum biomarkers: influence of obstructive jaundice on their performance. *Br. J. Cancer* **108,** 1846–1853 (2013).

103. Nie, S. *et al.* Glycoprotein Biomarker Panel for Pancreatic Cancer Discovered by Quantitative Proteomics Analysis. *J. Proteome Res.* **13,** 1873–1884 (2014).

104. Shaw, V. E. *et al.* Serum cytokine biomarker panels for discriminating pancreatic cancer from benign pancreatic disease. *Mol. Cancer* **13,** 114 (2014).

105. Sener, S. F., Fremgen, A., Menck, H. R. & Winchester, D. P. Pancreatic cancer: a report of treatment and survival trends for 100,313 patients diagnosed from 1985-1995, using the National Cancer Database. *J. Am. Coll. Surg.* **189,** 1–7 (1999).

106. Jenkinson, C. *et al.* Evaluation in pre-diagnosis samples discounts ICAM-1 and TIMP-1 as biomarkers for earlier diagnosis of pancreatic cancer. *J. Proteomics* **113,** 400–402 (2015).

107. Pan, S. *et al.* A multiplex targeted proteomic assay for biomarker detection in plasma: a pancreatic cancer biomarker case study. *J. Proteome Res.* **11,** 1937–1948 (2012).

108. Makawita, S. *et al.* Validation of four candidate pancreatic cancer serological biomarkers that improve the performance of CA19.9. *BMC Cancer* **13,** 404 (2013).

109. Faca, V. M. *et al.* A Mouse to Human Search for Plasma Proteome Changes Associated with Pancreatic Tumor Development. *PLoS Med* **5,** e123 (2008).

110. Mirus, J. E. *et al.* Cross-Species Antibody Microarray Interrogation Identifies a 3-Protein Panel of Plasma Biomarkers for Early Diagnosis of Pancreas Cancer. *Clin. Cancer Res.* **21,** 1764–1771 (2015).

111. Zeh, H. J. *et al.* Multianalyte profiling of serum cytokines for detection of pancreatic cancer. *Cancer Biomark. Sect. Dis. Markers* **1,** 259–269 (2005).

112. Tomaino, B. *et al.* Circulating autoantibodies to phosphorylated α-enolase are a hallmark of pancreatic cancer. *J. Proteome Res.* **10,** 105–112 (2011).

113. Bracci, P. M., Zhou, M., Young, S. & Wiemels, J. Serum autoantibodies to pancreatic cancer antigens as biomarkers of pancreas cancer in a San Francisco Bay Area case-control study. *Cancer* **118,** 5384–5394 (2012).

114. Capello, M. *et al.* Autoantibodies to Ezrin are an early sign of pancreatic cancer in humans and in genetically engineered mouse models. *J. Hematol. Oncol.J Hematol Oncol* **6,** 67 (2013).

115. Radon, T. P. *et al.* Identification of a Three-Biomarker Panel in Urine for Early Detection of Pancreatic Adenocarcinoma. *Clin. Cancer Res.* **21,** 3512–3521 (2015).

116. Mitchell, P. S. *et al.* Circulating microRNAs as stable blood-based markers for cancer detection. *Proc. Natl. Acad. Sci. U. S. A.* **105,** 10513–10518 (2008).

117. Morimura, R. *et al.* Novel diagnostic value of circulating miR-18a in plasma of patients with pancreatic cancer. *Br. J. Cancer* **105,** 1733–1740 (2011).

118. Baraniskin, A. *et al.* Circulating U2 small nuclear RNA fragments as a novel diagnostic biomarker for pancreatic and colorectal adenocarcinoma. *Int. J. Cancer* **132,** E48–E57 (2013).

119. Li, A. *et al.* Epigenetic silencing of transcription factor SIP1 in pancreatic cancer cells is associated with elevated expression and blood serum levels of microRNAs miR-200a,b. *Cancer Res.* **70,** 5226–5237 (2010).

120. Melo, S. A. *et al.* Glypican-1 identifies cancer exosomes and detects early pancreatic cancer. *Nature* **523,** 177–182 (2015).

121. Dunbar, S. A. Applications of Luminex® xMAP™ technology for rapid, high-throughput multiplexed nucleic acid detection. *Clin. Chim. Acta* **363,** 71–82 (2006).

122. Dive, C. *et al.* Considerations for the use of plasma cytokeratin 18 as a biomarker in pancreatic cancer. *Br. J. Cancer* **102,** 577–582 (2010).

123. Ballehaninna, U. K. & Chamberlain, R. S. The clinical utility of serum CA 19-9 in the diagnosis, prognosis and management of pancreatic adenocarcinoma: An evidence based appraisal. *J. Gastrointest. Oncol.* **3,** 105–119 (2012).

124. Bedi, M. M. S. *et al.* CA 19-9 to differentiate benign and malignant masses in chronic pancreatitis: is there any benefit? *Indian J. Gastroenterol.* **28,** 24–27 (2009).

125. Menon, U. *et al.* Sensitivity and specificity of multimodal and ultrasound screening for ovarian cancer, and stage distribution of detected cancers: results of the prevalence screen of the UK Collaborative Trial of Ovarian Cancer Screening (UKCTOCS). *Lancet Oncol.* **10,** 327–340 (2009).

126. Hosmer, D. W., Jr., Lemeshow, S. & Sturdivant, R. X. *Applied Logistic Regression*. (John Wiley & Sons, 2013).

127. Peduzzi, P., Concato, J., Kemper, E., Holford, T. R. & Feinstein, A. R. A simulation study of the number of events per variable in logistic regression analysis. *J. Clin. Epidemiol.* **49,** 1373–1379 (1996).

128. Vittinghoff, E. & McCulloch, C. E. Relaxing the rule of ten events per variable in logistic and Cox regression. *Am. J. Epidemiol.* **165,** 710–718 (2007).

129. O'Brien, D. P. *et al.* Serum CA19-9 is significantly upregulated up to 2 years before diagnosis with pancreatic cancer: implications for early disease detection. *Clin. Cancer Res. Off. J. Am. Assoc. Cancer Res.* **21,** 622–631 (2015).

130. Drucker, E. & Krapfenbauer, K. Pitfalls and limitations in translation from biomarker discovery to clinical utility in predictive and personalised medicine. *EPMA J.* **4,** 7 (2013).

131. Wang, F. *et al.* RNAscope: A Novel in Situ RNA Analysis Platform for Formalin-Fixed, Paraffin-Embedded Tissues. *J. Mol. Diagn. JMD* **14,** 22–29 (2012).

132. Midwood, K. S., Hussenet, T., Langlois, B. & Orend, G. Advances in tenascin-C biology. *Cell. Mol. Life Sci.* **68,** 3175–3199 (2011).

133. Midwood, K. S. & Orend, G. The role of tenascin-C in tissue injury and tumorigenesis. *J. Cell Commun. Signal.* **3,** 287–310 (2009).

134. Imanaka-Yoshida, K. Tenascin-C in cardiovascular tissue remodeling: from development to inflammation and repair. *Circ. J. Off. J. Jpn. Circ. Soc.* **76,** 2513–2520 (2012).

135. Jenkinson, C. *et al.* Decreased serum thrombospondin-1 levels in pancreatic cancer patients up to 24 months prior to clinical diagnosis: association with diabetes mellitus. *Clin. Cancer Res.* **(Accepted manuscript),** (2015).

136. Armstrong, A. J. *et al.* Long-term Survival and Biomarker Correlates of Tasquinimod Efficacy in a Multicenter Randomized Study of Men with Minimally Symptomatic Metastatic Castration-Resistant Prostate Cancer. *Clin. Cancer Res.* **19,** 6891–6901 (2013).

137. Pitteri, S. J. *et al.* Integrated Proteomic Analysis of Human Cancer Cells and Plasma from Tumor Bearing Mice for Ovarian Cancer Biomarker Discovery. *PLoS ONE* **4,** (2009).

138. Rifai, N., Gillette, M. A. & Carr, S. A. Protein biomarker discovery and validation: the long and uncertain path to clinical utility. *Nat. Biotechnol.* **24,** 971–983 (2006).

139. Hoofnagle, A. N. & Wener, M. H. The fundamental flaws of immunoassays and potential solutions using tandem mass spectrometry. *J. Immunol. Methods* **347,** 3–11 (2009).

140. Jaffe, E. A. *et al.* Cultured human fibroblasts synthesize and secrete thrombospondin and incorporate it into extracellular matrix. *Proc. Natl. Acad. Sci. U. S. A.* **80,** 998–1002 (1983).

141. Raugi, G. J., Mumby, S. M., Abbott-Brown, D. & Bornstein, P. Thrombospondin: synthesis and secretion by cells in culture. *J. Cell Biol.* **95,** 351–354 (1982).

142. Annis, D. S., Murphy-Ullrich, J. E. & Mosher, D. F. Function-blocking antithrombospondin-1 monoclonal antibodies. *J. Thromb. Haemost. JTH* **4,** 459–468 (2006).

143. Hingorani, S. R. *et al.* Trp53R172H and KrasG12D cooperate to promote chromosomal instability and widely metastatic pancreatic ductal adenocarcinoma in mice. *Cancer Cell* **7,** 469–483 (2005).

144. Ruifrok, A. C. & Johnston, D. A. Quantification of histochemical staining by color deconvolution. *Anal. Quant. Cytol. Histol. Int. Acad. Cytol. Am. Soc. Cytol.* **23,** 291–299 (2001).

145. Carvalho, F. M. *et al.* Prognostic value of podoplanin expression in intratumoral stroma and neoplastic cells of uterine cervical carcinomas. *Clinics* **65,** 1279–1283 (2010).

146. Ono, S. *et al.* Podoplanin-positive cancer-associated fibroblasts could have prognostic value independent of cancer cell phenotype in stage i lung squamous

cell carcinoma: Usefulness of combining analysis of both cancer cell phenotype and cancer-associated fibroblast phenotype. *Chest* **143,** 963–970 (2013).

147. Martinez, F. O., Gordon, S., Locati, M. & Mantovani, A. Transcriptional Profiling of the Human Monocyte-to-Macrophage Differentiation and Polarization: New Molecules and Patterns of Gene Expression. *J. Immunol.* **177,** 7303–7311 (2006).
148. Bubendorf, L., Nocito, A., Moch, H. & Sauter, G. Tissue microarray (TMA) technology: miniaturized pathology archives for high-throughput in situ studies. *J. Pathol.* **195,** 72–79 (2001).
149. Camp, R. L., Neumeister, V. & Rimm, D. L. A Decade of Tissue Microarrays: Progress in the Discovery and Validation of Cancer Biomarkers. *J. Clin. Oncol.* **26,** 5630–5637 (2008).
150. Ilyas, M. *et al.* Guidelines and considerations for conducting experiments using tissue microarrays. *Histopathology* **62,** 827–839 (2013).
151. Goethals, L. *et al.* A new approach to the validation of tissue microarrays. *J. Pathol.* **208,** 607–614 (2006).
152. Schmidt, L. H. *et al.* Tissue microarrays are reliable tools for the clinicopathological characterization of lung cancer tissue. *Anticancer Res.* **29,** 201–209 (2009).
153. Rubin, M. A., Dunn, R., Strawderman, M. & Pienta, K. J. Tissue microarray sampling strategy for prostate cancer biomarker analysis. *Am. J. Surg. Pathol.* **26,** 312–319 (2002).
154. Giblin, S. P. & Midwood, K. S. Tenascin-C: Form versus function. *Cell Adhes. Migr.* **9,** 48–82 (2014).
155. Paron, I. *et al.* Tenascin-C Enhances Pancreatic Cancer Cell Growth and Motility and Affects Cell Adhesion through Activation of the Integrin Pathway. *PLoS ONE* **6,** (2011).

156. Raimondi, S., Lowenfels, A. B., Morselli-Labate, A. M., Maisonneuve, P. & Pezzilli, R. Pancreatic cancer in chronic pancreatitis; aetiology, incidence, and early detection. *Best Pract. Res. Clin. Gastroenterol.* **24,** 349–358 (2010).

157. Esposito, I. *et al.* Tenascin C and annexin II expression in the process of pancreatic carcinogenesis. *J. Pathol.* **208,** 673–685 (2006).

158. Juuti, A., Nordling, S., Louhimo, J., Lundin, J. & Haglund, C. Tenascin C expression is upregulated in pancreatic cancer and correlates with differentiation. *J. Clin. Pathol.* **57,** 1151–1155 (2004).

159. Boja, E. S. & Rodriguez, H. Mass spectrometry-based targeted quantitative proteomics: Achieving sensitive and reproducible detection of proteins. *PROTEOMICS* **12,** 1093–1110 (2012).

160. Pérez–Mancera, P. A., Guerra, C., Barbacid, M. & Tuveson, D. A. What We Have Learned About Pancreatic Cancer From Mouse Models. *Gastroenterology* **142,** 1079–1092 (2012).

161. Henkin, J. & Volpert, O. V. Therapies using anti-angiogenic peptide mimetics of thrombospondin-1. *Expert Opin. Ther. Targets* **15,** 1369–1386 (2011).

162. Lawler, P. R. & Lawler, J. Molecular Basis for the Regulation of Angiogenesis by Thrombospondin-1 and -2. *Cold Spring Harb. Perspect. Med.* **2,** (2012).

163. Bigbee, W. L. *et al.* A Multiplexed Serum Biomarker Immunoassay Panel Discriminates Clinical Lung Cancer Patients from High-Risk Individuals Found to be Cancer-Free by CT Screening. *J. Thorac. Oncol.* **7,** 698–708 (2012).

164. Shafer, M. W., Mangold, L., Partin, A. W. & Haab, B. B. Antibody array profiling reveals serum TSP-1 as a marker to distinguish benign from malignant prostatic disease. *The Prostate* **67,** 255–267 (2007).

165. Suh, E. J. *et al.* Comparative profiling of plasma proteome from breast cancer patients reveals thrombospondin-1 and BRWD3 as serological biomarkers. *Exp. Mol. Med.* **44,** 36–44 (2012).

166. Pan, S. *et al.* Protein alterations associated with pancreatic cancer and chronic pancreatitis found in human plasma using global quantitative proteomics profiling. *J. Proteome Res.* **10,** 2359–2376 (2011).

167. Pannala, R., Basu, A., Petersen, G. M. & Chari, S. T. New-onset Diabetes: A Potential Clue to the Early Diagnosis of Pancreatic Cancer. *Lancet Oncol.* **10,** 88–95 (2009).

168. Ene-Obong, A. *et al.* Activated Pancreatic Stellate Cells Sequester CD8+ T-Cells to Reduce Their Infiltration of the Juxtatumoral Compartment of Pancreatic Ductal Adenocarcinoma. *Gastroenterology* **145,** 1121–1132 (2013).

169. Drifka, C. R. *et al.* Periductal stromal collagen topology of pancreatic ductal adenocarcinoma differs from that of normal and chronic pancreatitis. *Mod. Pathol.* (2015). doi:10.1038/modpathol.2015.97

170. Greenhalf, W. *et al.* Pancreatic Cancer hENT1 Expression and Survival From Gemcitabine in Patients From the ESPAC-3 Trial. *J. Natl. Cancer Inst.* **106,** djt347 (2014).